Title
Phytochemical Regulation of Tumor Suppressive MicroRNA in Human Breast Cancer Cells

Author
Hargraves, Kristina G.H.

Publication Date
2013

Peer reviewed|Thesis/dissertation

Phytochemical Regulation of Tumor Suppressive MicroRNA in Human Breast Cancer Cells

by

Kristina G. H. Hargraves

A dissertation submitted in partial satisfaction of the requirements for the degree of

Doctor of Philosophy

in

Endocrinology

in the

Graduate Division

of the

University of California, Berkeley

Committee in charge:

Professor Gary L. Firestone, Chair

Professor G. Steven Martin

Professor Jen-Chywan Wang

Fall 2013

Phytochemical Regulation of Tumor Suppressive MicroRNA in Human Breast Cancer Cells

By

Kristina G. H. Hargraves

ABSTRACT

Phytochemical Regulation of Tumor Suppressive MicroRNA in Human Breast Cancer Cells

by

Kristina G. H. Hargraves

Doctor of Philosophy in Endocrinology

University of California, Berkeley

Professor Gary L. Firestone, Chair

MicroRNA post-transcriptionally regulate more than half of the transcribed human genome and could be potential targets of anti-cancer therapeutics. The microRNA family, miR-34, is a component of the p53 tumor suppressor pathway and has been shown to mediate induction of cell cycle arrest, senescence, and apoptosis in cancer cells. Indole-3-carbinol (I3C) derived from cruciferous vegetables, artemisinin isolated from the sweet wormwood plant and artesunate derived from the carbonyl reduction of artemisinin effect components of the p53 pathway to growth arrest human cancer cells, implicating a potential role for miR-34a in their anti-proliferative effects.

Flow cytometry and Taqman semi-quantitative PCR analysis of I3C, artemisinin and artesunate treated human breast cancer cells indicate all three phytochemicals upregulate miR-34a in a dose and time-dependant manner that correlates with a pronounced G1 cell cycle arrest. Western blot analysis revealed miR-34a upregulation correlates with induction of functional p53 by I3C as well as artesunate and artemisinin mediated decreases in estrogen-receptor alpha (ERα) and the cyclin-dependant kinase CDK4, a known target of miR-34a inhibition. Luciferase assays in which cells were transfected with the miR-34a binding site of CDK4 mRNA attached to the firefly luciferase reporter gene confirmed miR-34a directly inhibits CDK4 expression in cells growth arrested by artemisinin or artesunate. Functional miR-34a appears critical for the anti-proliferative effects of I3C and artemisinin as transfection of non-translatable miR-34a inhibitors prevented I3C mediated growth inhibition and reversed artemisinin mediated down-regulation of CDK4. Artemisinin mediated down-regulation of ERα was also reversed in cells transfected with miR-34a inhibitors, implicating a novel role for miR-34a in the regulation of hormonal signaling. Transfection of dominant negative p53 prevented I3C upregulation of miR-34a in growth arrested cells containing wild-type p53 yet had no effect on artemisinin regulation of miR-34a, indicating a p53-indepedent mechanism of miR-34a regulation. Artemisinin and artesunate also upregulate miR-34a expression levels in breast cancer cell lines containing non-functional p53.

All of these data suggest that miR-34a plays a critical role in the anti-proliferative effects of artemisinin, artesunate and indole-3-carbinol in human breast cancer cells. Such evidence elucidates the therapeutic potential of each phytochemical to ectopically express tumor suppressive microRNA while implicating the use of miR-34a expression levels to determine the efficacy of phytochemical treatment. Artemisinin, artesunate and I3C could represent an efficacious means of increasing tumor suppressive microRNA *in vivo*.

Dedicated to KDHH

TABLE OF CONTENTS

LIST OF FIGURES

Chapter 1

Chapter 2

Chapter 3

INTRODUCTION

MicroRNA Introduction

MicroRNA (miRNA) are small, non-coding RNA molecules that post-transcriptionally regulate gene expression. They are transcribed in the nucleus as long primary transcripts that are trimmed by the Drosha enzyme to produce a stem-looped precursor molecule. Upon entry into the cytoplasm, each precursor is cleaved by the Dicer ribonuclease into a single-stranded mature microRNA molecule approximately 18-24 nucleotides in length. Mature microRNA form an RNA-induced silencing complex (RISC) with Argonaute proteins to silence gene expression by preventing translation of mRNA. The 6-8 nucleotide "seed" region at the 5' end of the miRNA either partially or perfectly pairs with the 3' un-translated region of its target mRNA. Imperfect base pairing physically prevents translation by inhibiting its initiation or by marking the mRNA for degradation by destabilization of the mRNA strand. Perfect complementarity between mRNA and miRNA induce mRNA cleavage through the RNA interference pathway (RNAi) (Yates 2013, Zinoyev 2013, Kim 2009, Filipowitz 2008, He 2007). Figure 1 provides a summary of the canonical pathway of microRNA biogenesis and action.

Since their discovery in 1993, miRNA have been shown to play a vital role in biological processes including development, growth and cellular differentiation. Most microRNA bind imperfectly to mRNA, permitting each molecule to target a large number of mRNA sequences. In this manner, microRNA provide a means by which a single cellular signal can down-regulate thousands of proteins. Bioinformatics as well as microarray analyses suggest that miRNA regulate more than half of the transcribed human genome (Friedman 2009, Lewis 2005, Xie 2005). MicroRNA are thus essential components of a cells regulatory machinery with aberrant expression levels implicated in disease states such as cancer.

The discovery of two miRNA clusters commonly deleted in B-cell chronic lymphocytic leukemia's in 2002 spurred researchers to further investigate the potential role of miRNA in cancer (Lujambio 2012, Croce 2006). By hybridizing RNA isolated from tumor samples and cultured cell lines to arrays containing miRNA libraries, cancer-specific miRNA expression profiles were generated for every type of analyzed cancer. MiRNA genes are often located within genomic sites frequently manipulated in cancer, leading to their mis-regulation as the cancer develops. The function of miRNA within each cancer type has been suggested by its expression levels and transcriptional targets. MiRNA over-expressed in cancer are classified as oncogenic or "oncomiRs" while down-regulated miRNA are classified as tumor-suppressors. One of the first microRNA families to be integrated into a known tumor suppressor pathway is the microRNA family miR-34.

Figure 1

microRNA Biogenesis & Action

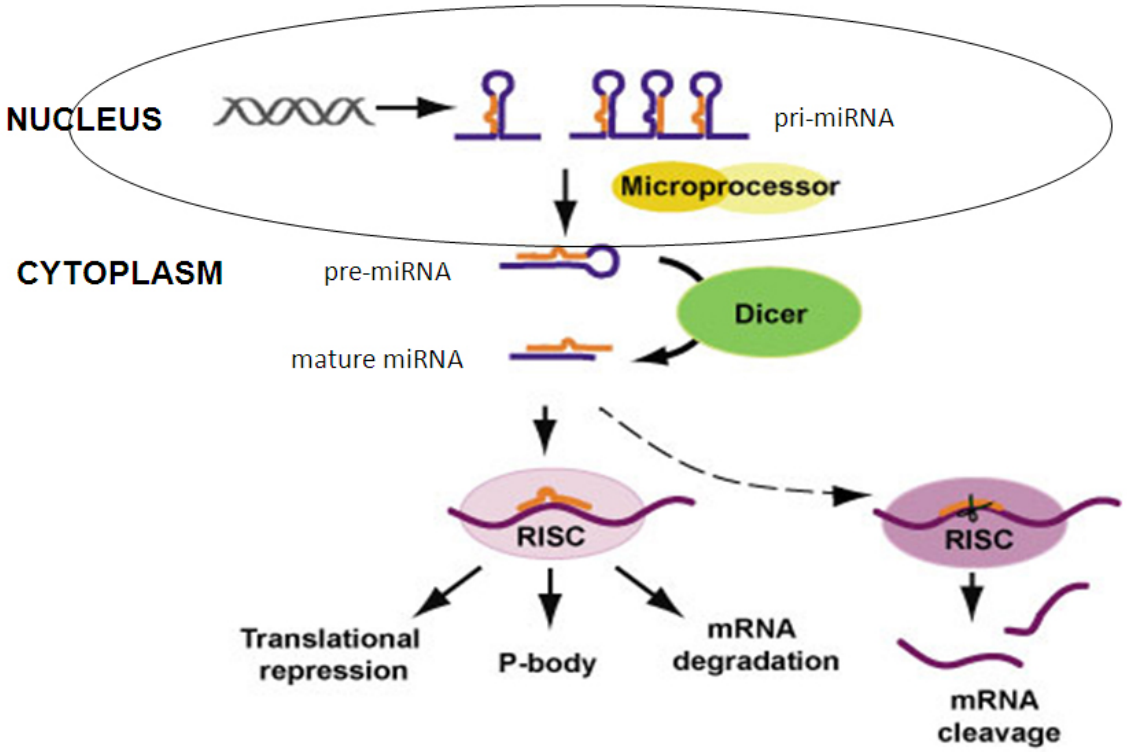

He Lin, et al. (2007) *Nature Review Cancer*. 7, 819-822.

miR-34 family and p53

MiR-34 is an evolutionarily conserved miRNA family containing three isoforms: miR-34a, miR-34b and miR-34c. In humans, the gene for miR-34a is located at chromosome 1p36 while miR-34b and miR-34c are co-transcribed from chromosome 11q23. Each molecule is approximately 23 nucleotides with a seed sequence of GGCAGUGU and 18 nucleotides shared between all three family members (Wong 2011, Hermeking 2009, He 2007). Figure 2 provides the structure and chromosomal location of each miR-34. In mice, miR-34a is the predominant isoform, with highest expression in the brain, while miR-34b and c are mainly expressed in lung tissue and osteoblast development (Wei 2012, Lodygin 2008, Bommer 2007).

In vitro assays including Western blots, microarray analysis, Luciferase assays, and the complementarity of mRNA to the miR-34 seed region, identified potential miR-34 target genes involved in cell cycle progression, microRNA processing, cellular migration and apoptosis. miR-34a directly down-regulates the cell cycle regulators CDK4, CDK6 and cyclin E2 as well as the anti-apoptotic protein Bcl-2, to induce cell cycle arrest and apoptosis within cancer cell lines while miR-34b/c expression correlates with inhibition of the transcription factor Myb, migratory protein CAV1 and microRNA metabolic regulator SFRS2 (Wong 2011, Hermeking 2009, He-review 2007). All three microRNA inhibit the tyrosine kinase MET while each miR-34 target different isoforms of the Myc transcription factor family: miR-34a can inhibit N-Myc while miR-34b/c suppresses c-Myc expression. In normal cells, miR-34 expression and target gene regulation has been implicated in a variety of processes including hematopoiesis, nervous system development, spermatogenesis, stem cell differentiation, and cold-resistance in insects (Soni 2013, Lyons 2013, Jiang 2012, Liu 2012, Courteau 2012, He 2011, Standanlick 2011, Wong, 2011, Arhana 2011, Bouhallier 2010, Tarantino 2010, Bak 2008, Sempere 2004, Miska 2004).

All three microRNA were first linked to cancer through their observed down-regulation in lung and neuroblastomas, implicating their possible role as tumor suppressors (Hermeking 2009, Cole 2008, He 2007-review). Six studies in 2007 indicated through genome-wide analysis for p53 induced miRNA, direct correlation of p53 status to miR-34 expression levels and identification of a consensus p53 binding site within the miR-34 promoter that the miR-34 family is an active component of the p53 tumor suppressor pathway and could provide the necessary inhibitory activity of p53 (Bommer 2007, Chang 2007, Corney 2007, He 2007, Raver-Shapira 2007, Tarasov 2007). p53 is also derived from the same chromosomal locus as miR-34a: 1p36.

Figure 2

miR-34 Structure and Loci

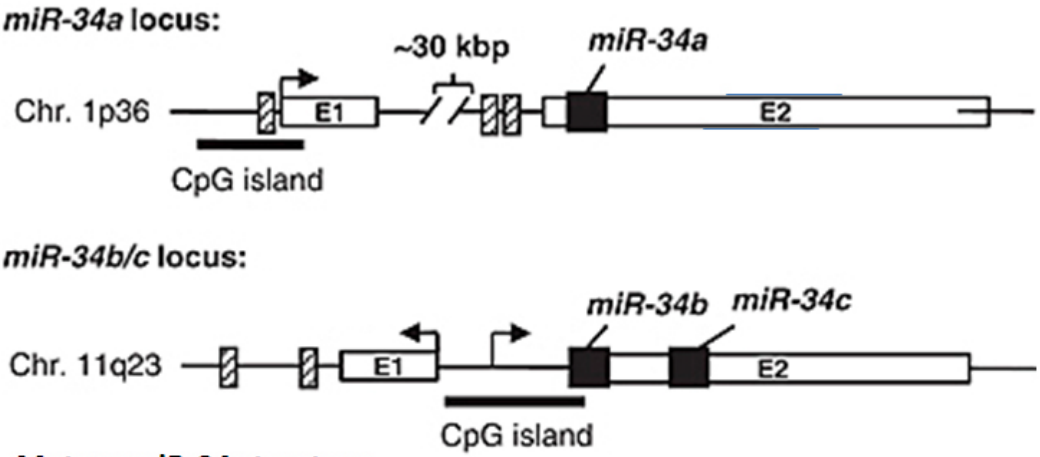

Mature miR-34 structure

Seed Region

```
miR-34a     5′-UGGCAGUGUC-UUAGCUGGUUGU-3′
miR-34b    5′-UAGGCAGUGUCAUUAGCUGAUUG-3′
miR-34c     5′-AGGCAGUGUAGUUAGCUGAUUGC-3′
```

Heikio Hermeking (2009). *Cell Death and Differentiation*. 17

p53 is a protein tetramer considered the guardian of the genome due to its induction of apoptosis, DNA repair or stalling of cell cycle progression in response to DNA damage (Caraval 2013, Riley 2008, Vogelstein 2000). Activation of p53 directly correlates with the regulation of genes involved each of these processes including upregulation of the cyclin-dependent kinase inhibitor p21, DNA polymerase pol κ, and pro-apoptotic protein Bax as well as the repression of Bcl-2. For years, researchers knew p53's activity as a transcription factor could explain its ability to upregulate the expression of particular genes yet were unable to explain its ability to inhibit expression of others. The integration of miR-34 into the p53 pathway could explain such inhibition, with miR-34 suppressing known p53 repression targets.

The following canonical pathway of p53 and miR-34 regulation has been proposed (Wong 2011, Hermeking 2009, He 2007-review). In healthy cells, p53 is rapidly degraded through proteosomal degradation mediated by the ubiquitin ligase MDM2. Upon DNA damage, the PI3-kinase related kinase ATM phosphorylates p53 at residues preventing MDM2 mediated ubiquitination. The newly stabilized protein then upregulates the transcription of target genes including miR-34, resulting in the repression of pro-cell survival and anti-apoptotic genes and subsequent death or growth arrest of the cell. miR-34a also provides a positive feedback loop on p53 activity by directly inhibiting SIRT-1, an NAD-dependent deacetylase that can destabilize p53, as well as the p53 binding protein, MDM4 (Arhana 2011, Luan 2010, Zhao 2010, Yamakuchi 2009, Yamakuchi 2008, Fujita 2008).

In cancerous lesions, alterations in the p53 and miR-34 gene locus interrupt their inhibition on cell proliferation. The chromosomal locus 1p36 is one of the most frequently deleted in cancer, providing a possible explanation for the loss of p53 activity and low miR-34 levels observed in several cancer types (Wong 2011, Hermeking 2009, He-review 2007, Welch 2007, Chang 2007, Bommer 2007). The p53 gene is mutated in nearly half of all human tumors while CpG methylation of all three miR-34 promoters has been detected in the most commonly diagnosed carcinomas, sarcomas and associated cell lines (Serra 2012, Vogt 2011, Olivier 2010, Lodygin 2008, Toyota 2008, Lujambio 2008, Kozaki 2008, Vogelstein 2000). p53 and miR-34 thus have clinical value as diagnostic indicators for cancer and therapeutically activating the powerful tumor-suppressive miR-34 family could be a potential cancer treatment (Wong 2011, Olivier 2010). The role of miR-34a in breast cancer as well as possible induction by plant based chemotherapeutics is the subject of this dissertation.

Breast Cancer and microRNA

Breast cancer is the most diagnosed form of cancer in American women excluding skin cancers with one in eight women (12%) likely to develop breast cancer in their life time (American Cancer Society 2013). 232, 340 women were diagnosed with breast cancer this year alone, and 39,600 die annually from the disease. While mortality rates for the disease have decreased in the past two decades, breast cancer is the second leading cause of cancer related death in women and incidence remains high.

The phenotype of breast cancer is often categorized by tumor grade including differentiation status, proliferation rate and metastatic potential as well as aberration in expression levels of molecular markers such as estrogen receptor, progesterone receptor and the epidermal growth factor receptor, Her-2/Neu (American Cancer Society 2013, Koboldt 2012, Carey 2010, Dawood 2011). The mutation status of the tumor suppressor protein p53 is also used to diagnose breast cancer.

Early stages of the disease are often slow-growing, poor to mildly invasive and express wild-type p53 as well as estrogen and progesterone receptor. Such cases represent 2/3 of breast cancer diagnoses and generally respond well to radiation and hormone targeted chemotherapy treatments such as the anti-estrogen therapies tamoxifen (Nolvadex) which is an estrogen receptor antagonist and aromatase inhibitors, Letrozole (Femara) and Exemestane (Aromasin) which prevent the conversions of androgens into estrogens (American Cancer Society 2013, Colozza 2008).

Molecular classifications of early stage breast cancer include the luminal A and luminal B subtype which are estrogen receptor positive and share physiology and genetic markers with normal epithelial cells lining the inner space or "lumen" of breast glands and ducts. Luminal A tumors possess fewer genetic mutations, grow more slowly and are associated with a slightly more favorable outcome than Luminal B tumors which may express Her-2/Neu. Luminal A breast cancer is often investigated in the laboratory setting by using the MCF-7 and T47D human breast cancer cell lines derived from the metastatic adenocarcinoma of a 69-year-old patient and the invasive ductal carcinoma of 54-year-old patient respectively (Kao 2009, Levenson 1997, Keydar 1979). Both cell lines are hormone responsive, weakly tumorigenic, estrogen and progesterone receptor positive and Her-2/Neu receptor negative. MCF-7 cells contain wild-type p53 while T47D cells possess a mutant form of the tumor suppressor. A cell line often used to represent more normalized tissue is the spontaneously immortalized human mammary epithelial cell line, MCF-10A (Cowell 2005, Soule 1990). MCF-10A cells possess a molecular and phenotypic profile resembling normal breast epithelial cells including low estrogen and progesterone receptor expression, wild-type p53 and limited to no expression of the Her-2 receptor.

Her-2/Neu receptor positive and hormone receptor negative breast cancers often represent a more advanced stage of the disease that is associated with poor prognosis (American Cancer Society 2013). Tumors grow rapidly and are highly invasive, requiring targeted therapies to address the high-level of self-sustaining growth factors produced by gene mutations. Her-2 positive cancers represent 1/5 of diagnoses and are molecularly characterized by amplification of the Her-2 gene. While unresponsive to hormone therapy, such cancers can be successfully treated with targeted agents that inhibit the Her-2 receptor such as trastuzamab (Herceptin) or lapatanib (Tykerb) given in combination with general chemotherapy.

Hormone receptor negative or "triple-negative" breast cancers lack estrogen receptor, progesterone receptor and elevated levels of Her-2 making treatment options more difficult. Hormone receptor negative cancers can also be classified as basal-like as they often share molecular markers with the outer or basal layer of cells lining breast ducts and glands. The triple negative MDA-MB-231 cell line derived from the metastatic adenocarcinoma of a 51-year-old patient is often used to represent this stage of the disease experimentally while the Her-2 positive breast cancer cell line SKBR3 isolated from the metastatic adenocarcinoma of a 43-year-old patient is representative of Her-2 receptor positive breast cancer (Chavez 2010, Calileu 1973, Fogh 1977). Both cell lines contain mutant p53.

In the past eight years, microarray and Northern blot analysis of tumor samples and commonly used cell lines in comparison with normal breast tissue enabled researchers to develop a microRNA signature for breast cancer phenotypes. Estrogen receptor positive breast cancers are associated with decreased miR-30 while breast cancers with poor prognosis indicators such as lymph node metastasis', increased vascularization and a high proliferation index can be identified by decreased levels of the tumor suppressive microRNA let-7a-f, miR-125b and miR-145 and elevated levels of the oncogenic microRNA miR-21and miR-155 (Liu 2013, O'Day 2010, Shi 2009, Cheng 2009, Blenkinron 2007, Iori 2005). Luminal A and Luminal B breast cancers are associated with elevated levels of let-7f and decreased levels of miR-155 while basal and Her-2+ disease states feature the reverse profile (Blenkiron 2007).

Alterations in miR-125b, miR-145 and miR-21 levels also enable differentiation between normal tissue, human breast cancer cell lines and breast cancer tumors. Elevated levels of the tumor suppressive microRNA miR-145 and miR-125b can be detected in the basal compartment of normal breast tissue while the oncogenic miR-21 is barely detected (Bockmeyer 2011, Sempere 2007, Iori 2005). This profile is reversed when comparing normal breast tissue to tumor samples of increasing tumor grade with miR-125b and miR-145 levels decreasing and miR-21 levels increasing with the progression of the disease (Bockmeyer 2011, Iori 2005).

Human preneoplastic and breast cancer cell lines reflect a similar microRNA profile as their associated tissues with MCF-10A cells expressing elevated levels of tumor suppressive miR-34a and miR-125b and low levels of oncogenic miR-21, MCF-7 and T47D cell lines expressing moderate levels of both, and MDA-MB-231 cells, indicative of triple-negative breast cancer phenotype, possessing high levels of miR-21 and low levels of miR-34a (Yang 2013, Mackiewicz 2011, Iori 2005). A summary of the microRNA profile as well as the clinical classifications of each cell line is provided in Figure 3.

Figure 3

Human Breast Cancer Cell Lines

		MCF-10A	MCF-7	T47D	MDA-MB-231	SKBR3
Breast cancer phenotype		Preneoplastic	Luminal A	Luminal A	Triple-Negative/ Basal	Her2+
Tumorigenic		No	Yes	Yes	Yes	Yes
p53 status		WT	WT	Mutant	Mutant	Mutant
Hormone responsive		Yes	Yes	Yes	No	No
microRNA levels	**34a**	High	Medium	Medium	Low	High
	125b	High	Low	Medium	High	Low
	21	Low	Medium	Medium	High	Low

microRNA levels and their associated targets in breast cancer indicate their potential role in the disease. The molecular targets of miR-125b and miR-145 include known oncogenes such as N-Myc and Akt while miR-21 can inhibit the expression of tumor suppressor genes such as TGFβ and PTEN. Ectopically expressing miR-34a in human breast cancer cell lines has been shown to suppress cell proliferation and metastasis through inhibition of Akt signaling and direct suppression of the receptor tyrosine kinase AXL (Yang 2013, Mackiewicz 2011). Elevated levels of miR-34a in breast cancer patients are also associated with decreased lymph node metastasis and a lower risk of recurrence or death from the disease (Yang 2013, Peurala 2011).

miR-34a as well as the oncogenic microRNA miR-221/222 have also been found to play a role in breast cancer chemoresistance. Ectopically expressing miR-34a in breast cancer cells resistant to the chemotherapy agent adriamycin increased sensitivity to the drug through inhibition of the transmembrane receptor Notch-1 while elevated levels of miR-221/222 is associated with tamoxifen resistance in breast cancer (Li 2012, Zhao 2008, Miller 2008). Knockdown of miR-221/222 sensitizes resistant cells to tamoxifen while over-expression confers resistance through down-regulation of the cell cycle inhibitor, p27. miR-221/222 also directly inhibits estrogen-receptor alpha (ERα), providing an additional level of microRNA regulation. Other microRNA that have been shown to regulate key signaling pathways in breast cancer include the tumor suppressive microRNA miR-205 and miR-206 that directly inhibit ERα and Her-2 respectively and are often downregulated in advanced stages of the disease (Li 2013).

All of these data not only implicates the critical role of microRNA in breast cancer progression and diagnosis but the need for targeted therapies to chemically restore the microRNA signature of normal breast tissue. To date, no study has yet achieved targeted delivery of microRNA therapeutics however recent research has implicated possible methods of microRNA regulation *in vivo* (Liu 2012, Iorio 2011, Shi 2009). Tumor suppressive microRNA can be ectopically expressed by microRNA replacement methods such as lipid nanoparticle delivery of double stranded precursor molecules or viral delivery of microRNA coding vectors. Adenovirus or lentiviral delivery of vectors expressing the tumor suppressors let-7a or miR-26a reduced tumor formation and inhibited cancer cell proliferation in murine models of lung and liver cancer respectively while lipid-based delivery of double stranded pre-miR-34a successfully stalled the *in vivo* progression of human lung and colon cancer as well as the lung metastasis of murine melanoma cells (Trang 2010, Esquela-Kerscher 2008, Kota 2009, Wiggins 2010, Chen 2010, Tazawa 2007). microRNA inhibitors such as non-translatable complimentary targets known as “antagomirs” or the more stable form of locked nucleic acid antisense oligos (LNAs) have been used *in vitro* and *in vivo* to inhibit oncogenic microRNA. Systemic treatment of tumor-bearing mice with miR-10b antagomirs suppressed breast cancer metastasis while LNA inhibition of miR-122, a known promoter of hepatitis C virus (HCV) replication in the liver, dramatically reduced HCV RNA levels in infected patients (Janssen 2013).

Limitations of current microRNA therapeutics include off-target side-effects, potential toxicity due to high concentrations and inefficient delivery methods. High levels of shRNA required to silence microRNA expression in the mouse liver induced off-target side-effects including interferon response activation and liver damage resulting in death while several patients in a miR-122 clinical trial expressed headache and nausea like symptoms (Janssen 2013, Grimm 2006). Clearly, there is need for more efficacious treatment options with microRNA regulation specificity and limited side-effects. Plant-based anti-cancer therapeutics represent one such possibility and the regulation of the tumor suppressive microRNA miR-34 by indole-3-carbinol derived from cruciferous vegetables and artemisinins extracted from the sweet wormwood plant is the subject of this dissertation.

Indole-3-carbinol and Cancer

Indole-3-carbinol (I3C) is a bioactive phytochemical derived from the cooking or crushing of cruciferous vegetables such as broccoli, cauliflower and cabbage. Diets rich in cruciferous vegetables have long been associated with decreased cancer risk in humans and biochemical studies as early as 1978 identified I3C as one of the critical components to elicit an anti-cancer effect (Liu 2013, Hoezl 2008, Higdon 2007, Altundag 2006, Kristal 2004, Kristal 2002, Terry 2001, Cohen 2000, Verhoeven 1996, Sharma 1994, Wattenberg 1985, Wattenberg 1978).

I3C is synthesized from its precursor glucobrassicin when cruciferous vegetables undergo physical force (such as cooking or chewing), initiating glucobrassicins exposure to the enzyme myrosinase. Myrosinase hydrolyzes glucobrassicin into I3C and acid hydrolysis within the stomach converts some of the I3C into biologically active dimer and trimers including 3'3-diindoylmethane (DIM) (Acharya 2010, Weng 2008, Aggarwal 2005). The chemical structure and derivation of I3C is provided in Figure 4.

Epidemiological as well as laboratory studies have revealed I3C and DIM have substantial anti-cancer effects. Increased consumption of cruciferous vegetables in postmenopausal women inversely correlated with their risk of developing breast cancer while mice fed a diet rich in cruciferous vegetables or with I3C or DIM alone exhibited decreased risk of spontaneous mammary tumor formation (Terry 2002, Bradlow 1991). Completed clinical trials suggest both compounds are well-tolerated and beneficial in the treatment of breast and cervical cancers while trials are currently ongoing for the treatment of prostate cancer (Del Priore 2009, Reed 2005, Dalessandri 2004, Terry 2001, Bell 2000, ClinicalTrials.gov). I3C and DIM also decrease tumor size, volume and level of vascularization upon administration to mice implanted with xenografts of human cancer cells (Weng 2008).

Figure 4

Indole Biogenesis

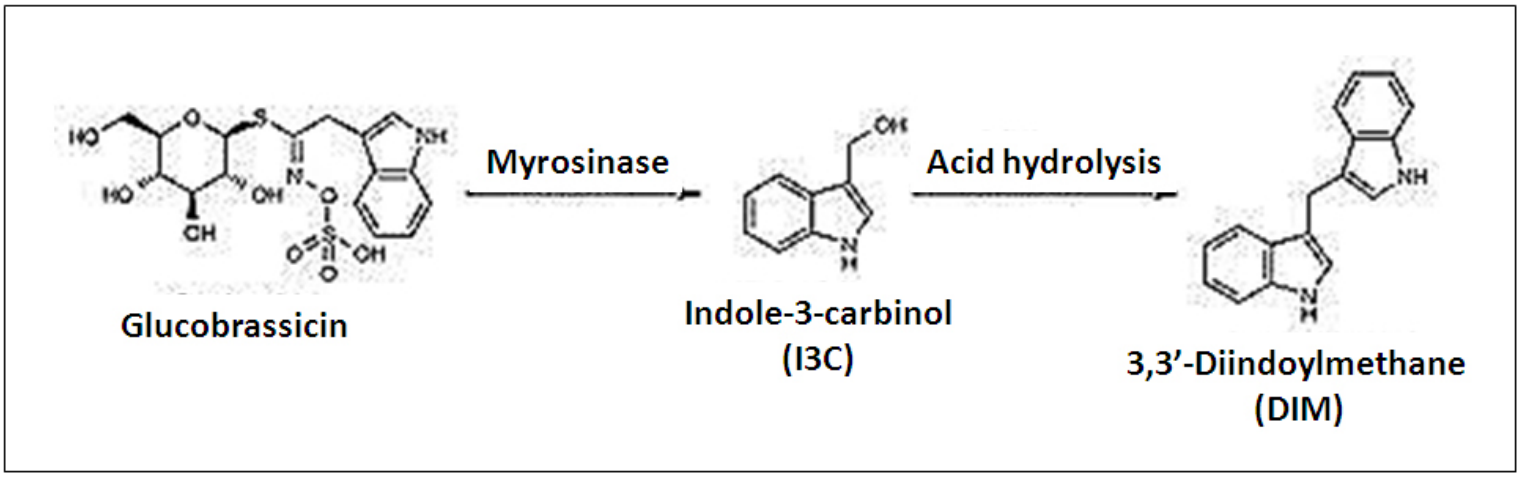

Mechanistic studies with human cancer cell lines revealed that I3C and DIM partially exert their anti-cancer effects through alterations in cell cycle progression, immune function and apoptosis. Both compounds decrease levels of the anti-apoptotic factor Bcl-2, inactivate Akt/NF-κB nuclear signaling, increase interferon-gamma responsiveness and reduce CDK2 enzymatic activity to growth arrest and induce apoptosis in human breast cancer cells as well as non-tumorigenic breast epithelial cells (Aronchik 2010, Xue 2008, Rahnman 2007, Riby 2006, McGuire 2006, Xue 2005, Garcia 2005, Chatterji 2004, Rahman 2003, Hong 2002, Hong 2001).

Other molecular targets known to be negatively affected by I3C include CDK6, cyclin E, and components of hormone receptor signaling such as estrogen receptor-alpha (Acharya 2010, Firestone 2009, Weng 2008, Sundar 2006, Weng 2006, Aggarwal 2005, Kim 2005). Research within our lab identified human neutrophil elastase as the only known direct molecular target of I3C inhibition, resulting in the G1 cell cycle arrest of human breast cancer cells (Aronchik 2012, Aronchik 2010, Ngyuyen 2008). I3C treatment of human breast cancer cells also negatively impacts telomerase expression, insulin-growth factor signaling, proliferation and cellular motility while DIM can inhibit angiogenesis and tumor invasion while sensitizing cells to chemotherapeutic agents (Marconett 2012, Marconett 2011, Brew 2009, Garcia 2005, Cram 2001, Cover 1998, Rahimi 2010, Riby 2008, Rahman 2007, McGuire 2006, Chang 2005).

Previous research within our lab indicated that I3C stabilizes p53 to induce the G1 cell cycle arrest of the non-tumorigenic human mammary epithelial cell line, MCF-10A (Brew 2006). I3C treatment increases ATM phosphorylation status independent of DNA damage, resulting in an increase in total as well as phosphorylated forms of p53, upregulated p21 levels and subsequent G1 cell cycle arrest. Transfection of dominant negative p53 reverses this effect suggesting that I3C mediated cell cycle arrest of this cell line is p53-dependent.

The activation of p53 suggests that I3C could potentially utilize the downstream transcriptional target and known tumor suppressive microRNA family miR-34 to exert its anti-proliferative effects. Chapter 1 of this dissertation indicates that I3C upregulates miR-34a in a dose and time dependent manner that requires functional p53. Inhibition of miR-34a prevents I3C mediated growth inhibition indicating miR-34a is a critical component of I3C's anti-proliferative effects in human breast cancer cells.

Artemisinin, Artesunate and Cancer

Artemisinin, a sesquiterpene lactone extracted from the leaves of the sweet wormwood plant, *Artemisia annua* L., is an anti-malarial compound that exhibits potent anti-cancer effects both *in vitro* and *in vivo.* The sweet wormwood plant has been used as an herbal remedy for over two thousand years yet a single reference to its use as a treatment for malaria symptoms in the *Handbook of Prescriptions for Emergencies* by Ge Hong (284-346 C.E) prompted Chinese researchers to investigate *Artemisia* as a potential treatment for North Vietnamese soldiers afflicted with malaria during the early Vietnam war (Miller 2011, Tu 2011, Efferth 2009).

Artemisinin was first isolated in 1972 and since that time has been successfully used as a combination therapy for drug-resistant and severe forms of the disease in 67 malaria-endemic countries (Miller 2013, Cui 2009, Bosman 2007).

Artemisinin can drastically reduce the parasite load within hours however its short half-life, insolubility in water and poor bioavailability have lead to the generation of more effective semi-synthetic derivatives, such as artesunate, an artemisinin compound with a reduced carbonyl group. The chemical structure of artemisinin and artesunate can be found in Figure 5. Artesunate is more clinically effective than its parent compound and is currently the most commonly used derivative partner used to treat malaria (Haynes 2007, Adjuik 2004). Both compounds are well tolerated in humans with limited side-effects (Sinclair 2012, Efferth 2010, Adjuik 2004, Meschnick 2002).

Artemisinin and artesunate exert their anti-malarial effects through cleavage of the endoperoxide bridge. The malaria parasite consumes hemoglobin within the red blood cells of its host, resulting in the release of heme-iron. Heme-iron cleaves the endoperoxide bridge of artemsinin and the subsequent generation of reactive oxygen species irreparably damages the food vacuoles of the parasite (Efferth 2009, Gautam 2009, Cui 2009, Meschnick 2002).

The observation that cancer cells often possess much greater iron content than their primary tissue counterparts prompted researchers to investigate the anti-cancer activity of artemisinins (Efferth 2009, Nakase 2008). In the past twenty years, *in vitro* and *in vivo* studies have shown artemsinin and artesunate are cytotoxic against several cancer types including leukemia, melanoma, breast, lung, prostate, pancreatic, ovarian and colon cancer (McGovern 2010, Efferth 2009, Sundar 2009). Oral or intravenous treatment of artemisinin and artesunate decreases tumor size, volume and level of vascularization upon administration to mice implanted with xenografts of human cancer cells while *in vitro* treatment induces apoptosis, inhibits cell proliferation and prevents angiogenesis (Tin 2012, Sundar 2009, Langroudi 2010, Du 2010, Hou 2008, Zhou 2007, Lai 2009, Lai and Singh 2006). Both compounds have limited effects on primary cells of the cancer tissue origin and clinical trials for the artesunate treatment of metastatic breast cancer are currently ongoing (ClinicalTrials.gov, Gong 2013, Hamacher-Brady 2011, Tin 2012, Hou 2008, Efferth 2004). Artemisinins also demonstrate potential as adjuvant cancer treatments. Combination treatments of artesunate and the chemotherapeutic lenlidomide greatly enhanced the cytotoxic effects of either drug in breast, colon, lung and prostate cancer while artemisinin can synergize with the anti-estrogen fulvestrant to growth arrest human breast cancer cells (Liu 2011, Sundar 2008).

Figure 5

Synthesis of Artemisinins

Artemisia Annua L.

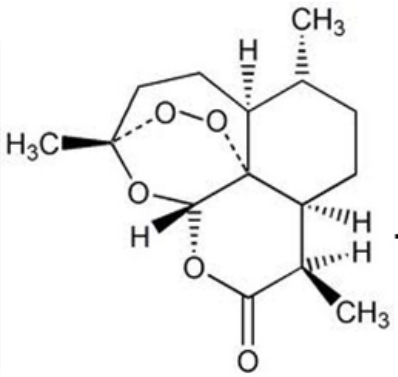

Artemisinin

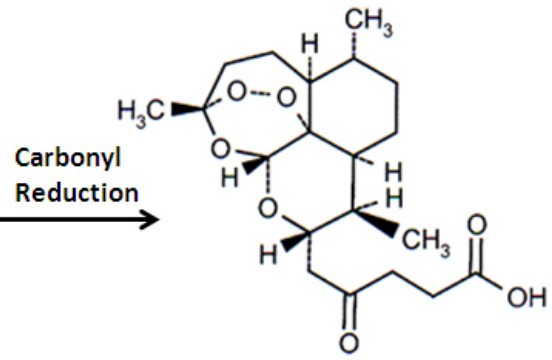

Artesunate

In vitro studies as well as microarray analysis suggest artemisinins primarily exert their anti-cancer effects through regulation of target genes involved in cell cycle regulation, apoptosis, angiogenesis and oncogene activity (Gao 2013, Zhou 2012, Nakase 2009, Anfosso 2006, Efferth 2004, Efferth 2003, Wartenberg 2003, Efferth 2002, Sadava 2002). Artemisinin or artesunate treatment of human lung, hepatoma, breast, prostate or colon cancer cell lines downregulates levels of CDK4 and cyclin D1 to induce a G1 cell cycle arrest (Gong 2013, Tin 2012, McGovern 2010, Liu 2011, Sundar 2008, Hou 2008, Willoughby 2006). Both compounds also inhibit CDK2 levels and activity in human breast cancer while artemisinin treatment alone attenuates estrogen signaling by decreasing the levels and activity of estrogen-receptor alpha (Tin 2012, Sundar 2009, Sundar 2008, Efferth 2003). Other molecular targets inhibited by both compounds include the oncogene c-Myc, pro-angiogenic signaling component vascular endothelial growth factor (VEGF) and the anti-apoptotic factor Bcl-2 (Gong 2013, He 2011, Sertel 2010, Zhou 2007, Wartenberg 2003). p53 mutation status does not appear to affect cell line sensitivity to artesunate while functional p53 is required for the artemisinin mediated cell cycle arrest of human gastric cancer cells (Zhang 2013, Sertel 2010, Efferth 2004, Efferth 2003).

To date, no research has been published on microRNA regulation by artemisinins. Chapters 2 and 3 of this dissertation indicate artemsinin and artesunate upregulate miR-34a in a p53-independent manner to directly inhibit CDK4 in human breast cancer cells. Such data further elucidates the anti-cancer potential of artemisinins while providing evidence of phytochemical regulation of tumor suppressive microRNA.

Phytochemical Regulation of microRNA

MicroRNA have only recently been linked to the anti-cancer activity of phytochemicals. In the past five years, microarray and qPCR detection of microRNA levels in phytochemically treated cancer cells and tumor samples have determined plant-based compounds such as isoflavone found in soy, I3C and 3,3'-diindolymethane (DIM) derived from cruciferous vegetables, and epigallocatechin-3-gallate isolated from green tea regulate microRNA levels in association with apoptosis, reversal of the epithelial-to-mesenchymal transition, enhanced efficacy of conventional chemotherapy and decreased cell proliferation (Li 2010, Sarkar 2010).

Current research indicates the I3C metabolite, DIM, inhibits the invasive capability of pancreatic and prostate cancer cells while up-regulating the tumor-suppressive microRNA families, miR-200, let-7 and miR-146a. DIM treatment of pancreatic cancer cell lines correlated with a dose and time-dependent increase in each microRNA family as well as a decrease in protein and RNA levels of metastasis related target proteins such as protein membrane-1 matrix metalloproteinase (MT1-MMP) known to be directly inhibited by miR-200 and interleukin 1 receptor-associated kinase 1 (IRAK-1), a target of miR-146a inhibition and activator of the transcription factor, NF-kB (Soubani 2012, Li 2010). DIM induction of the miR-200 family also increased sensitivity of pancreatic cells to the chemotherapy agent gemcitabine while increased levels of let-7 upon DIM treatment of prostate cancer cells decreased self-renewal capacity

through inhibition of the epithelial-to-mesenchymal regulator, Enhancer of Zeste homolog 2(EZH2) (Li-Sarkar 2009, Kong-Sarkar 2012). DIM has also been implicated in the adjuvant regulation of microRNA in human breast cancer cells. DIM in combination with the chemotherapy drug Herceptin increased miR-200 levels within Her-2+ human breast cancer cells to down-regulate the transcription factor FoxM1 and induce apoptosis (Ahmad 2013). Transfection of miR-200 inhibitors reversed this effect, indicating a functional requirement of miR-200 in DIM/Herceptin mediated apoptosis.

The phytochemicals I3C, artemisinin and artesunate may also utilize miRNA to induce their affects. Two studies in 2010 implicated I3C regulation of microRNA in lung cancer. Both studies found that dietary uptake of I3C reversed carcinogen induced alterations in microRNA levels in mouse and rat lung tumors induced by vinyl-carbamate or cigarette smoke, respectively (Izzotti 2010, Melkamu 2010). In addition, I3C treatment of pancreatic cancer cells correlated with decreased levels of the oncogenic microRNA, miR-21 (Paik 2013). While each study implies a connection between I3C treatment and microRNA regulation, it has yet to be determined if microRNA are necessary for I3C mediated anti-cancer affects and what role they may play.

No research is currently published linking microRNA to the anti-cancer effects of artemisinin or its derivatives. Computational studies have been performed to predict microRNA involvement in artemisinin biosynthesis yet a pharmaceutical analysis of artemsinin regulated microRNA has yet to be performed (Perez-Quintero 2012, Pani 2011).

My thesis provides the first evidence of regulation of the tumor-suppressive microRNA, miR-34a, by indole-3-carbinol, artemisinin, and artesunate in human breast cancer cells. Such research not only provides further evidence of the anti-cancer properties of artemisinins and I3C but elucidates the potential use of miR-34a as a diagnostic mechanism for determining viability of phytochemical treatment.

ACKNOWLEDGEMENTS

I would like to thank my mentor, Dr. Gary Firestone, for his assistance and advice. I have gained solid scientific insight and immeasurable technical skills from his tutelage.

I would also like to thank the members of my thesis committee, Dr. G. Steven Martin and Dr. Jen-Chywan Wang for their guidance, as well as, Dr. Lin He and members of her laboratory for their collaboration on the miR-34 aspect of my project. I am grateful to Firestone lab members past and present and my faculty family at Mills College for their advice throughout the years.

Thank you to my grandmother, the late Dr. Wanda Broussard Hall, for initiating the doctoral legacy I am proud and pleased to have joined. Thank you also to family members, friends, neighbors and unknown supporters who were placed in my path to share a kind word, gesture, or inspiration. In closing, I bestow this body of work to my father, mother and sister. Your unconditional support was paramount to this successful conclusion. Please know that none of this would have been possible without you.

CHAPTER 1

Indole-3-carbinol upregulates miR-34a by p53 to Inhibit Proliferation of Preneoplastic and Human Breast Cancer Cells

ABSTRACT

Indole-3-carbinol, a bioactive phytochemical derived from cruciferous vegetables, has pronounced anti-cancer effects *in vitro* and *in vivo* however a direct link to tumor suppressive microRNA has yet to be established. In this study, quantitative PCR analysis demonstrates that I3C upregulates mature levels of the tumor suppressive microRNA miR-34a in a dose and time-dependent manner correlating with induction of a G1 cell cycle arrest in human preneoplastic and breast cancer cell lines. Functional p53 is required for I3C regulation of miR-34a as transfection of dominant negative p53 ablates miR-34a induction. Luciferase and RT-PCR experiments reveal that under conditions of mature miR-34a induction by I3C, expression of the miR-34a promoter is down-regulated while levels of miR-34a primary transcript remain the same, suggesting I3C regulates microRNA processing to increase levels of mature miR-34a. Transfection of miR-34a inhibitors significantly reduced I3C inhibition of cell proliferation. Taken together, these data suggest that miR-34a is a critical component of I3C's anti-proliferative effects in human breast cancer cells and is regulated in a p53-dependent manner.

INTRODUCTION

Indole-3-carbinol (I3C) is a potential anti-cancer therapeutic derived from the cooking and crushing of cruciferous vegetables. Diets rich in cruciferous vegetables have long been associated with decreased cancer risk in humans and biochemical as well as short-term bioassays indentified I3C as one of the active components to elicit an anti-cancer effect (Liu 2013, Hoezl 2008, Higdon 2007, Altundag 2006, Kristal 2004, Kristal 2002, Terry 2001, Cohen 2000, Verhoeven 1996, Sharma 1994, Wattenberg 1985, Wattenberg 1978). I3C has been shown to possess anti-tumorigenic and pro-apoptotic properties in a variety of cancer cell lines and animal models while completed clinical trials suggest it is beneficial for the treatment of breast and cervical cancer (Terry 2002, Bradlow 1991, Weng 2008, Del Priore 2009, Reed 2005, Dalessandri 2004, Terry 2001, Bell 2000).

Previous research in our lab demonstrated the potential of I3C as an anti-cancer therapeutic in the treatment of breast cancer. I3C induces a G1 cell cycle arrest of both estrogen-responsive and estrogen-unresponsive cell lines through alterations in cell cycle components including inhibition of the cyclin-dependent kinase 6 (CDK6) promoter, decreased enzymatic activity of CDK2 and CDK4, and alterations in cyclin E processing (Nguyen 2010, Nguyen 2008, Jump 2008, Garcia 2005, Firestone 2003, Cram 2001, Cover 1998). I3C also decreases tumor volume in breast cancer xenografts while inhibiting telomerase expression and hormonal signaling in the estrogen-responsive MCF-7 cell line through degradation of estrogen receptor alpha (ERα) (Marconett, 2011, Marconett 2010, Nguyen 2010, Sundar 2006). Recent work with the highly invasive MDA-MB-231 cell line revealed I3C directly binds to the serine protease human neutrophil elastase to reduce CDK2 enzymatic activity (Nguyen 2008). I3C inhibition of extracellular elastase prevents proteolytic cleavage of the tumor necrosis factor receptor, CD40 resulting in a regulatory cascade that disrupts cell survival and proliferative responses mediated by the transcription factor NFκB (Aronchik 2010). I3C can also suppress cell motility through Rho kinase activation and growth arrests the preneoplastic human mammary epithelial cell line, MCF-10A through stabilization of the tumor suppressor protein p53 (Brew 2009, Nguyen 2008, Brew 2006).

p53 is a transcription factor whose inactivation is often required for successful cancer progression (Olivier 2010, Juntilla 2009). Activation of p53 directly correlates with the regulation of genes involved in cell cycle progression, DNA repair and apoptosis including the cyclin-dependent kinase inhibitor p21, DNA polymerase pol κ, and the anti-apoptotic factor Bcl-2 (Caraval 2013, Riley 2008, Vogelstein 2000). Six studies in 2007 integrated the tumor suppressive microRNA family miR-34 into the p53 signaling pathway. MiR-34 consists of three isoforms (miR-34a, miR-34b and miR-34c) that post-transcriptionally regulate gene expression by inhibition of target mRNA (Bommer 2007, Chang 2007, Corney 2007, He 2007, Raver-Shapria 2007, Tarasov 2007). All three microRNA were significantly down-regulated in p53 mutant or null cell lines while a canonical p53 binding site was identified in the miR-34

promoters. Activation of p53 significantly increased miR-34 levels while luciferase assays in which the miR-34 binding site in the mRNA of potential target genes was attached to the firefly luciferase gene revealed miR-34's inhibition of known p53 repression targets such as Bcl-2. Researchers thus propose that upon activation in normal cells, p53 transcriptionally upregulates the miR-34 family to exert its repressive effects.

Activation of tumor suppressive microRNA could be a novel form of anti-cancer treatment (Wong 2011, Wong 2008). Imperfect base pairing between microRNA and its target mRNA sequence permit a single molecule to down-regulate the expression of thousands of genes and aberrant microRNA expression profiles have been associated with every type of analyzed cancer (Lujambio 2012, Friedman 2009, Croce 2006, Lewis 2005, Xie 2005). Previous research in our lab demonstrated that I3C mediated growth arrest in human preneoplastic mammary epithelial cells requires functional p53 (Brew 2006). I3C treatment increases ATM phosphorylation status independent of DNA damage, resulting in an increase in total as well as phosphorylated forms of p53, upregulated p21 levels and subsequent G1 cell cycle arrest. Transfection of dominant negative p53 reverses this effect suggesting that I3C mediated cell cycle arrest of this cell line is p53-dependent.

I3C activation of p53 could represent a novel means of up-regulating the miR-34 tumor suppressive family. This study demonstrates that I3C upregulates miR-34a in dose and time-dependent manner to growth arrest human preneoplastic and breast cancer cells. Functional p53 is required for miR-34a activation and miR-34a inhibition prevents I3C's restriction on cell proliferation.

MATERIALS & METHODS

Cell Culture

Cells were grown to sub-confluency in a humidified incubator at 37°C containing 5% CO2. MCF10A cells were maintained in Dulbecco modified Eagle medium (DMEM)-F-12 medium supplemented with 10% fetal bovine serum, penicillin/streptomycin (Cambrex/Biowhittaker, Walkersville, MD), 10ug/ml insulin (bovine), 0.1 µg/ml cholera toxin (Sigma Chemical, St. Louis, MO), recombinant epidermal growth factor (Promega, Madison, WI) and 0.5 µg/ml hydrocortisone (ICN Biochemical, Irvine, CA). The cell lines MCF10A-Neo (stably transfected with the retroviral vector, LTR-gene X-simian virus 40-Neo) and MCF10A-DNp53 (transfected with pLSXN-p53DD, a murine dominant-negative p53 construct from M. Oren) were described previously (Sheen 2002, Shaulian 1992). MCF-7 cell lines were cultured as described by the American Tissue Culture Collection (Manassas, VA). Cells were treated for the indicated time points in complete medium with I3C (Sigma-Aldrich, Milwaukee, WI) dissolved 1000X in DMSO (Sigma-Aldrich, Milwaukee, WI). Pure DMSO was used as a control. The medium was changed every 24 hours for the duration of each experiment.

Flow cytometry

For cell cycle analysis, attached and non-adherent cells treated in 6-well plates were collected within the media, rinsed with PBS and hypotonically lysed in 0.5 ml of propidium iodide buffer (0.5mg/ml propidium iodide, 0.1% sodium citrate, 0.05% Triton X-100). Samples were analyzed on a Beckman-Coulter (Fullerton, CA) EPICS XL flow cytometer with laser output adjusted to deliver 15 MW at 488 nm. Ten thousand cells were counted. Cell cycle analysis was then performed using MultiCycle software WinCycle 32 (Phoenix Flow Systems, San Diego, CA).

RNA extraction

Cells were harvested in 1.0 ml TRIzol reagent (Invitrogen, Carlsbad, CA) and total RNA extracted following the manufacturer's protocol with the phase separation procedure being performed twice to extract microRNA. Removal of contaminating DNA was performed on 10µg of extracted RNA using a DNA-free Kit (Invitrogen, Carlsbad, CA) per the manufacturer's protocol. RNA integrity was confirmed by running a 1.5% formaldehyde (Sigma Chemical, St. Louis, MO) denaturing agarose gel (Invitrogen, Carlsbad, CA) using 1µg of RNA per sample and visualizing intact bands corresponding to the molecular weights of the 28S and 18S subunits of ribosomal RNA, the most abundant RNA species. Gels contained GelRed Nucleic Acid Gel Stain (Biotium, Hayward, CA) diluted to a 2X concentration for band visualization using short wavelength ultraviolet light.

Reverse Transcription and PCR

Total RNA was reverse transcribed using stem loop primers for miR-34a, miR-34b and miR-34c as well as random primers for GAPDH, a housekeeping gene insensitive to I3C treatment. Each reverse transcriptase reaction contained 10XRT buffer, 100mM dNTPS, 50U/µl MultiScribe reverse transcriptase, and 20U/µl RNAse inhibitor (Applied Biosystems, Foster City, California) dissolved in nuclease-free water. The reverse transcription reaction for GAPDH contained 100ng of purified total RNA as well as 10X random primers while the reaction for microRNA reverse transcription contained 560ng of purified total RNA and 5X miR-34a stem-loop RT primer (Applied Biosystems, Foster City, California). The microRNA reactions were incubated in a thermal cycler for 30 minutes at 16°C, 30 minutes at 42°C, and 5 minutes at 85°C while reactions for the control gene were incubated for 10 minutes at 25°C, 120 minutes at 37°C, and 5 minutes at 85°C.

Real-time PCR reactions for each miRNA (10 µl volume) were performed in triplicate, and each reaction mixture included 4 µl of diluted RT product (1:2 dilution), 5 µl of 2X TaqMan Universal PCR Master Mix, 0.2 µM TaqMan probe, 1.5 µM forward primer, 0.7 µM reverse primer with the probes and primers specific to mature miR-34a, mature miR-34b, mature miR-34c or human GAPDH (Applied Biosystems, Foster City, CA). Reactions were incubated in an Applied Biosystems 7900HT Fast Real-Time PCR system in 96-well plates at 95°C for 10 min, followed by 40 cycles at 95°C for 15 seconds and 60°C for 1 min. Changes in fluorescence levels of miR-34 were normalized to GAPDH, and fold changes compared between the target sample (miR-34 levels in cells treated with I3C) and calibrator samples (miR-34 levels in DMSO treated cells).

Qualitative PCR reactions (50µl volume) employed 1.5ug of purified RNA and a reaction mixture of 10X PCR Master Mix, 2.5mM dNTP mixture, 10pmol forward primer, 10pmol reverse primer and .25µl Taq DNA polymerase (Applied Biosystems, Foster City, CA). The following primer sets and conditions were used:
pri-34a_Forward: 5'-CGTCACCTCTTAGGCTTGGA-3'
pri-34a_Reverse: 5'-CATTGGTGTCGTTGTGCTCT-3'
Sirt-1_Forward:5'-TGGCAAAGGAGCAGATTAGTAGG -3'
Sirt-1_Reverse: 5'- CTGCCACAAGAACTAGAGGATAAGA-3'
MDM4_Foward: 5'-ATCTGACAGTGCTTGCAGGA-3'
MDM4_Reverse: 5'- GCTGCATGCAAAATCTTCAA-3'
c-Myc_Forward: 5'- CCTCGGATTCTCTGCTCTC-3'
c-Myc_Reverse: 5'-TTCTTGTTCCTCCTCAGAGTC -3'
N-Myc_Forward: 5'-CTTCGGTCCAGCTTTCTCAC -3'
N-Myc_Reverse: 5'- TCTTGCCTGCAATTTTTCCT-3'
Gapdh_Forward: 5'-GAAGGTGAAGGTCGGAGTC-3'
Gapdh_Reverse: 5'-GAAGATGGTGATGGGATTTC-3'

GAPDH: 45s at 94°C, 30s at 94°C, 1 min at 72°C for 27 cycles, pri-34a and SIRT-1: 30s at 95°C, 30s at 55°C, 30s at 68°C for 38 cycles, c-Myc: 30s at 95°C, 30s at 53°C, 30s min at 68°C for 35 cycles, N-Myc: 30s at 95°C, 30s at 52°C, 30s at 68°C for 35 cycles, MDM4: 30s at 95°C, 30s at 51°C, 30s at 68°C for 35 cycles. All PCR products were combined with 6X DNA loading dye, fractionated by electrophoresis on a 1.5% agarose gel containing .01% GelRed Nucleic Acid Gel Stain (Biotium, Hayward, CA)and visualized with an ultraviolet transilluminator.

Immunoblotting

Cell extracts were harvested in RIPA lysis buffer containing inhibitors, and standardized to 20-30ug protein using the Bradford protein assay. Equal protein amounts were subjected to SDS-PAGE on an 8% or 10% poly-acrylamide gel, transferred onto nitrocellulose membranes, and incubated for 1 hour at room temperature with blocking solution (5% milk dissolved in TBST). Primary antibodies to p53, p53 phosphorylated at serine residue 15 (Cell Signaling Technology, Beverly, MA) p21, actin, CDK4 and CDK6 (Santa Cruz Biotechnologies, Santa Cruz, CA) were incubated overnight at 4°C. After three washes in 5% milk dissolved in TBST, membranes were incubated with anti-mouse or anti-rabbit horseradish peroxidase-conjugated antibodies for 1.5 hours at room temperature. Following an additional five washes in 5% milk, chemo luminescent signals were generated by incubation with Western Lightning ECL reagents according to the manufactures instructions (Perkin Elmer, Shelton, CT) and the results transferred to ECL-sensitive film (GE Healthcare, United Kingdom). Phosphorylated proteins were incubated and washed in TBST instead of 5% milk.

Transfections and Luciferase Assay

100nM miR-34a or control locked nucleic acid inhibitors (Exiqon, Woburn, MA) were transfected according to the manufacturer's instructions into MCF-7 cells with Lipofectamine 2000 reagent (Applied Biosystems, Mountain View) while 2µg dominant negative p53 or miR-34a promoter plasmids were transfected using Superfect reagent (Qiagen, Germantown, Maryland). Upon overnight incubation, cells containing the miR-34a promoter were treated with or without 200µM I3C for 24, 48 or 72 hours and harvested in ice-cold PBS. The cells were then centrifuged at 14,000 rpm for 5 minutes at 4°C, combined with 1X Passive lysis buffer, and Promega Luciferase assay performed according to the manufacturer's instructions (Promega, San Luis Obispo, CA). Relative light units were normalized to protein expression as determined by the Bradford protein assay. Dominant negative p53 was purchased from Clontech Laboratories (Mountain View, CA) while miR-34a promoter plasmids were a kind gift of Dr. Xueqing Xu, Third Military Medical University (Chongqing, China).

Cell Proliferation Assay

MCF-7 cells were seeded in 24-well plates at 50% confluence and upon overnight incubation, 100nM miR-34a or control locked nucleic acid inhibitors transfected into cells with Lipofectamine 2000 reagent (Applied Biosystems, Mountain View, CA). The culture medium was replaced with fresh medium 24 hours later containing either 200μM I3C or DMSO with a second treatment occurring at 48 hours. Cells were then subjected to the CCK-8 Cell Counting Proliferation Assay (Dojindo Molecular Technologies Inc, Rockville, MD) according to the manufacturer's instructions in which the amount of orange-colored formazan dye generated by dehydrogenase reduction of tetrazolium salt is directly proportional to the number of living cells.

RESULTS

I3C upregulates miR-34a under conditions of cell cycle arrest in human preneoplastic and breast cancer cells

To assess the possibility of I3C regulation of miR-34 family expression under conditions of cell cycle arrest, the human preneoplastic mammary epithelial cell line MCF-10A and human breast cancer cell line MCF-7 were treated with I3C or the vehicle control DMSO under conditions optimized for cell cycle arrest. Upon treatment with 300μM (MCF-10A) or 200μM (MCF-7) I3C for 24, 48 and 72 hours, the propidium-iodide stained DNA content of each sample was assessed for specific stages of the cell cycle by flow cytometry analysis. Maximal cell cycle arrest without cell death was obtained at 48 hours (Figure 1A-1B). I3C treatment at 48 hours caused a 16.9%-25% arrest in the G1 phase of the cell cycle with a concomitant decrease in cells within the G2/M phase for MCF-10A cells or S phase for MCF-7 cells (Figure 1C). Cells also arrested at 72 hours, however, phenotypic changes characteristic of cell death (blebbing, floating cells, sub-G1 peak in the flow cytometry profile) become apparent (Figure 1A-1B) Thus, I3C treatment at 48 hours maximally growth arrests MCF-10A and MCF-7 cells in the G1 phase of the cell cycle without observed cell death.

Taqman semi quantitative RT-PCR was performed on purified RNA extracted from I3C or DMSO treated cells to assess the levels of mature miR-34a. Taqman qPCR is one of the most commonly used means of detecting mature microRNA levels, given its high specificity and ability to resolve as few as seven copies of mature microRNA in a PCR reaction (Chen 2005, Heid 1996). Total RNA was reverse transcribed using stem loop primers for miR-34a, miR-34b and miR-34c and the cDNA amplified in real-time using primers and dual-labeled fluorogenic probes specific to miR-34 or GAPDH, a housekeeping gene insensitive to I3C treatment. Changes in fluorescence levels of miR-34a were normalized to GAPDH, and fold changes compared between the target sample (miR-34 levels in I3C treated cells) and calibrator samples (miR-34 levels in DMSO treated cells). I3C treatment caused a greater than two-fold increase in miR-34a levels at 48 hours in both MCF-10A and MCF-7 cells (Figure 2A-2B**).** I3C treatment also upregulated miR-34b and miR-34c levels in MCF-10A cells while levels of miR-34b and miR-34c were minimally altered and undetected in MCF-7 cells.

In semi-quantitative PCR, a fold change indicates the difference in how many doublings of gene amplicons occurred within the target vs. calibrator samples (Livak 2001). A fold change of two indicates the target sample contains twice as many amplicons as the calibrator and is considered the significance threshold in microRNA research (He 2007, Croce 2006, Iorio 2005). I3C upregulated miR-34a greater than two-fold in MCF-7 and MCF-10A cells, implicating miR-34a is significantly affected by I3C treatment and could play a critical role in I3C mediated cell cycle arrest in human preneoplastic and breast cancer cells.

Figure 1. I3C growth arrests human breast cancer cells.
A) MCF-10A cells were treated with or without 300μM I3C for 24, 48 and 72 hours and subjected to flow cytometry analysis of the cell cycle as described in "Materials and Methods." The bar graphs indicate the average DNA content corresponding to the phases of the cell cycle as detected in three independent experiments and error bars represent standard deviation. The presence of cell death as indicated by visual observation of cellular blebbing or a sub-G1 peak in the flow cytometry profile at each time point are indicated by a + or - mark.
B) MCF-7 cells were treated with or without 200μM I3C for 24, 48 and 72 hours and subjected to flow cytometry analysis of the cell cycle as described in "Materials and Methods."The bar graphs indicate the average DNA content corresponding to the phases of the cell cycle as detected in three independent experiments and error bars represent standard deviation. The presence of cell death as indicated by visual observation of cellular blebbing or a sub-G1 peak in the flow cytometry profile at each time point are indicated by a + or - mark.
C) Representative flow cytometry profiles for cells treated for 48 hours with or without I3C at concentrations of 200μM (MCF-7) or 300μM (MCF-10A). **D)** MCF-7 cells were treated for 48 hours with or without the indicated concentrations of I3C for 48 hours. The bar graphs indicate the average DNA content corresponding to the phases of the cell cycle as detected in three independent experiments and error bars represent standard deviation.

Figure 1A

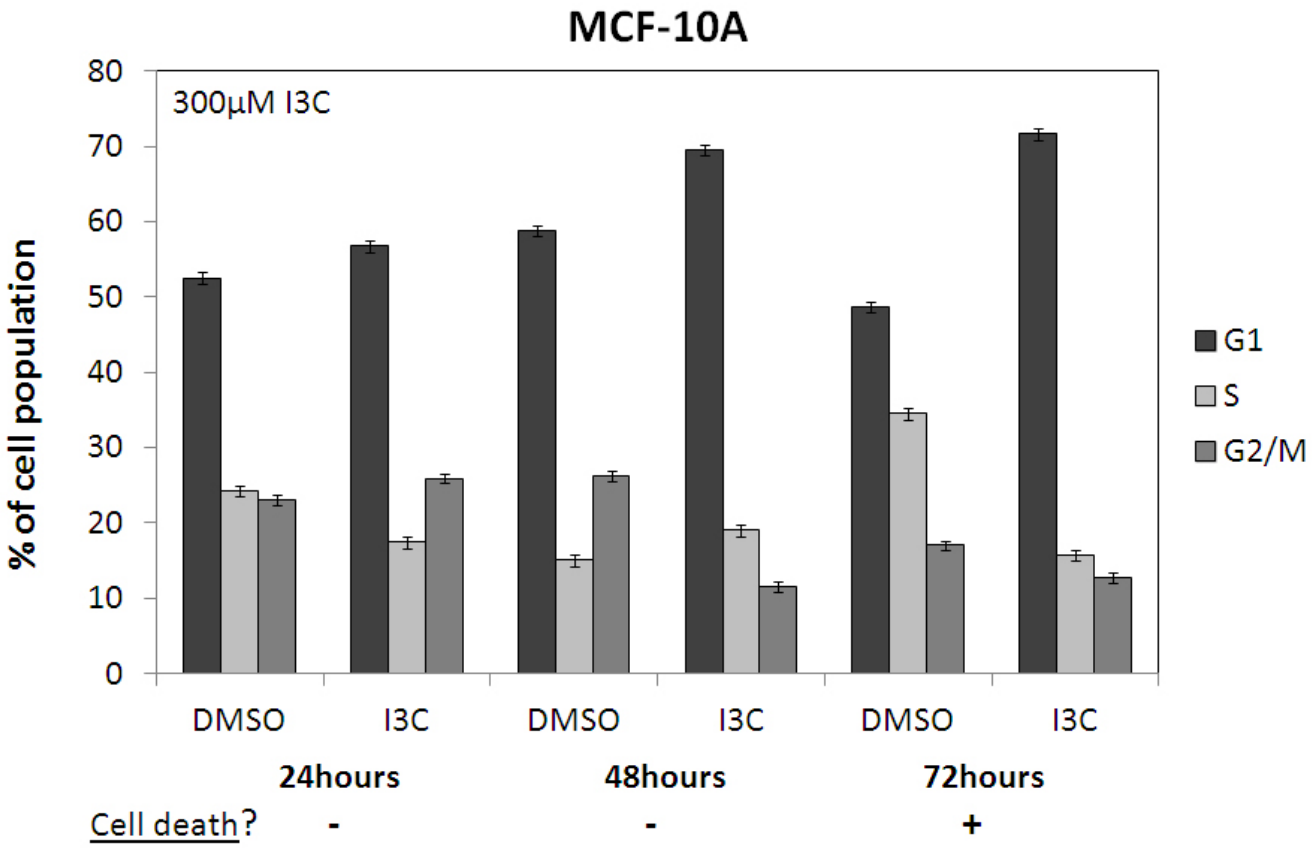
MCF-10A
300µM I3C
% of cell population
80
70
60
50
40
30
20
10
0
G1
S
G2/M
DMSO
I3C
DMSO
I3C
DMSO
I3C
24hours
48hours
72hours
Cell death?
-
-
+

Figure 1B

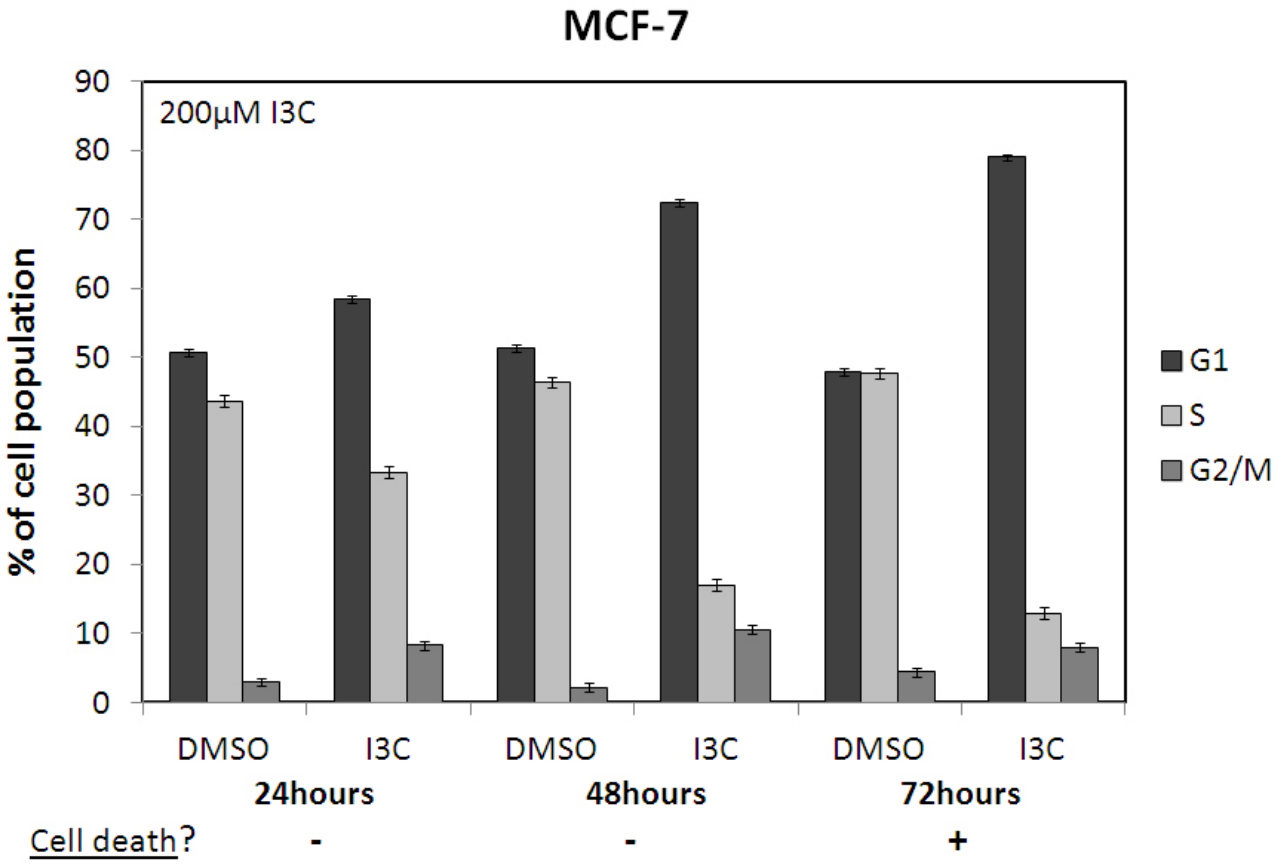
MCF-7
200µM I3C
% of cell population
90
80
70
60
50
40
30
20
10
0
DMSO
I3C
DMSO
I3C
DMSO
I3C
24hours
48hours
72hours
Cell death?
-
-
+
G1
S
G2/M

Figure 1C

48 hours

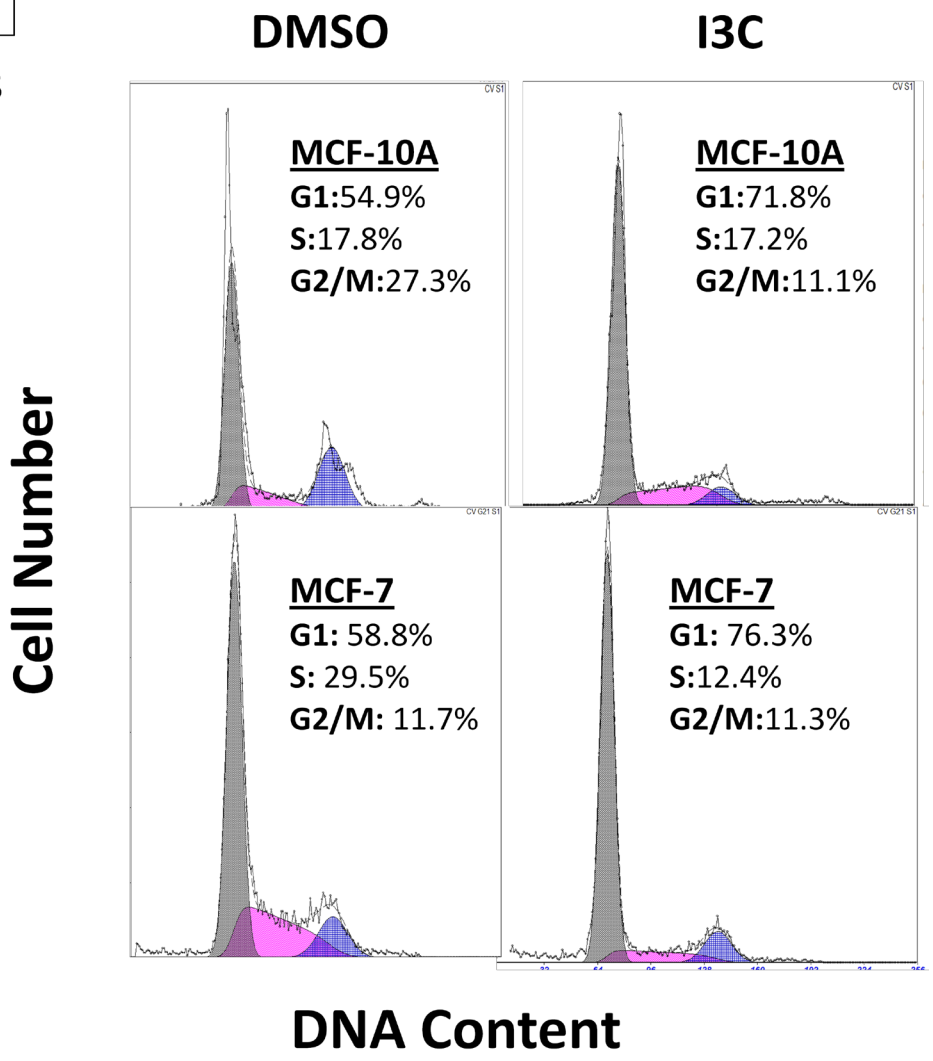

Figure 1D

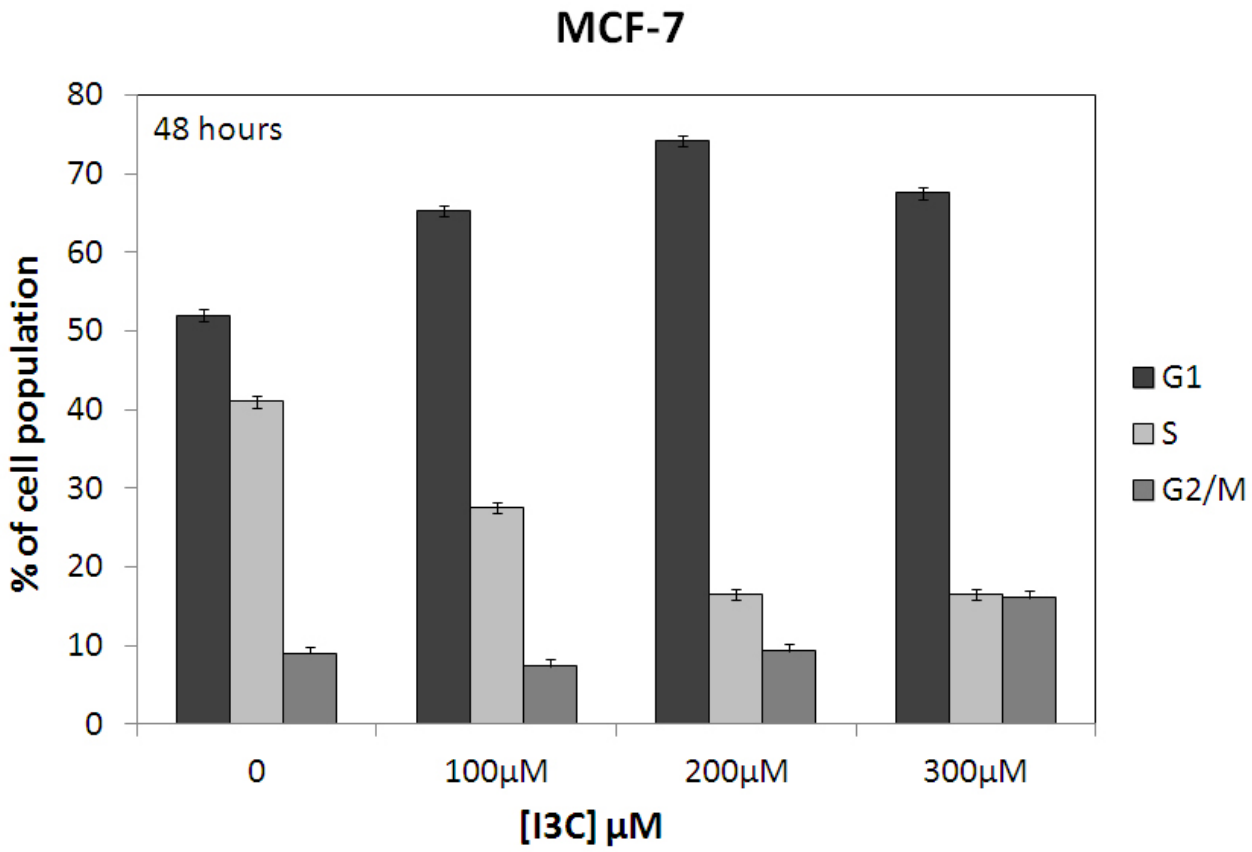
MCF-7
48 hours
% of cell population
80
70
60
50
40
30
20
10
0
0
100µM
200µM
300µM
[I3C] µM
G1
S
G2/M

Figure 2. I3C treatment upregulates miR-34a in a time dependent manner.
A) MCF-10A cells were treated with or without 300μM I3C for the indicated time points. Reverse transcription with stem-looped primers for each member of the miR-34 family or random primers for GAPDH was performed on purified RNA extracts followed by Taqman semi-quantitative PCR using dual-labeled fluorogenic probes for mature miR-34a, miR-34b, miR-34c and GAPDH, a housekeeping gene insensitive to I3C treatment. Triplicate results were normalized to expression of GAPDH and bar graphs represent average fold change in miR-34a, miR-34b and miR-34c levels as determined in three independent experiments. Dotted line represents the two-fold significance threshold of microRNA experiments and error bars indicate standard deviation.
B) MCF-7 cells were treated with or without 200μM I3C for the indicated time points and Taqman qPCR performed as described above. Triplicate results were normalized to expression of GAPDH and bar graphs represent average fold change in miR-34a and miR-34b levels as determined in three independent experiments. miR-34c was undetected. The dotted line represents the two-fold significance threshold of microRNA experiments and error bars indicate standard deviation.

Figure 2A

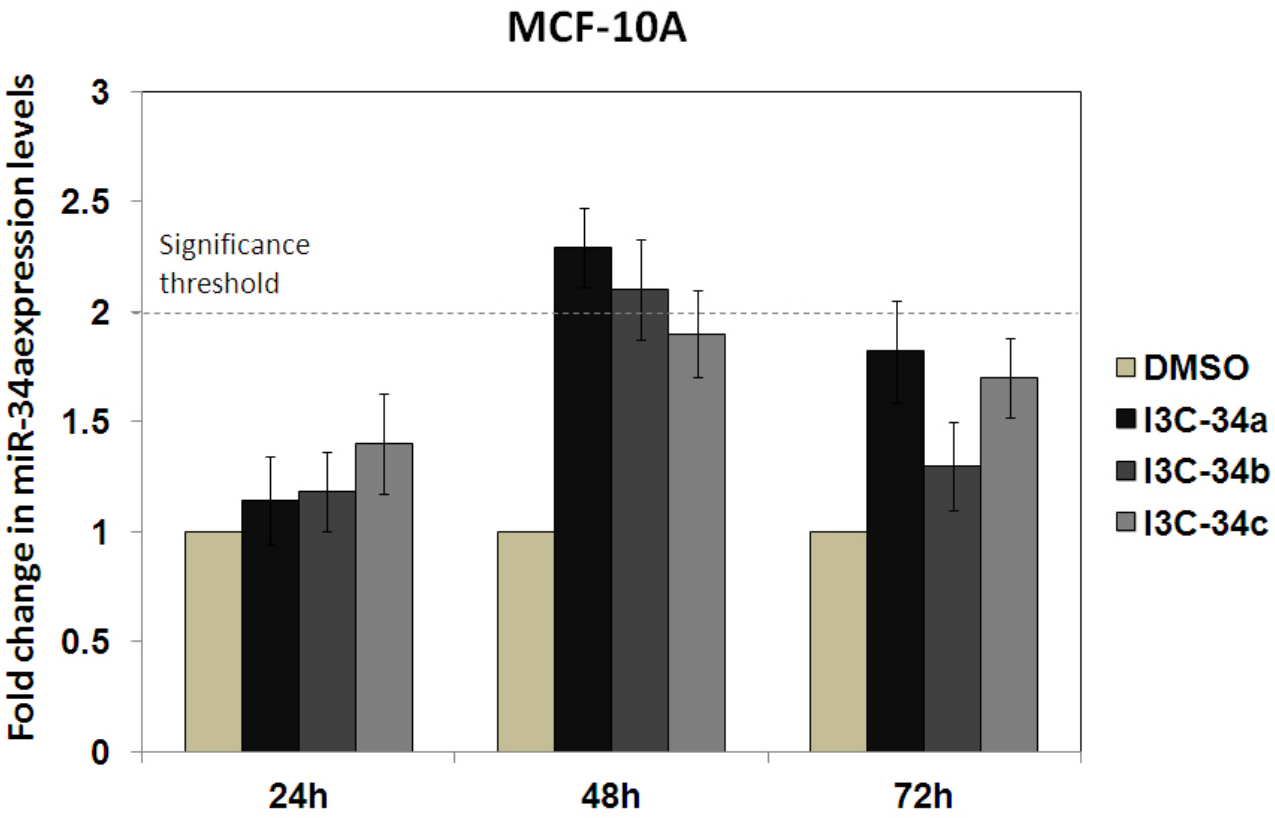
MCF-10A
Fold change in miR-34aexpression levels
3
2.5
2
1.5
1
0.5
0
Significance threshold
24h
48h
72h
DMSO
I3C-34a
I3C-34b
I3C-34c

Figure 2B

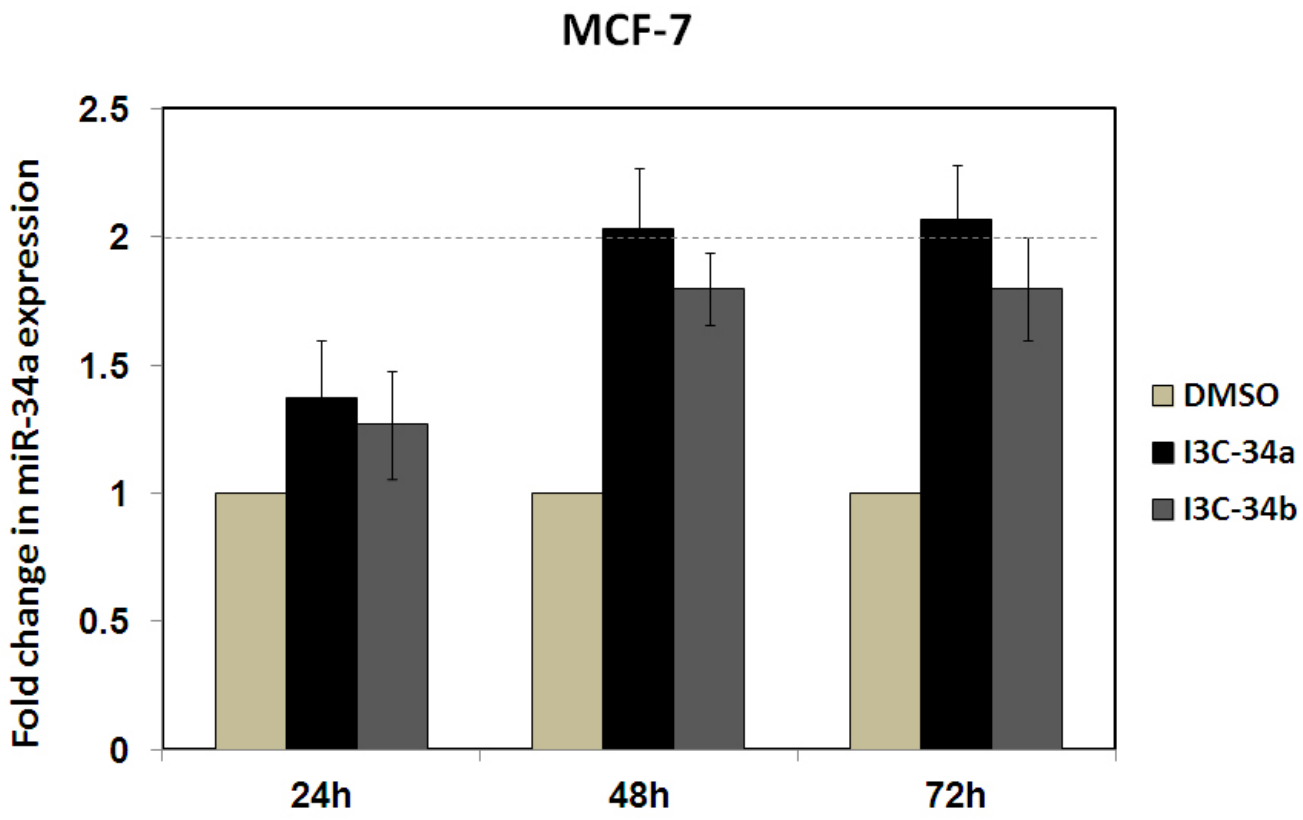
MCF-7
Fold change in miR-34a expression
2.5
2
1.5
1
0.5
0
24h
48h
72h
DMSO
I3C-34a
I3C-34b

I3C dose dependently induces miR-34a levels in MCF-7 cells. Taqman qPCR performed on RNA extracts of cells treated with 100μM, 200μM or 300μM I3C for 48 hours revealed I3C increased miR-34a levels 1.5 to three-fold respectively (Figure 3**)**. Each dose also caused cells to arrest in the G1 phase of the cell cycle **(**Figure 1D) with 200μM I3C inducing the greatest cell cycle arrest. miR-34c was undetected while miR-34b levels were only significantly upregulated with 300μM I3C.

I3C upregulates p53 levels and downregulates cell cycle proteins in human breast cancer cells

Previous research in our lab indicated I3C upregulated levels of total and phosphorylated p53 in growth-arrested human mammary epithelial cells (Brew 2006). To determine if I3C also regulates p53 levels in human breast cancer cells, Western blot analysis was performed on protein extracts of MCF-7 cells treated with or without increasing concentrations of I3C or 200μM I3C for 24, 48 and 72 hours. I3C treatment increased levels of total p53, p53 phosphorylated at serine 15 and the p53 transcriptional target, p21 in a time and dose-dependent manner (Figure 4). p53 could play an important role in I3C mediated miR-34a regulation in MCF-7 cells as the dose and time-dependent upregulation correlates with the induction profile of miR-34a (Figure 2B, Figure 3).

Western blot analysis also indicated a decrease in protein levels of the cyclin-dependent kinase, CDK6 at all time points as well as 200μM and 300μM I3C treatment while CDK4 levels did not change (Figure 4). CDK6 phosphorylates the retinoblastoma protein to regulate the G1 to S phase transition in the cell cycle (Reed 1997). It is also a known transcriptional target of miR-34a suggesting miR-34a could be inducing I3C mediated cell cycle arrest through CDK6 inhibition (Hermeking 2007).

Functional p53 is required for I3C induction of miR-34a

miR-34a is a known transcriptional target of p53. To investigate a possible link between I3C induction of p53 and regulation of miR-34a, MCF-10A and MCF-7 cells were transiently transfected with dominant negative p53 (DNp53) or an empty neomycin control vector (Neo). Upon overnight incubation, transfected cells were treated with or without 300μM (MCF-10A) or 200μM (MCF-7) I3C for 48 hours. Western blot analysis revealed dominant negative p53 expression prevented I3C upregulation of p53 in both cell lines (Figure 5B). I3C treatment upregulated mature miR-34a levels greater than two fold in MCF-10A-Neo and MCF-7-Neo cells as detected by quantitative PCR yet such expression was severely ablated in either cell line containing dominant negative p53 (Figure 5A). Such data suggests that functional p53 is necessary for I3C mediated regulation of miR-34a in preneoplastic and human breast cancer cells.

Figure 3. I3C regulation of miR-34a is dose-dependent in human breast cancer cells. MCF-7 cells were treated with or without indicated concentrations of I3C for 48 hours and Taqman qPCR performed as described in "Materials and Methods." Triplicate results were normalized to expression of GAPDH and bar graphs represent average fold change in miR-34a and miR-34b levels as determined in three independent experiments. miR-34c was undetected. The dotted line represents the two-fold significance threshold of microRNA experiments and error bars indicate standard deviation.

Figure 3

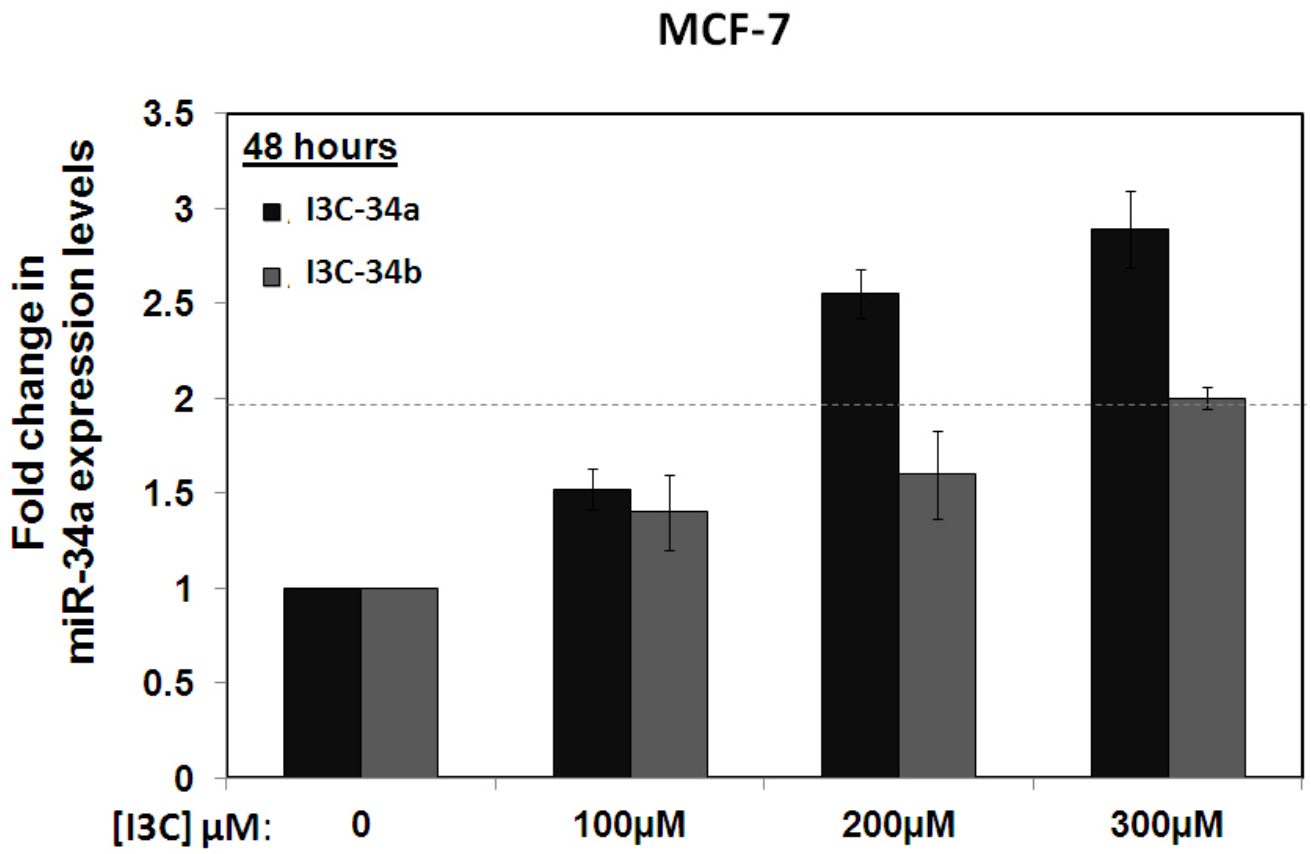
MCF-7
48 hours
I3C-34a
I3C-34b
Fold change in miR-34a expression levels
3.5
3
2.5
2
1.5
1
0.5
0
[I3C] µM:
0
100µM
200µM
300µM

Figure 4. I3C upregulates p53 levels while downregulating cell cycle proteins. MCF-7 cells were treated with or without I3C at the indicated concentrations or time points and protein levels of p53, p53 phosphorylated at serine 15 (p53.s15), p21, CDK4 and CDK6 determined by Western blot as described in "Materials and Methods." Actin was used as a loading control.

Figure 4

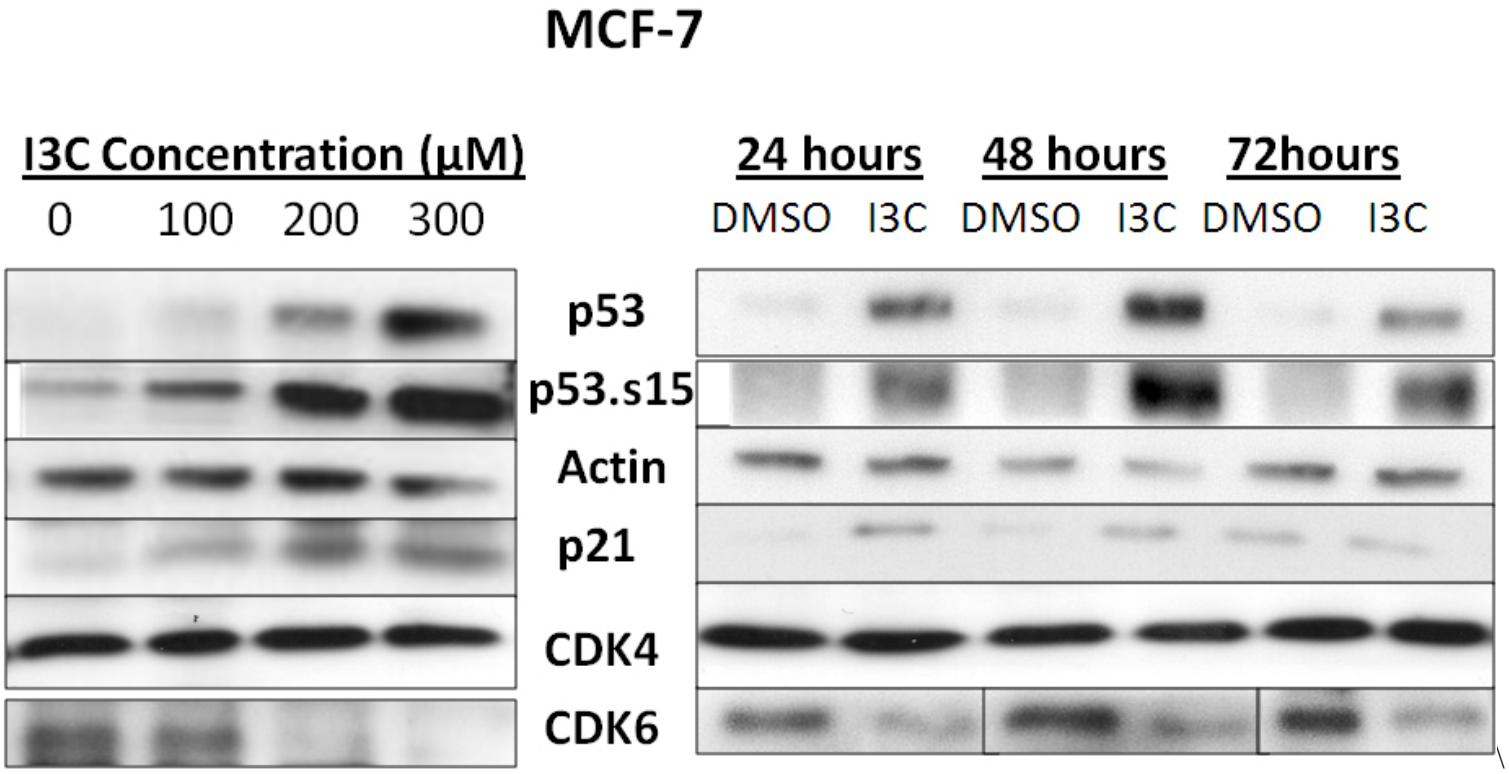
MCF-7
I3C Concentration (µM)
0
100
200
300
24 hours
48 hours
72hours
DMSO
I3C
DMSO
I3C
DMSO
I3C
p53
p53.s15
Actin
p21
CDK4
CDK6

Figure 5. Functional p53 is required for I3C induction of miR-34a.
MCF-10A and MCF-7 cells were transfected with dominant negative p53 (10A-DNp53, MCF-7-DNp53) or an empty vector control (10A-Neo, MCF-7-Neo). Upon overnight incubation, transfected cells were treated with or without I3C at concentrations of 200μM (MCF-7) or 300μM (MCF-10A) for 48 hours and total RNA and protein harvested. **A)** Taqman semi-quantitative PCR analysis was performed on RNA extracts to detect mature miR-34a levels as described in "Materials and Methods." Triplicate results were normalized to expression of GAPDH and bar graphs represent average fold change in miR-34a levels as determined in three independent experiments. Dotted line represents the two-fold significance threshold of microRNA experiments and error bars indicate standard deviation. **B)** p53 protein levels were determined by Western blot analysis as described in "Materials and Methods" using actin as a loading control.

Figure 5

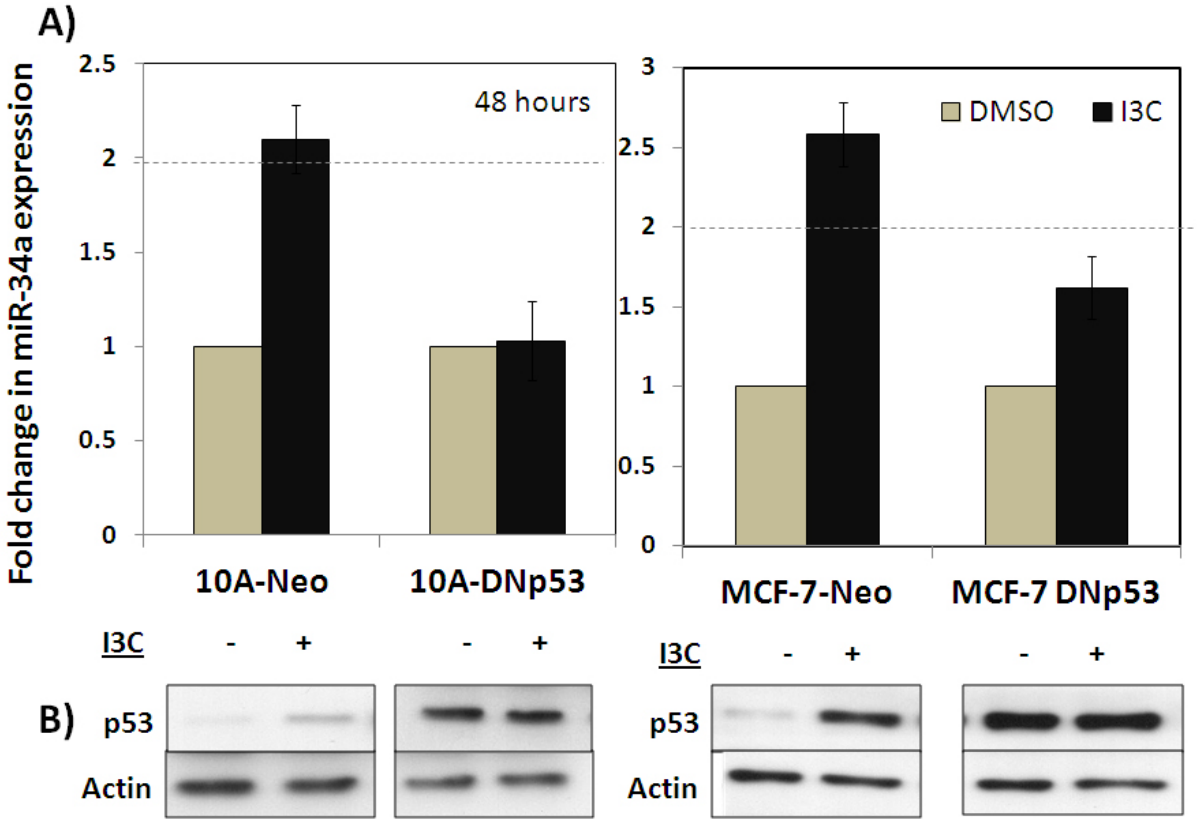
A)
Fold change in miR-34a expression
48 hours
DMSO
I3C
2.5
2
1.5
1
0.5
0
3
2.5
2
1.5
1
0.5
0
10A-Neo
10A-DNp53
MCF-7-Neo
MCF-7 DNp53
I3C
-
+
-
+
I3C
-
+
-
+
B)
p53
Actin
p53
Actin

I3C inhibits expression of the miR-34a promoter while primarymiR-34a transcript levels do not change

I3C regulation of the miR-34a promoter could be responsible for the observed increase in mature miR-34a levels. To investigate this possibility, MCF-7 cells were transfected with or without a segment of the miR-34a promoter containing the canonical p53 binding site inserted upstream of the luciferase gene. A vector expressing luciferase under the control of an unregulated promoter or an empty neomycin vector were used as positive and negative controls respectively. Upon transfection, cells were treated with or without 200μM I3C for 24, 48 or 72 hours and a luciferase assay performed on the harvested cells. Normalized luciferase activity revealed I3C does not upregulate the miR-34a promoter at time points correlating with an increase in mature miR-34a (Figure 6A). Promoter expression does not change at 24hours yet decrease at 48 and 72hours when mature miR-34a levels are at their peak (Figure 2B, 6A). This suggests that I3C treatment mildly inhibits the miR-34a promoter and upregulates mature miR-34a levels through alternate means.

microRNA undergo two processing steps before reaching the maturation stage. They are transcribed as long primary transcripts (pri-miRNA) containing multiple microRNA copies that are cleaved in the nucleus to produce a single stem-looped precursor molecule (pre-miRNA). Upon entry into the cytoplasm, one strand of the pre-miRNA is degraded and the resulting single stranded mature microRNA loaded in the RNA induced silencing complex to prevent translation of target mRNA sequences. I3C treatment could upregulate mature miR-34a levels by altering microRNA processing. To investigate this possibility, qualitative PCR analysis was performed using primers for pri-miR-34a on RNA extracts in which mature miR-34a levels were confirmed to be upregulated by I3C. Gel electrophoresis of the PCR products revealed pri-34a levels remain the same while mature miR-34a levels increase in a dose and time-dependent manner (Figure 6B). This suggests that I3C does not transcriptionally regulate miR-34a gene expression but alters microRNA biogenesis to increase mature miR-34a levels.

Loss of functional miR-34a reverses I3C mediated growth inhibition

To determine if miR-34a is critical for I3C inhibition of cell proliferation, MCF-7 cells were transfected with locked nucleic acid inhibitors (LNA) against miR-34a. LNA's are non-translatable microRNA targets that reduce microRNA function by sequestering their target microRNA in highly stable heteroduplexes. They exhibit higher affinity for a target microRNA than its endogenous mRNA targets and have minimal effects on total microRNA levels. MCF-7 cells were transfected with 100nM miR-34a inhibitor or a non-specific control inhibitor, and upon overnight incubation, treated with or without 200μM I3C for 48 hours. Cell viability was then assessed by the Cell Counting Kit-8 proliferation assay which correlates formazan dye formation to cell viability. Normalized dye absorbance showed I3C reduced viability in cells transfected with the control inhibitor by 25% yet had no effect on LNA transfected cells (Figure 7A). Such data suggests that functional miR-34a is required for I3C mediated growth inhibition.

Figure 6. I3C inhibits expression of the miR-34a promoter while primary miR-34a transcript levels do not change. A) MCF-7 cells were transfected with or without a segment of the miR-34a promoter containing the canonical p53 binding site inserted upstream of the luciferase gene. Upon overnight incubation, cells were treated with or without 200μM I3C for the indicated time points and a luciferase assay performed on the harvested cells as described in "Materials and Methods." Relative light units were normalized to protein expression as detected by the Bradford protein assay. **B)** The transcript levels of primary miR-34a (pri-34a) and GAPDH were determined by qualitative RT-PCR analysis using specific primers as described in "Materials and Methods." Products were fractionated by electrophoresis on a 1.5% agarose gel and visualized with an ultraviolet transilluminator. GAPDH was used as a loading control. Fold change in mature miR-34a levels as detected by Taqman qPCR analysis of the same RNA extracts is indicated.

Figure 6A

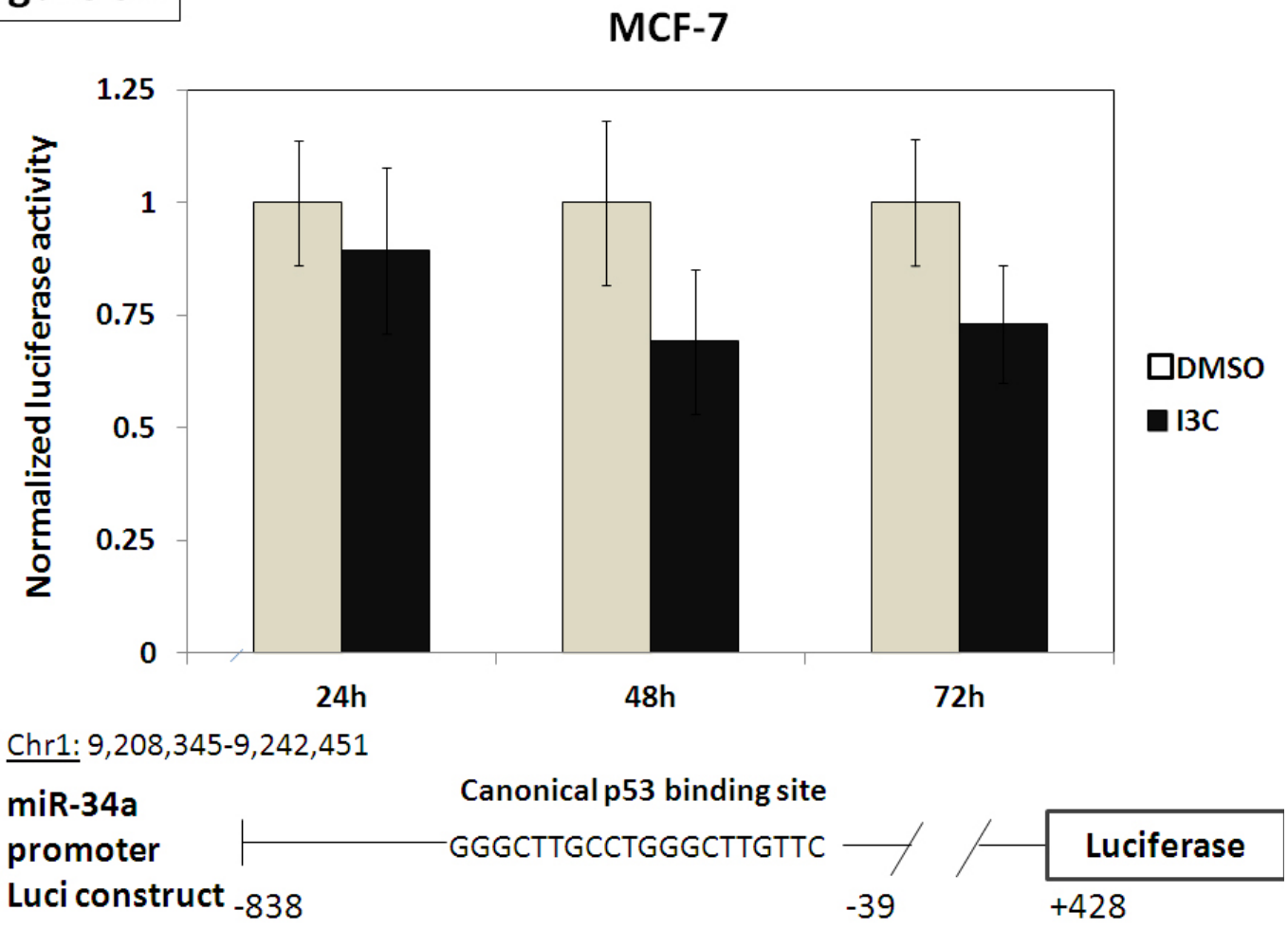
MCF-7
Normalized luciferase activity
1.25
1
0.75
0.5
0.25
0
24h
48h
72h
DMSO
I3C
Chr1: 9,208,345-9,242,451
miR-34a promoter Luci construct
Canonical p53 binding site
GGGCTTGCCTGGGCTTGTTC
Luciferase
-838
-39
+428

Figure 6B

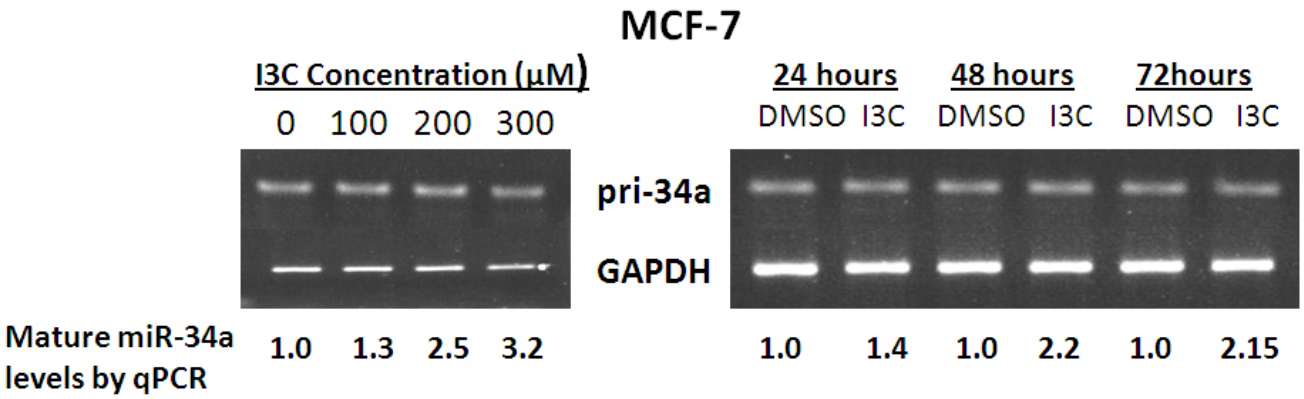
MCF-7
I3C Concentration (μM)
0 100 200 300
24 hours
48 hours
72hours
DMSO I3C DMSO I3C DMSO I3C
pri-34a
GAPDH
Mature miR-34a levels by qPCR
1.0 1.3 2.5 3.2
1.0 1.4 1.0 2.2 1.0 2.15

Figure 7. Loss of functional miR-34a reverses I3C mediated growth inhibition. A) MCF-7 cells were transfected with 100nM control or locked nucleic acid inhibitors (LNA's) against miR-34a and upon overnight incubation, treated with or without 200μM I3C for 48 hours. LNA's are non-translatable microRNA targets that reduce microRNA function by sequestering their target microRNA in highly stable heteroduplexes. Cell viability was then assessed by the Cell Counting Kit-8 proliferation in which formazan dye formation directly correlates with cell viability. The assay was performed as described in "Materials and Methods" and bar graphs represent average cell viability as determined from three independent experiments. Error bars indicate standard deviation. **B)** Western blot analysis was performed on protein extracts from cells transfected with or without miR-34a inhibitors and treated with DMSO or 200μM I3C for 48 hours. Antibodies specific to CDK6, p53, p53 phosphorylated at serine 15 (p53.s15), and actin were used and the procedure performed as described in "Materials and Methods." Actin was used as a loading control.

Figure 7A

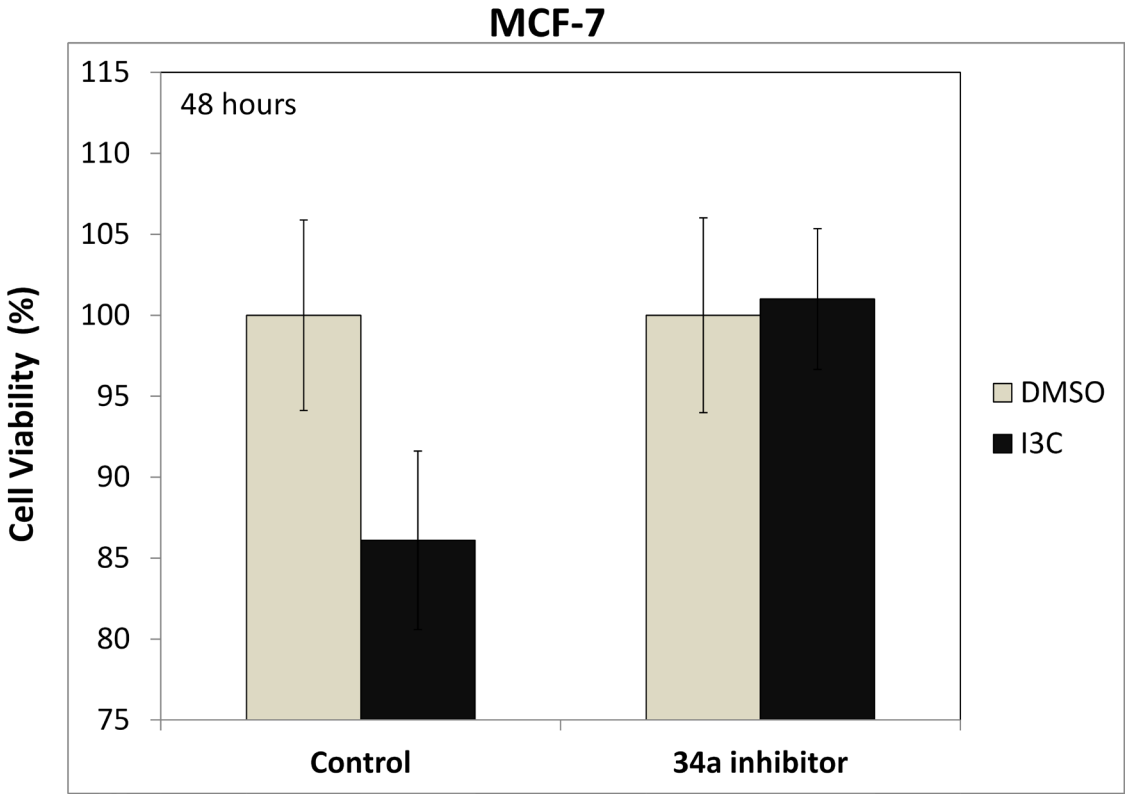
MCF-7
48 hours
Cell Viability (%)
115
110
105
100
95
90
85
80
75
Control
34a inhibitor
DMSO
I3C

To determine the molecular mechanism by which miR-34a induces I3C mediated cell cycle arrest and growth inhibition, potential gene targets were screened via Western blot and RT-PCR. Western blot analysis of miR-34a target gene expression in I3C treated LNA transfected cells showed no change in I3C regulation of total and phosphorylated p53 as well as the cyclin-dependent kinase and G1 cell cycle mediator, CDK6 (Figure 7B). I3C treatment of both control and LNA-miR-34a transfected cells decreased CDK6 protein levels while up-regulating total p53 and p53 phosphorylated at serine 15. This suggests that miR-34a does not inhibit CDK6 nor effects p53 stabilization to induce its I3C mediated effects.

Additional miR-34a target genes involved in cell proliferation were screened by RT-PCR analysis using primers specific to N-Myc, c-Myc, SIRT-1, HDMX and GAPDH as a loading control. N-Myc and c-myc are oncogenic transcription factors that promote cell proliferation by increasing expression of target genes including cyclin D1, cyclin E, and the epidermal growth factor receptor (EGFR) (Perini 2005, Dang 1999). Luciferase analysis and miR-34 over-expression assays indicate miR-34b/c and miR-34a directly inhibit c-Myc and N-myc to induce a G1 cell cycle arrest in human cancer cell lines (Wei 2008, Cole 2008, Leucci 2008, Lujambio 2008). miR-34a can also inhibit cell proliferation by enhancing p53 activity through repression of the NAD-dependent deacetylase, SIRT-1 and the p53 binding protein MDM4 (He 2007, Markey 2008 from Hermeking, Arhana 2011, Luan 2010, Zhao 2010, Yamakuchi 2009, Yamakuchi 2008, Fujita 2008).

RT-PCR analysis suggest I3C downregulates N-Myc in a dose dependent manner while having no effect on c-Myc and the p53 inhibitors, MDM4 and Sirt-1 (Figure 8A). N-Myc could be a potential target of miR-34a regulation as the doses in which N-Myc expression is fully ablated correlate with the greatest induction of miR-34a by I3C. RT-PCR analysis of cells treated with 200μM I3C for 24, 48 and 72 hours further confirmed I3C down-regulation of N-Myc at the time points of greatest miR-34a induction (Figure 8B). To determine if miR-34a is responsible for I3C inhibition of N-Myc expression, RT-PCR analysis was performed on RNA extracts of MCF-7 cells transfected with a control or miR-34a inhibitor and treated with 200μM I3C for 48 hours. I3C decreased N-Myc expression in both control and LNA transfected cells, indicating that functional miR-34a is not required for I3C regulation of N-Myc expression (Figure 9). All of these data suggest that miR-34a is critical for I3C mediated inhibition of cell proliferation however the molecular mechanism is yet to be determined.

Figure 7B

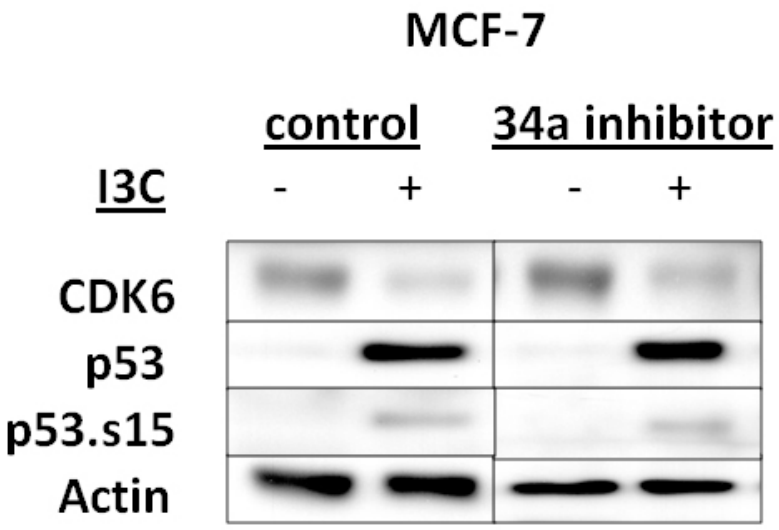

Figure 8. I3C downregulates N-Myc transcript levels. MCF-7 cells were treated with or without I3C at the indicated **A)** concentrations and **B)** time points. The transcript levels of MDM4, Sirt-1, c-Myc, N-Myc and GAPDH were determined by qualitative RT-PCR analysis using specific primers as described in "Materials and Methods." Products were fractionated by electrophoresis on a 1.5% agarose gel and visualized with an ultraviolet transilluminator. GAPDH was used as a loading control. Fold change in mature miR-34a levels as detected by Taqman qPCR analysis of the same RNA extracts is indicated.

Figure 8

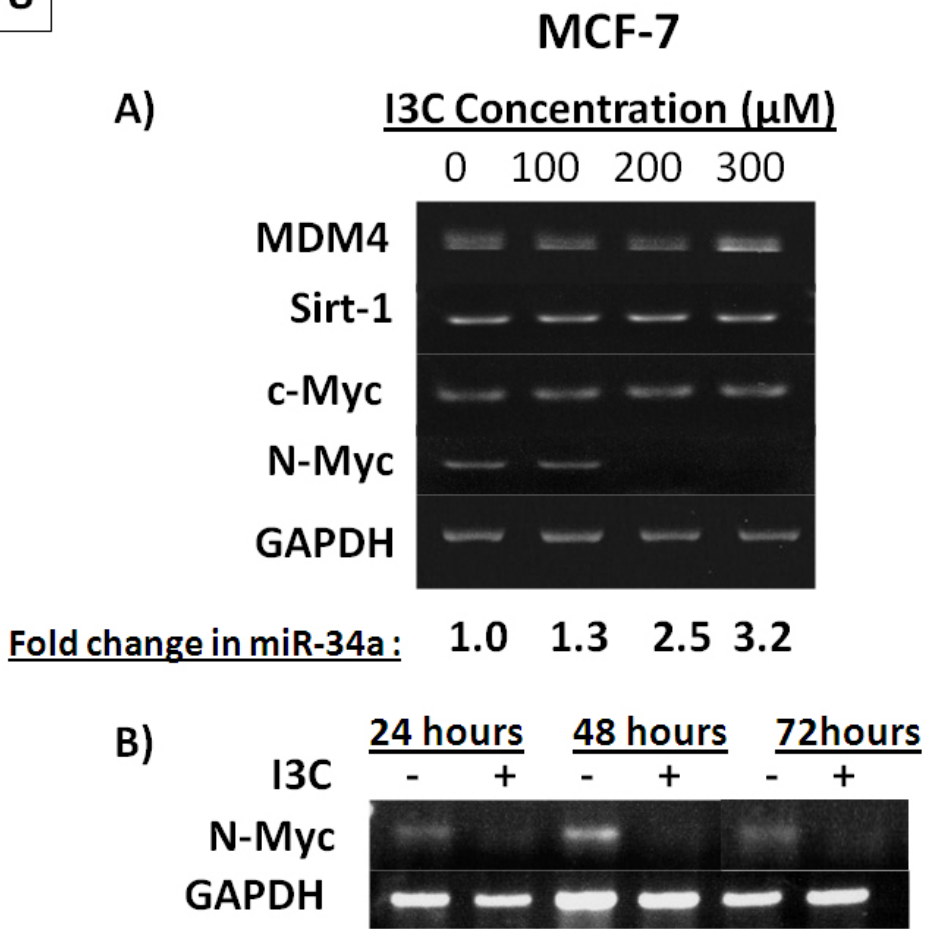
MCF-7
A)
I3C Concentration (µM)
0 100 200 300
MDM4
Sirt-1
c-Myc
N-Myc
GAPDH
Fold change in miR-34a : 1.0 1.3 2.5 3.2
B)
24 hours
48 hours
72hours
I3C
- + - + - +
N-Myc
GAPDH

Figure 9. miR-34a inhibition does not affect I3C regulation of N-Myc. MCF-7 cells were transfected with 100nM control or miR-34a inhibitors and upon overnight incubation, treated with or without 200μM I3C for 48 hours. N-Myc and GAPDH transcript levels were determined by qualitative RT-PCR analysis using specific primers as described in "Materials and Methods." Products were fractionated by electrophoresis on a 1.5% agarose gel and visualized with an ultraviolet transilluminator. GAPDH was used as a loading control.

Figure 9

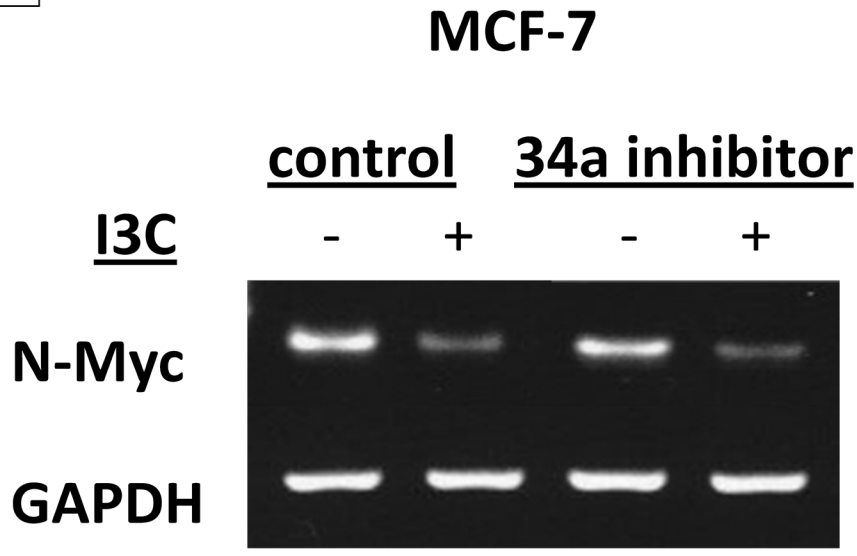

DISCUSSION

My study demonstrates that I3C utilizes the tumor-suppressive microRNA miR-34a to induce its anti-proliferative effects in human breast cancer cells. I3C treatment upregulates mature miR-34a levels in a dose and time-dependent manner that correlates with a G1 cell cycle arrest and down-regulation of cell cycle proteins as well as an increase in total and phosphorylated p53. Transfection with dominant negative p53 ablates miR-34a induction in both preneoplastic as well as human breast cancer cell lines containing wild-type p53, indicating that functional p53 is required for I3C regulation of miR-34a.

miR-34a is a known transcriptional target of p53 which suggests I3C could be increasing miR-34a levels through p53 regulation of the miR-34a promoter. Luciferase assays in which the segment of the miR-34a promoter containing the canonical p53 binding site were transfected into human breast cancer cells reveal I3C treatment actually decreases promoter activity at time points in which mature miR-34a levels increase. MicroRNA are transcriptionally expressed as long primary molecules (pri-miRNA) that undergo two processing steps: once within the nucleus in which the Drosha enzyme cleaves pri-miRNA to produce a single stem looped precursor molecule and a second time in the cytoplasm by the Dicer ribonuclease, resulting a single-stranded mature microRNA molecule approximately 18-24 nucleotides in length. To determine if I3C could be increasing mature miR-34a levels through regulation of miR-34a processing instead of promoter expression, pri-miR-34a levels were detected by RT-PCR using RNA extracts in which mature miR-34a levels were confirmed to have increased. Gel electrophoresis of PCR products revealed levels of pri-miR-34a levels remained the same with I3C treatment. This confirms that I3C is not up-regulating miR-34a transcription but could instead be influencing the processing of pri-miR-34a into mature miR-34a.

p53 was recently shown to influence microRNA processing in human cancer cells through Drosha complex interactions mediated by the DEAD –box RNA helicases, p68 and p72 (Suzuki 2010, Suzuki 2009). The Drosha complex consists of the pri-microRNA processing enzyme Drosha, the RNA binding protein DiGeorge syndrome critical region 8 and multiple RNA associated proteins including p68 and p72, which are required for the maturation of several microRNAs (Fukuda 2007). Co-immunoprecipitation and RNA-chromatin immunoprecipitation experiments in human fibroblasts revealed increased association of p53 with the Drosha complex and select primary microRNA upon DNA damage while siRNA ablation of p68 or p72 reversed this effect. p53 recruitment of p68 and p72 increased Drosha processing activity *in vitro* and *in vivo*, greatly increasing the precursor and mature microRNA levels of select microRNA yet having no effect on pri-miRNA expression. I3C activation of p53 could increase Drosha processing of pri-miR-34a to increase mature miR-34a levels. Co-immunoprecipitation and RNA-chromatin immunoprecipitation experiments to detect p53 association with the Drosha complex as well as primary-miR-34a could be utilized to test this hypothesis. Integration of I3C regulation of miR-34a processing as well as promoter activity could reveal a self-regulating negative feedback loop in which I3C treatment increases p53 processing of primary miR-34a

transcripts while inhibiting promoter expression to restrict mature miR-34a expression to particular levels.

I3C mediated increase of mature miR-34a levels correlated with an increase in p53 phosphorylation at serine residue 15. Serine residue 15 is a key phosphorylation site of the PI3-kinase related kinase ataxia telangiectasia-mutated (ATM) suggesting I3C activation of ATM signaling could be responsible for the observed increase in p53 levels (Apella 2001). Previous research in our lab established that I3C activation of ATM was required for p53 activation in human preneoplastic mammary epithelial cells (Brew 2006). I3C treatment increased ATM phosphorylation resulting in increased phosphorylation of p53 at serine residue 15 and subsequent dissociation from the p53 inhibitor and ubiquitin ligase, MDM2. Pre-treating cells with ATM inhibitors, Western blot detection of ATM activation residues and co-immunoprecipitation experiments detecting p53-MDM2 association could be a potential way to investigate this possibility in I3C treated human breast cancer cells.

Loss of functional miR-34a reversed I3C mediated growth inhibition. Potential miR-34a target genes that regulate cell proliferation include the cyclin-dependent kinase CDK6 and transcription factor N-Myc (Sun 2008, Lujambio 2008, Wei 2008, Cole 2008). I3C upregulation of miR-34a in this study correlated with a dose and time-dependent decrease in CDK6 protein and N-Myc transcript levels, suggesting potential I3C mediated miR-34a inhibition of either protein. Transfection of miR-34a inhibitors had no effect on N-Myc expression while mildly attenuating I3C mediated down-regulation of CDK6. I3C treatment could direct miR-34a mediated repression of CDK6 however such regulation may only be a minimal component of I3C's effect on the gene. Previous research in our lab indicated I3C can downregulate CDK6 protein levels through disruption of transcription factor interactions with the CDK6 promoter (Firestone 2003, Cram 2001). Thus, I3C may utilize both promoter inhibition and miR-34a mediated translational repression to decrease CDK6 levels. Luciferase assays using constructs in which the miR-34a target region of CDK6 is attached to firefly luciferase mRNA could be utilized to confirm this hypothesis. Other potential I3C cell proliferation regulators and confirmed miR-34a target genes include the transcription factor Myb, transcriptional regulatory protein Hmga2, and the transmembrane signaling receptor Notch1 (Hermeking 2007).

The results of this study indicate I3C regulation of tumor suppressive microRNA is a critical component of its anti-cancer activity in human breast cancer. Future directions include determining the p53-dependent mechanism of miR-34a regulation and identifying direct targets of miR-34a inhibition.

:

CHAPTER 2

Artemisinin upregulates miR-34a in a p53-independent Manner to Growth Arrest Human Breast Cancer Cells via CDK4 Inhibition

ABSTRACT

Artemisinin, a sesquiterpene lactone derived from the sweet wormwood plant *Artemisia Annua*, is a malarial treatment with anti-tumorigenic properties. Previous research suggests artemisinin growth arrests human breast cancer cells yet the precise mechanism of action is still unknown. This study indicates that artemisinin upregulates the tumor suppressive microRNA miR-34a to growth arrest human breast cancer cells. qPCR analysis indicate artemisinin upregulates miR-34a in a dose and time-dependent manner that correlates with a G1 cell cycle arrest and decrease in protein levels of the cyclin dependent kinase, CDK4. Functional p53 is not required for miR-34a induction as miR-34a upregulation can occur in cell lines containing non-functional p53 and transfection of dominant negative p53 into a cell line containing wild-type p53 does not affect miR-34a induction. miR-34a is required for artemisinin mediated inhibition of CDK4 as transfection of miR-34a inhibitors prevented artemisinin down-regulation of the protein. Artemisinin treatment also decreases expression of a luciferase construct containing the wild-type miR-34a binding site of CDK4, indicating direct inhibition of CDK4 by miR-34a upon artemisinin treatment. Artemisinin transcriptionally regulates miR-34a in a region outside the p53 binding segment of the miR-34a promoter as luciferase and RT-PCR experiments show an increase in primary miR-34a levels yet no change in canonical promoter activity. All of these data suggest that miR-34a could be regulated in a p53-independent manner and is an essential component of artemisinin mediated cell cycle arrest in human breast cancer.

INTRODUCTION

One of the difficulties in developing anti-cancer therapeutics is finding those that exhibit potent activity against multiple stages of the disease. p53 is a transcription factor that is mutated in half of diagnosed cancers with its mutation state often indicative of poor prognosis and treatment resistance (Olivier 2010, Petitjan 2007). p53 mutations in human breast cancer correlate with aggressive Her-2+ or triple-negative cancers that are refractory against traditional chemotherapy agents and insensitive to radiation treatment (Langerod 2007, Petijan 2007, Olivier 2006, Aas 2003, Bergh 1998, Aas 1996). Naturally occurring plant compounds such as artemisinin extracted from the sweet wormwood plant demonstrate potent inhibitory effects against breast cancer and could be one possibility for treating both early stage and p53 mutant forms of the disease.

Most p53 mutations occur within contact points inside the DNA binding domain, preventing p53 from interacting with its regulatory sequence in target gene promoters. Such mutations disrupt multiple gene networks regulating cell proliferation and survival by preventing p53 mediated expression of cell cycle genes as well as induction of apoptosis and DNA repair (Caraval 2013, Riley 2008, Vogelstein 2000). p53 also participates in a negative feedback loop on its own expression by up-regulating gene expression of the ubiquitin ligase, MDM2. Mutant p53 is thus often expressed at much higher levels in cancer cells than its wild-type counterpart which may be due to its inability to transcriptionally regulate its own degradation (Blaksogonny 2000, Midgley 1997).

The recent integration of the tumor suppressive microRNA family miR-34 into the p53 regulatory network provides an additional node of misregulation in cancer cells. miR-34 is a transcriptional target of p53, thus p53 mutation status in cancer cells often correlates with decreased miR-34 levels and subsequent over-expression of miR-34 target genes including the cell cycle regulator cyclin D1, oncogenic transcription factor c-Myc, and anti-apoptotic factor Bcl-2 (Wong 2011, Hermeking 2007,Tarasov 2007, Chang 2007, Raver-Shapira 2007, He 2007). Disruptions in p53 and miR-34 activity can also influence chemotherapy resistance. p53 mutations in human breast cancer have been associated with increased resistance to the anti-cancer agents doxorubicin, epirubicin, tamoxifen, and 5-fluorouricil while over-expressing miR-34a in p53 mutant breast and prostate cancer cell lines increased sensitivity to adriamycin or camptothecin (Li 2012, Chrisianthar 2008, Fujita 2008, Geisler 2003, Aas 2003, Geisler 2001, Bergh 1998, Aas 1996). Clearly there is a need for novel anti-cancer therapies with the broad spectrum effectiveness to treat p53 mutant forms of the disease while restoring the activity of p53 transcriptional targets such as miR-34.

Artemisinin is an anti-malarial compound extracted from the sweet wormwood plant *Artemisia annua* that exhibits cytotoxic effects against human cancer cell lines and tumors in a p53 independent manner. Previous research in our lab showed artemisinin treatment induces a G1 cell cycle arrest in breast and prostate cancer cell lines regardless of p53 mutation status (Tin

2012, Willoughby 2009). Artemisinin treatment growth arrests both the estrogen-responsive, wild-type p53 MCF-7 cell line and estrogen-unresponsive, p53 mutant MDA-MB-231 breast cancer cell lines as well as the androgen-responsive, wild-type p53 LnCAP and androgen unresponsive, p53 mutant DU145 prostate cancer cell lines. Artemisinin mediated arrest in MCF-7 cells downregulates levels of estrogen-receptor alpha as well as expression of E2F1 transcription factor while artemisinin cell cycle arrest in LNCAP cells downregulates expression of the CDK4 promoter through disruption of Sp1 transcription factor signaling (Sundar 2008, Willoughby 2006).

Artemisinin could be a potential treatment for p53 mutant forms of breast cancer yet the direct effect of artemisinin on p53 expression as well as downstream targets such as miR-34 has yet to be investigated. This study demonstrates that artemisinin growth arrests human breast cancer cells regardless of p53 functionality and that such arrests correlates with a time and dose-dependent increase in mature miR-34a. Artemisinin has no effect on p53 expression levels and functional p53 is not required for miR-34a induction. miR-34a directly inhibits CDK4 upon artemisinin treatment and is required for artemisinin mediated down-regulation of the protein. Such data suggests miR-34a can be regulated in a p53-independent manner and tumor suppressive microRNA play a critical role in the anti-cancer activity of artemisinin.

MATERIALS & METHODS

Cell Culture

Cells were grown to sub-confluency in a humidified incubator at 37°C containing 5% CO2. MCF-7 and T47D cell lines were cultured as described by the American Tissue Culture Collection (Manassas, VA). Cells were treated for the indicated time points in complete medium with artemisinin (Sigma, St. Louis, Missouri) dissolved 1000X in DMSO. Pure DMSO (Sigma-Aldrich, Milwaukee, WI) was used as a control. The medium was changed every 24 hours for the duration of each experiment.

Flow cytometry

For cell cycle analysis, attached and non-adherent cells treated in 6-well plates were collected within the media, rinsed with PBS and hypotonically lysed in 0.5 ml of propidium iodide buffer (0.5mg/ml propidium iodide, 0.1% sodium citrate, 0.05% Triton X-100). Samples were analyzed on a Beckman-Coulter (Fullerton, CA) EPICS XL flow cytometer with laser output adjusted to deliver 15 MW at 488 nm. Ten thousand cells were counted. Cell cycle analysis was then performed using MultiCycle software WinCycle 32 (Phoenix Flow Systems, San Diego, CA).

RNA extraction

Cells were harvested in 1.0 ml TRIzol reagent (Invitrogen, Carlsbad, CA) and total RNA extracted following the manufacturer's protocol with the phase separation procedure being performed twice to extract microRNA. Removal of contaminating DNA was performed on 10µg of extracted RNA using a DNA-free Kit (Invitrogen, Carlsbad, CA) per the manufacturer's protocol. RNA integrity was confirmed by running a 1.5% formaldehyde (Sigma Chemical, St. Louis, MO) denaturing agarose gel (Invitrogen, Carlsbad, CA) using 1µg of RNA per sample and visualizing intact bands corresponding to the molecular weights of the 28S and 18S subunits of ribosomal RNA, the most abundant RNA species. Gels contained GelRed Nucleic Acid Gel Stain (Biotium, Hayward, CA) diluted to a 2X concentration for band visualization using short wavelength ultraviolet light.

Reverse Transcription and PCR

Total RNA was reverse transcribed using stem loop primers for miR-34a, miR-34b and miR-34c as well as random primers for β-actin, a housekeeping gene insensitive to artemisinin treatment. Each reverse transcriptase reaction contained 10XRT buffer, 100mM dNTPS, 50U/µl MultiScribe reverse transcriptase, and 20U/µl RNAse inhibitor (Applied Biosystems, Foster City, California) dissolved in nuclease-free water. The reverse transcription reaction for β-actin contained 100ng of purified total RNA as well as 10X random primers while the reaction for microRNA reverse transcription contained 560ng of purified total RNA and 5X miR-34a stem-loop RT primer (Applied Biosystems, Foster City, California). The microRNA reactions were

incubated in a thermal cycler for 30 minutes at 16°C, 30 minutes at 42°C, and 5 minutes at 85°C while reactions for the control gene were incubated for 10 minutes at 25°C, 120 minutes at 37°C, and 5 minutes at 85°C.

Real-time PCR reactions for each miRNA (10 µl volume) were performed in triplicate, and each reaction mixture included 4 µl of diluted RT product (1:2 dilution), 5 µl of 2X TaqMan Universal PCR Master Mix, 0.2 µM TaqMan probe, 1.5 µM forward primer, 0.7 µM reverse primer with the probes and primers specific to mature miR-34a, mature miR-34b, mature miR-34c or human β-actin(Applied Biosystems, Foster City, CA). Reactions were incubated in an Applied Biosystems 7900HT Fast Real-Time PCR system in 96-well plates at 95°C for 10 min, followed by 40 cycles at 95°C for 15 seconds and 60°C for 1 min. Changes in fluorescence levels of miR-34 were normalized to β-actin, and fold changes compared between the target sample (miR-34 levels in cells treated with artemisinin) and calibrator samples (miR-34 levels in DMSO treated cells).

Qualitative PCR reactions (50µl volume) employed 1.5ug of purified RNA and a reaction mixture of 10X PCR Master Mix, 2.5mM dNTP mixture, 10pmol forward primer, 10pmol reverse primer and .25µl Taq DNA polymerase (Applied Biosystems, Foster City, CA). The following primer sets and conditions were used:
pri-34a_Forward: 5'-CGTCACCTCTTAGGCTTGGA-3'
pri-34a_Reverse: 5'-CATTGGTGTCGTTGTGCTCT-3'
Gapdh_Forward: 5'-GAAGGTGAAGGTCGGAGTC-3'
Gapdh_Reverse: 5'-GAAGATGGTGATGGGATTTC-3'
GAPDH: 45s at 94°C, 30s at 94°C, 1 min at 72°C for 27 cycles, pri-34a: 30s at 95°C, 30s at 55°C, 30s at 68°C for 38 cycles. All PCR products were combined with 6X DNA loading dye, fractionated by electrophoresis on a 1.5% agarose gel containing .01% GelRed Nucleic Acid Gel Stain (Biotium, Hayward, CA)and visualized with an ultraviolet transilluminator.

Immunoblotting

Cell extracts were harvested in RIPA lysis buffer containing inhibitors, and standardized to 20-30ug protein using the Bradford protein assay. Equal protein amounts were subjected to SDS-PAGE on an 8% or 10% poly-acrylamide gel, transferred onto nitrocellulose membranes, and incubated for 1 hour at room temperature with blocking solution (5% milk dissolved in TBST). Primary antibodies to p53, HSP90 (Cell Signaling Technology, Beverly, MA) p21, actin, CDK4, CDK6, cyclin D1 and estrogen-receptor alpha (ERα) (Santa Cruz Biotechnologies, Santa Cruz, CA) were incubated overnight at 4°C. After three washes in 5% milk dissolved in TBST, membranes were incubated with anti-mouse or anti-rabbit horseradish peroxidase-conjugated antibodies for 1.5 hours at room temperature. Following an additional five washes in 5% milk, chemo luminescent signals were generated by incubation with Western Lightning ECL reagents according to the manufactures instructions (Perkin Elmer, Shelton, CT) and the results transferred to ECL-sensitive film (GE Healthcare, United Kingdom).

Transfections and Luciferase Assay

100nM miR-34a or control locked nucleic acid inhibitors (Exiqon, Woburn, MA) were transfected into MCF-7 and T47D according to the manufacturer's instructions with Lipofectamine 2000 reagent (Applied Biosystems, Mountain View) while 2μg of indicated plasmids were transfected using Superfect reagent (Qiagen, Germantown, Maryland). Upon overnight incubation, cells containing the miR-34a promoter were treated with or without 300μM artemisinin for 24, 48 or 72 hours and harvested in ice-cold PBS. CDK4-miR-34a luciferase constructs were transfected in a similar manner and treated with or without 300μM artemisinin for 48 hours. The cells were then centrifuged at 14,000 rpm for 5 minutes at 4°C, combined with 1X Passive lysis buffer, and Promega Luciferase assay performed according to the manufacturer's instructions (Promega, San Luis Obispo, CA). Relative light units were normalized to protein expression as determined by the Bradford protein assay. Dominant negative p53 was purchased from Clontech Laboratories (Mountain View, CA). CDK4-miR-34a luciferase constructs were a kind gift of Dr. Lin He, University of California, Berkeley while miR-34a promoter plasmids were a kind gift of Dr. Xueqing Xu, Third Military Medical University (Chongqing, China).

.

RESULTS

Artemisinin growth arrests human breast cancer cells irrespective of p53 status

Artemisinin has been shown to be growth arrest cancer cells in a p53 independent manner (Hou 2008, Tin 2012, Sundar 2008). To determine the role of p53 in the anti-cancer activity of artemisinin (Art), human breast cancer cell lines containing wild-type p53 (MCF-7) or mutant p53 (T47D) were treated with or without increasing concentrations of artemisinin at varying time points to determine the effects on the cell cycle. Cells were treated with 100μM, 200μM, 300μM or 400μM artemisinin or 300 μM artemisinin for 24, 48 or 72 hours and flow cytometry analysis using propidium iodide staining performed on the harvested extracts. Artemisinin treatment at 48 hours caused a 12%-34% arrest in the G1 phase of the cell cycle for MCF-7 and T47D cells with a concomitant decrease in cells in the S phase (Figure 1A). The minimum artemisinin concentration to maximize G1 cell cycle arrest was 300μM for both cell lines while 48 hours of treatment provided significant cell cycle arrest at the earliest time point (Figures 1B-1E).These data suggest that artemisinin growth arrests human breast cancer cells regardless of p53 mutation status with maximal cell cycle arrest occurring with 300μM treatment for 48 hours.

Artemisinin increases miR-34a levels and decreases cell cycle proteins in a dose and time-dependent manner

To assess the possibility of artemisinin regulation of miR-34 family expression under conditions of cell cycle arrest, MCF-7 and T47D cells were treated with or without increasing concentrations of artemisinin or 300μM artemisinin for 48 hours and Taqman quantitative PCR analysis performed on extracted RNA. Total RNA was reverse transcribed using stem loop primers for miR-34a, miR-34b and miR-34c and the cDNA amplified in real-time using primers and dual-labeled fluorogenic probes specific to miR-34a, miR-34b, miR-34c or β-actin as a negative control. Changes in fluorescence levels of miR-34 were normalized to β-actin, and fold changes compared between the target sample (miR-34 levels in artemisinin treated cells) and calibrator samples (miR-34 levels in DMSO treated cells). A fold-change of two is indicative of a significant change, thus artemisinin treatment upregulated miR-34a in a dose and time-dependent manner in MCF-7 and T47D cells (Figures 2A-2D). 300μM and 400μM increased miR-34a levels greater than two-fold in both cell lines (Figures 2B, 2D) while maximal induction occurred at 48 hours for MCF-7 cells and 72 hours for T47D cells (Figures 2A, 2C). miR-34b levels were minimally affected while mature miR-34c was undetected in either cell line. miR-34a was significantly upregulated at time points and doses correlating with artemisinin mediated cell cycle arrest (Figures 1B-1E), suggesting it could play a critical role in the process.

Figure 1. Artemisinin growth arrests human breast cancer cells.
A) Representative flow cytometry profiles for MCF-7(wild-type p53) and T47D (p53 mutant) cells treated for 48 hours with or without 300μM artemisinin. Flow cytometry analysis was performed using propidium iodide staining as described in "Materials and Methods." **B)** MCF-7 breast cancer cells were treated with or without artemisinin (Art) at the indicated time points or **D)** concentrations at 48 hours and subjected to flow cytometry analysis of the cell cycle as described in "Materials and Methods."The bar graphs indicate the average DNA content corresponding to the phases of the cell cycle as detected in three independent experiments. Error bars represent standard deviation. **C)** T47D breast cancer cells were treated with or without artemisinin (Art) at the indicated time points and **E)** concentrations and subjected to flow cytometry analysis of the cell cycle as described in "Materials and Methods." The bar graphs indicate the average DNA content corresponding to the phases of the cell cycle as detected in three independent experiments. Error bars represent standard deviation.

Figure 1A

48 hours

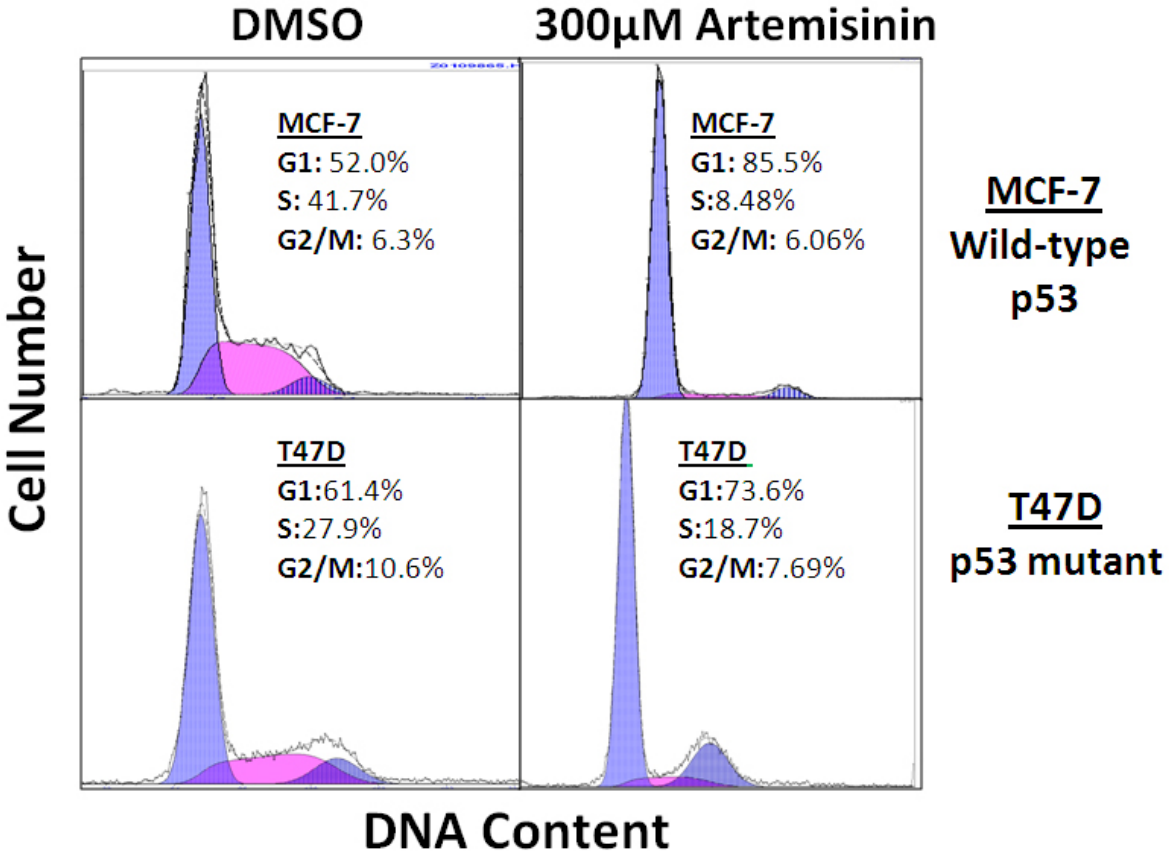

Figure 1B

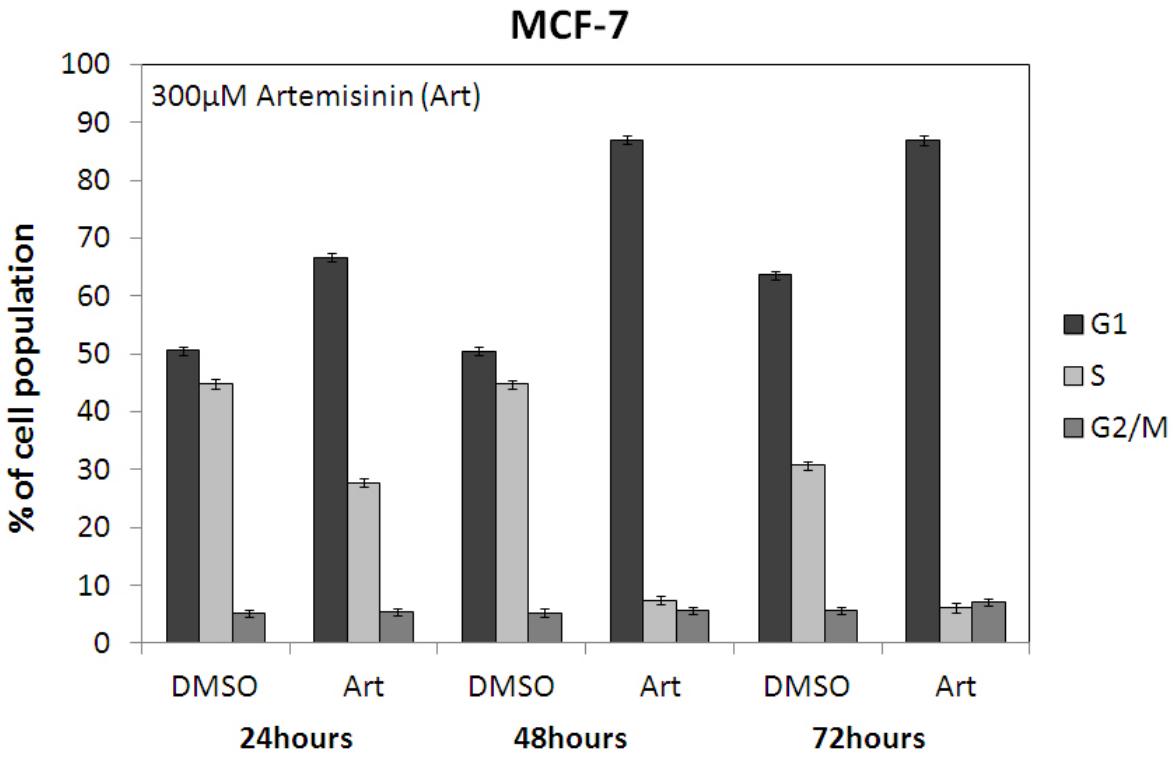

Figure 1C

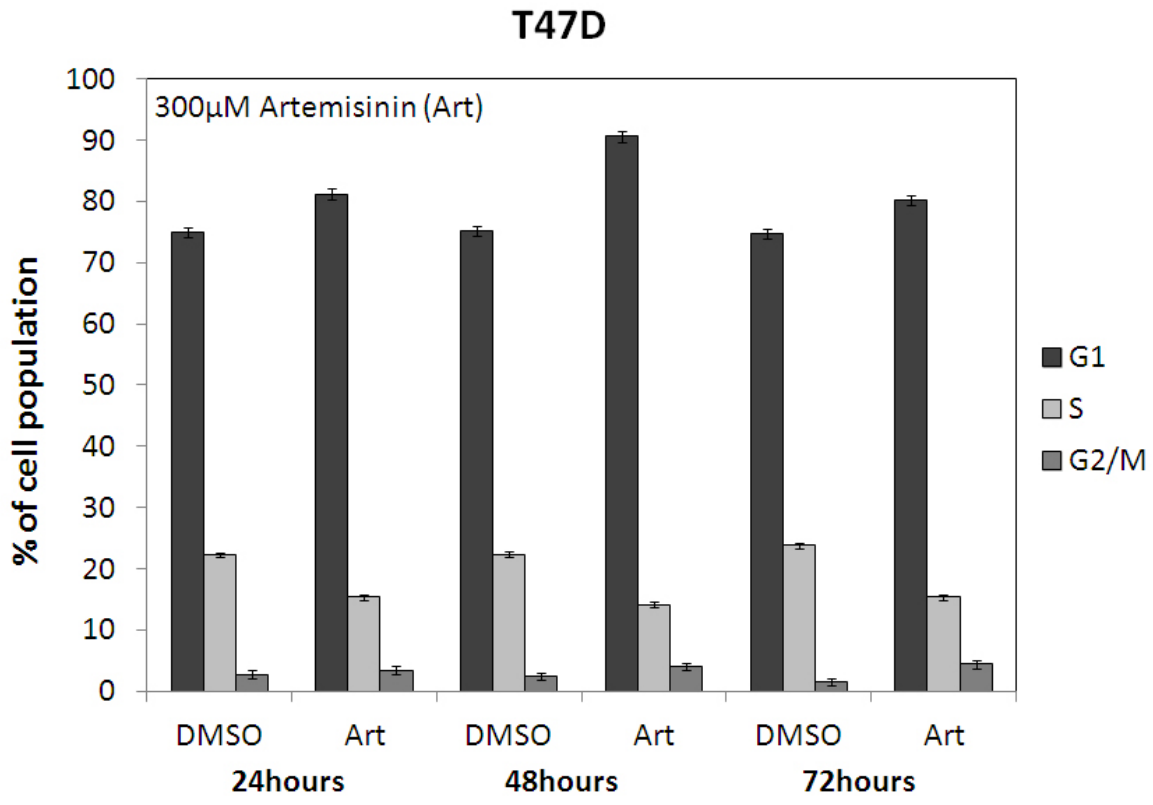

Figure 1D

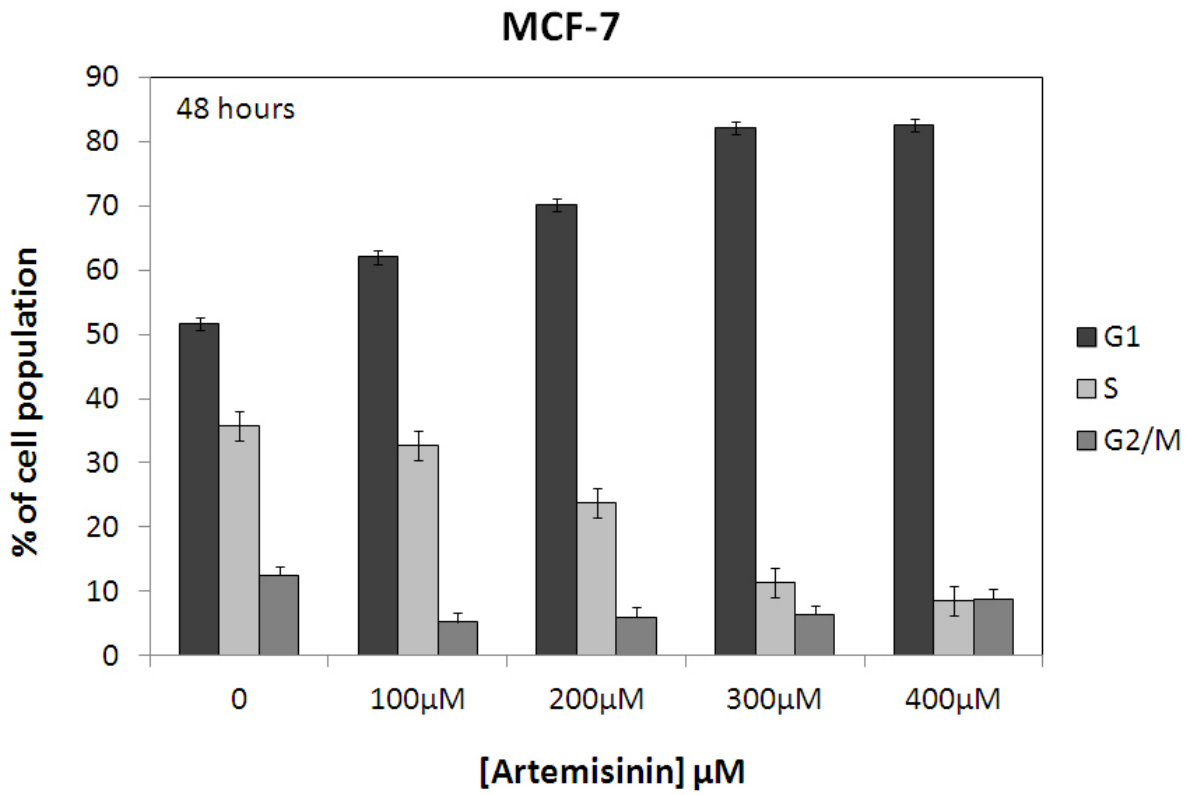

Figure 1E

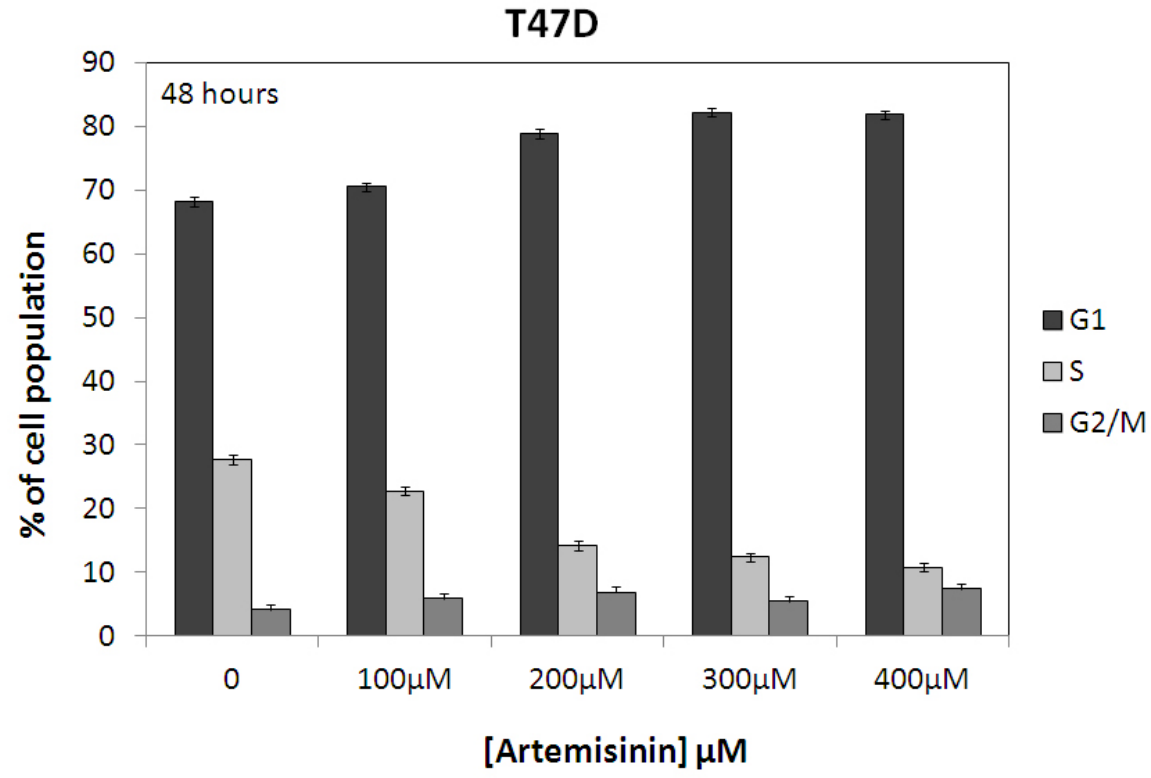

Figure 2. Artemisinin treatment upregulates miR-34a in a dose and time dependent manner. MCF-7cells were treated with or without artemisinin at the **A)** indicated time points or **B)** concentrations at 48 hours. Reverse transcription with stem-looped primers for each member of the miR-34 family or random primers for β-actin was performed on purified RNA extracts followed by Taqman semi-quantitative PCR using dual-labeled fluorogenic probes for mature miR-34a, miR-34b, miR-34c and β-actin, a housekeeping gene insensitive to artemisinin treatment. Triplicate results were normalized to expression of β-actin and bar graphs represent average fold change in miR-34a and miR-34b levels as determined in three independent experiments. miR-34c was undetected. Dotted line indicate the two-fold significance threshold of microRNA experiments and error bars represent standard deviation.T47D cells were treated with or without artemisinin at the **C)** indicated time points or **D)** concentrations at 48 hours and Taqman qPCR performed as described above to detect levels of mature miR-34 and miR-34b. miR-34c was undetected. Triplicate results were normalized to expression of β-actin and bar graphs represent average fold change in miR-34a and miR-34b levels as determined in three independent experiments. The dotted line represents the two-fold significance threshold of microRNA experiments and error bars indicate standard deviation.

Figure 2A

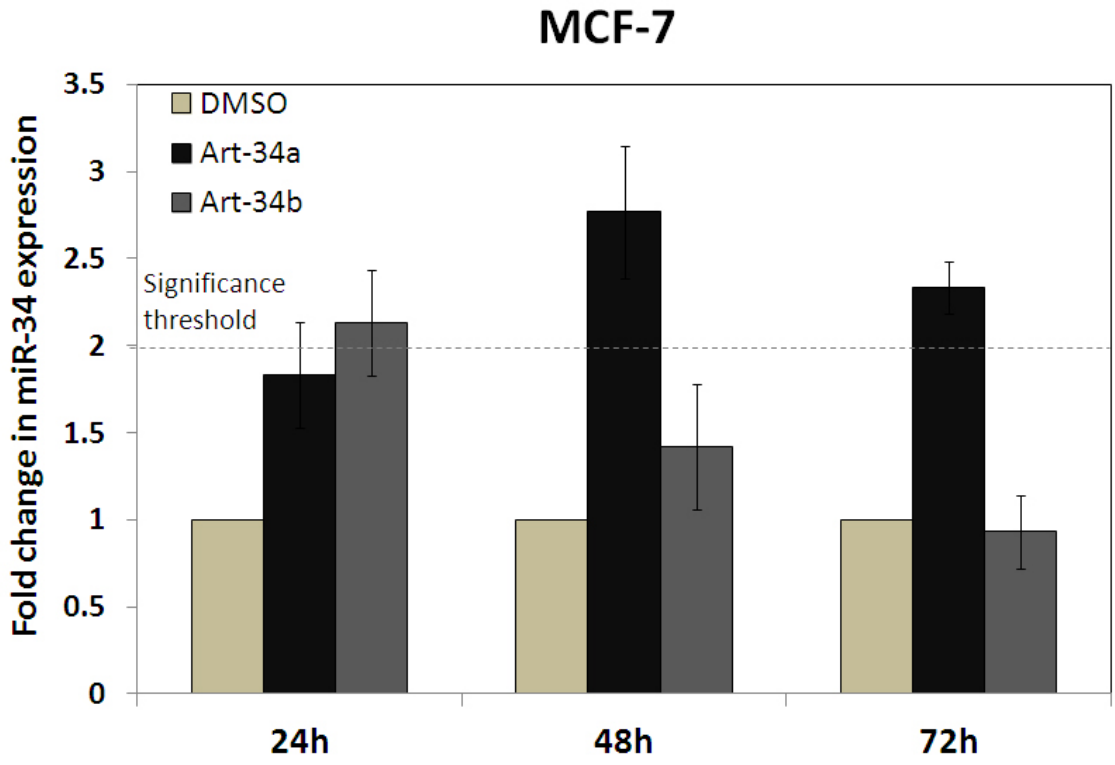

Figure 2B

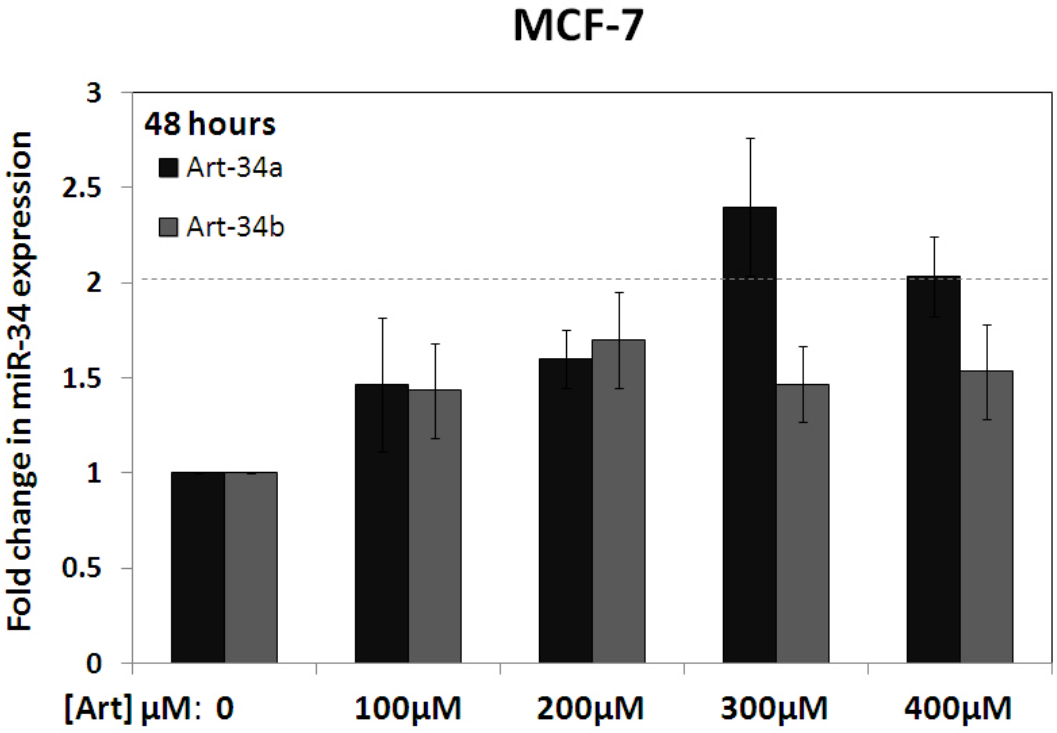

Figure 2C

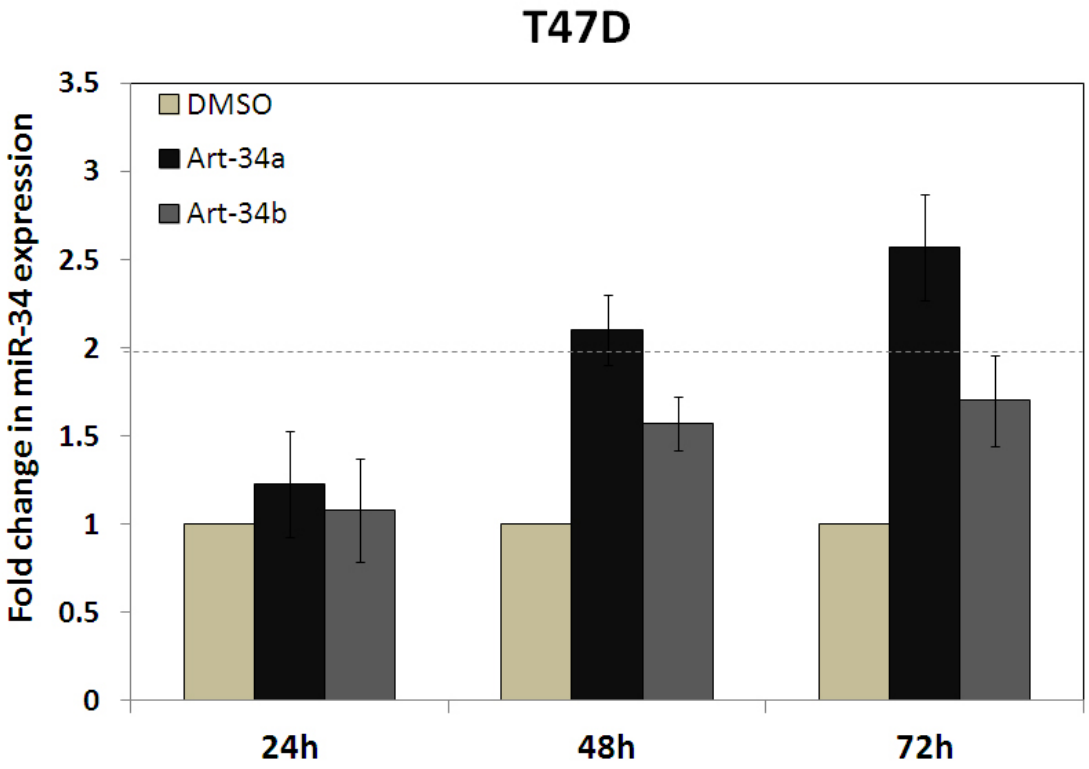

Figure 2D

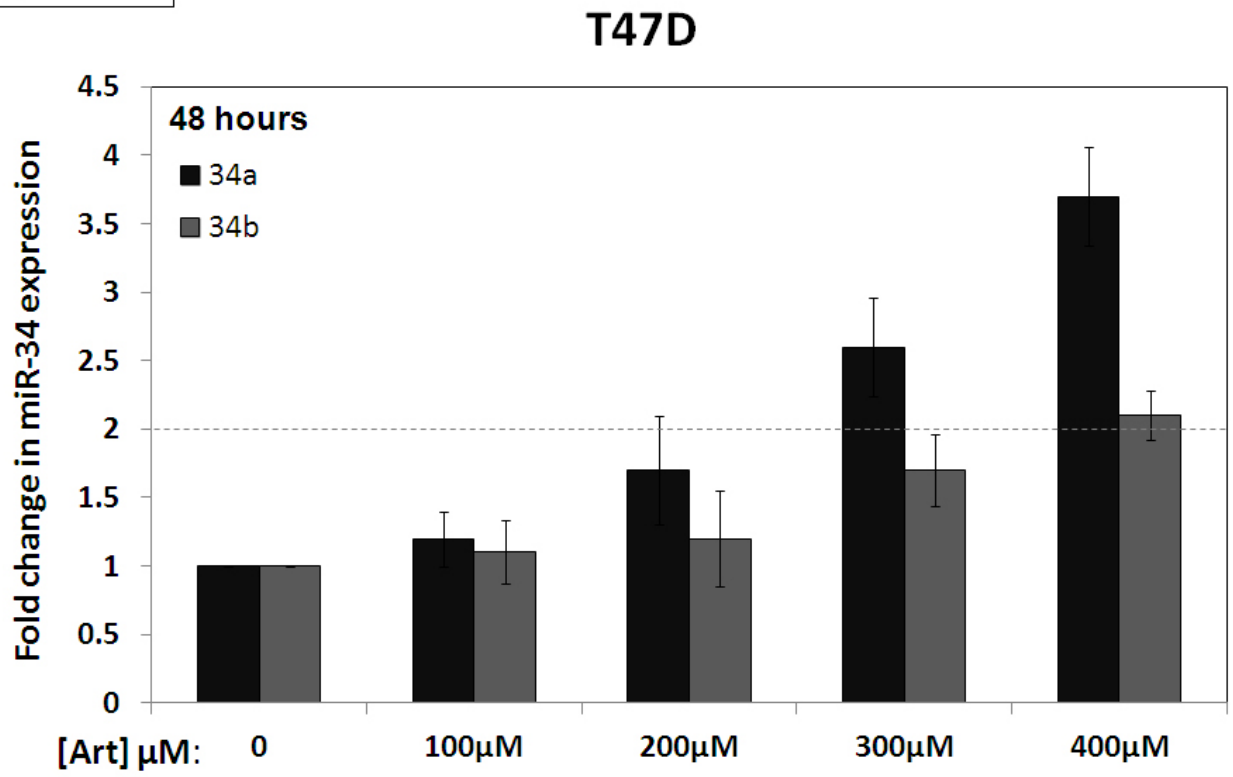

To determine if artemisinin also regulates p53 levels in human breast cancer cells, Western blot analysis was performed on protein extracts from MCF-7 or T47D cells treated with or without increasing concentrations of artemisinin or 300μM artemisinin for 24, 48 and 72 hours. p53 levels were undetected in artemisinin treated MCF-7 cells while expression levels remained high regardless of treatment in T47D cells (Figure 3A-3B). The p53 mutation within T47D cells occurs within the DNA binding domain, rendering the protein non-functional while increasing its stability (Lukashchuk 2007, Olivier 2010, Nigro 1989). The high expression of p53 detected in the Western blot is thus consistent with the behavior of mutant p53. Levels do not change upon artemisinin treatment, suggesting that artemisinin does not alter wild-type or mutant p53 expression in human breast cancer cells.

To determine artemisinins affect on G1 cell cycle regulators, levels of cyclin D1, CDK4, CDK6 and estrogen receptor-alpha (ERα) were also detected by Western blot. The cyclin-dependent kinases CDK4 and CDK6 phosphorylate the retinoblastoma protein to regulate the G1 to S phase transition in the cell cycle while cyclin D1 is the kinase activator of either protein (Reed 1997). ERα can also influence cell cycle progression through transcriptional upregulation of target genes such as cyclin D1 and the transcription factor c-Myc (Melmed 2008). Previous research in our lab also established ERα as a target of artemisinin-mediated down-regulation (Sundar 2008).

Western blot analysis indicates artemisinin treatment decreases cyclin D1, CDK4, and ERα in a time and dose-dependent manner in both cell lines while levels of CDK6 remain unaffected ((Figure 3A-3B). All of these data suggest artemisinin upregulates miR-34a in a dose and time-dependent manner in human breast cancer cells that correlates with the down-regulation of cell cycle regulatory proteins and a pronounced G1 cell cycle arrest. This process appears p53-independent as artemisinin treatment has no effect on total p53 levels and miR-34a induction occurs in cell lines containing wild-type or mutant p53.

Functional p53 is not required for miR-34a induction

To confirm miR-34a is upregulated in a p53 independent manner by artemisinin, the MCF-7 cell line containing wild-type p53 was transfected with dominant negative p53 (DNp53) or an empty neomycin control vector (Neo). Upon overnight incubation, transfected cells were treated with or without 300μM artemisinin for 48 hours. Western blot analysis revealed that artemisinin treatment had no effect on total p53 levels in either cell line while dominant negative p53 expression increased stabilization and thus detection of the protein in MCF-7 DNp53 cells (Figure 4B). Artemisinin treatment upregulated mature miR-34a levels greater than two fold in MCF-7-Neo and MCF-7-DNp53 cells as detected by qPCR analysis (Figure 4A.) Such data indicates functional p53 is not required for artemisinin regulation of miR-34a in human breast cancer cells.

Figure 3. Artemisinin does not affect p53 levels while downregulating cell cycle regulatory proteins. A) MCF-7 and **B)** T47D cells were treated with or without artemisinin at the indicated concentrations or time points and protein levels of p53, p21, ERα, CDK4, CDK6, cyclin D1 (CycD1), HSP90 and actin determined by Western blot as described in "Materials and Methods." Actin or HSP90 was used as a loading control.

Figure 3A

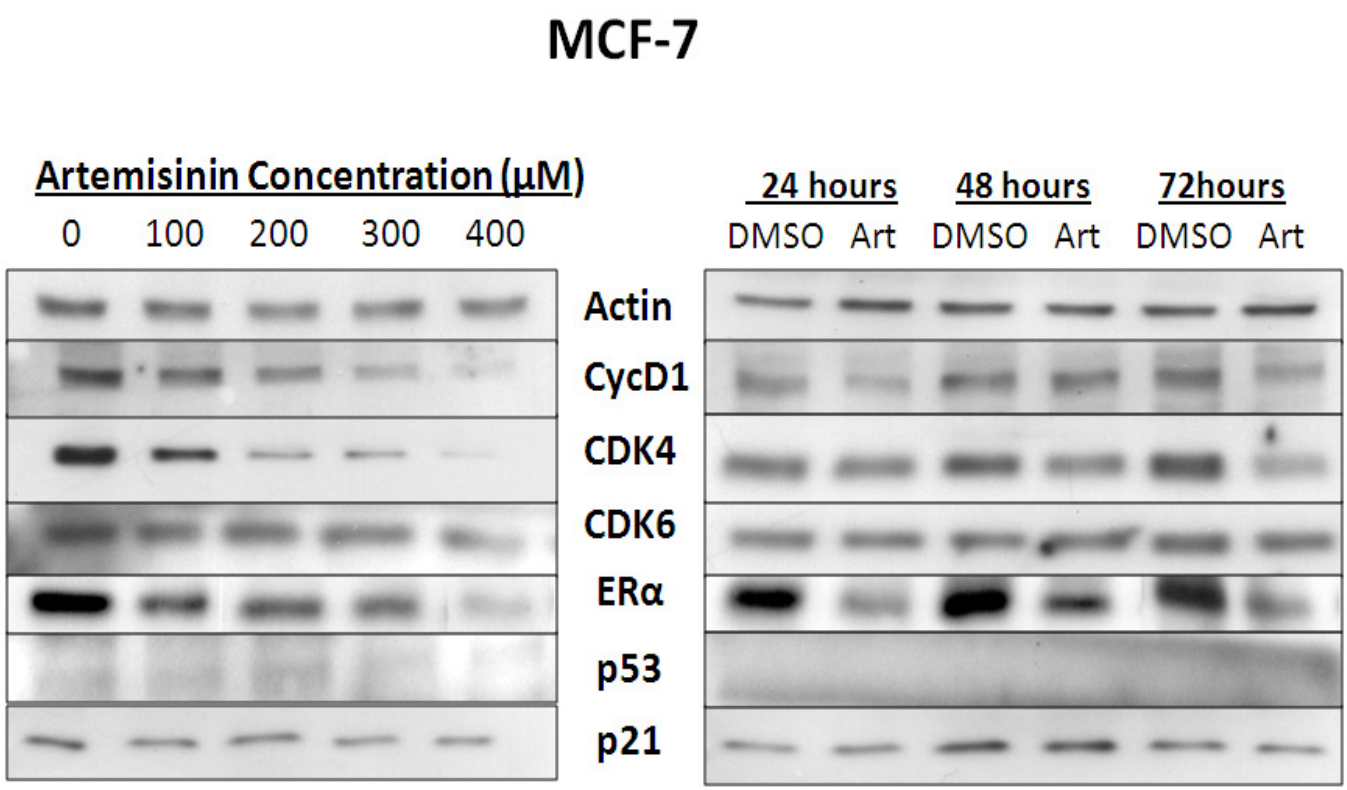
MCF-7
Artemisinin Concentration (μM)
0
100
200
300
400
24 hours
48 hours
72hours
DMSO
Art
DMSO
Art
DMSO
Art
Actin
CycD1
CDK4
CDK6
ERα
p53
p21

\

Figure 3B

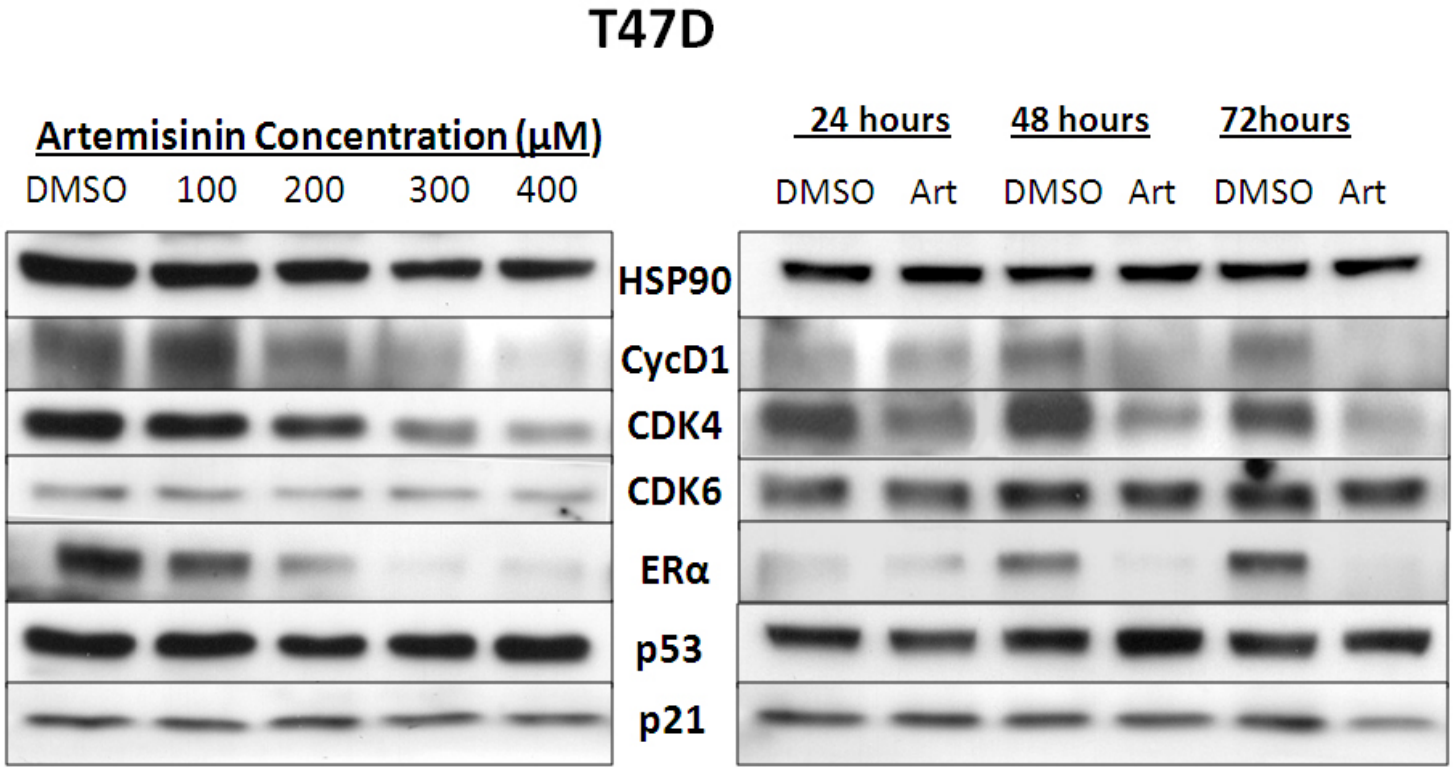
T47D
Artemisinin Concentration (μM)
DMSO 100 200 300 400
24 hours
48 hours
72hours
DMSO Art DMSO Art DMSO Art
HSP90
CycD1
CDK4
CDK6
ERα
p53
p21

Figure 4. Functional p53 is not required for artemisinin induction of miR-34a.
MCF-7 cells were transfected with dominant negative p53 (MCF-7-DNp53) or an empty vector control (MCF-7-Neo). Upon overnight incubation, transfected cells were treated with or without 300μM artemisinin for 48 hours and total RNA and protein harvested. **A)** Taqman semi-quantitative PCR analysis was performed on RNA extracts to detect mature miR-34a levels as described in "Materials and Methods." Triplicate results were normalized to expression of β-actin and bar graphs represent average fold change in miR-34a levels as determined in three independent experiments. The dotted line represents the two-fold significance threshold of microRNA experiments and error bars indicate standard deviation. **B)** p53 protein levels were determined by Western blot analysis as described in "Materials and Methods" using actin as a loading control.

Figure 4

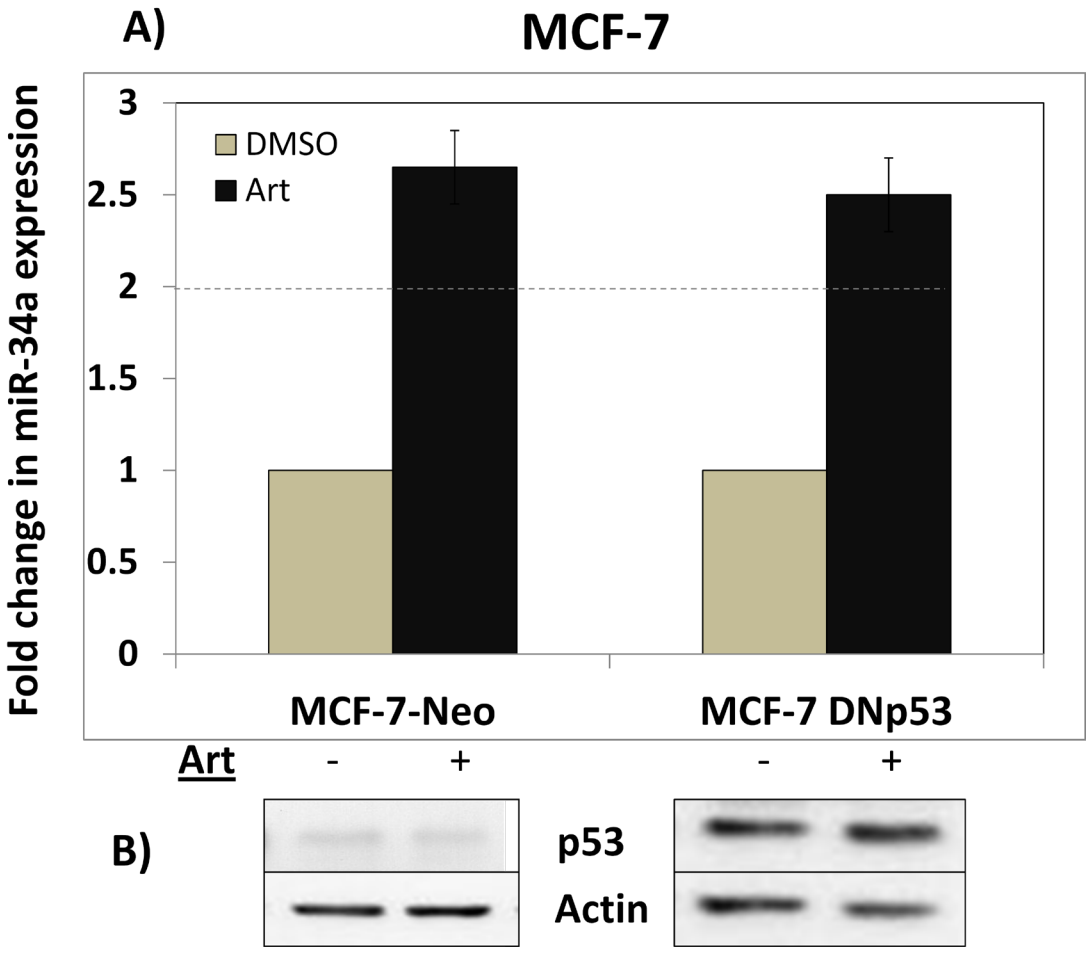
A)
MCF-7
Fold change in miR-34a expression
3
2.5
2
1.5
1
0.5
0
DMSO
Art
MCF-7-Neo
MCF-7 DNp53
Art
-
+
-
+
B)
p53
Actin

Artemisinin does not regulate the p53 binding region of the miR-34a promoter

To determine if artemisinin regulates the miR-34a promoter, MCF-7 and T47D cells were transfected with or without a segment of the miR-34a promoter containing the canonical p53 binding site inserted upstream of the luciferase gene. A vector expressing luciferase under the control of an unregulated promoter or an empty neomycin vector were used as positive and negative controls respectively. Upon transfection, cells were treated with or without 300μM artemisinin for 24, 48 or 72 hours and a luciferase assay performed on the harvested cells. Normalized luciferase activity revealed artemisinin does not upregulate the miR-34a promoter in either cell line at time points correlating with an increase in mature miR-34a (Figure 5A-5B). This suggests that artemisinin could upregulate miR-34a through transcriptional regulation at another region of the miR-34a promoter or by influencing microRNA processing.

microRNA are processed twice before reaching maturation. They are transcribed as long primary transcripts (pri-miRNA) containing multiple microRNA copies that are cleaved in the nucleus to produce a single stem-looped precursor molecule (pre-miRNA). Upon entry into the cytoplasm, one strand of the pre-miRNA is degraded and the resulting single stranded mature microRNA loaded in the RNA induced silencing complex to prevent translation of target mRNA sequences. Artemisinin treatment could upregulate mature miR-34a levels by altering microRNA processing. To investigate this possibility, qualitative PCR was performed using primers for pri-miR-34a on RNA extracts in which mature miR-34a levels were confirmed by Taqman qPCR to be upregulated by artemisinin. Gel electrophoresis of the PCR products revealed pri-34a levels increase substantially after 48 hours of artemisinin treatment in MCF-7 cells (Figure 6A) and upon 24 and 48 hours of artemisinin treatment in T47D cells (Figure 6B) These data suggest that artemisinin transcriptionally upregulates miR-34a gene expression to increase mature miR-34a levels and that the artemisinin responsive region of the miR-34a promoter lies outside the region containing the p53 binding site.

Figure 5. Artemisinin does not regulate the p53-binding region of the miR-34a promoter. **A)** MCF-7 cells and **B)** T47D were transfected with or without a segment of the miR-34a promoter containing the canonical p53 binding site inserted upstream of the luciferase gene. Upon overnight incubation, cells were treated with or without 300μM artemisinin for the indicated time points and a luciferase assay performed on the harvested cells as described in "Materials and Methods." Relative light units were normalized to protein expression as detected by the Bradford protein assay.

Figure 5A

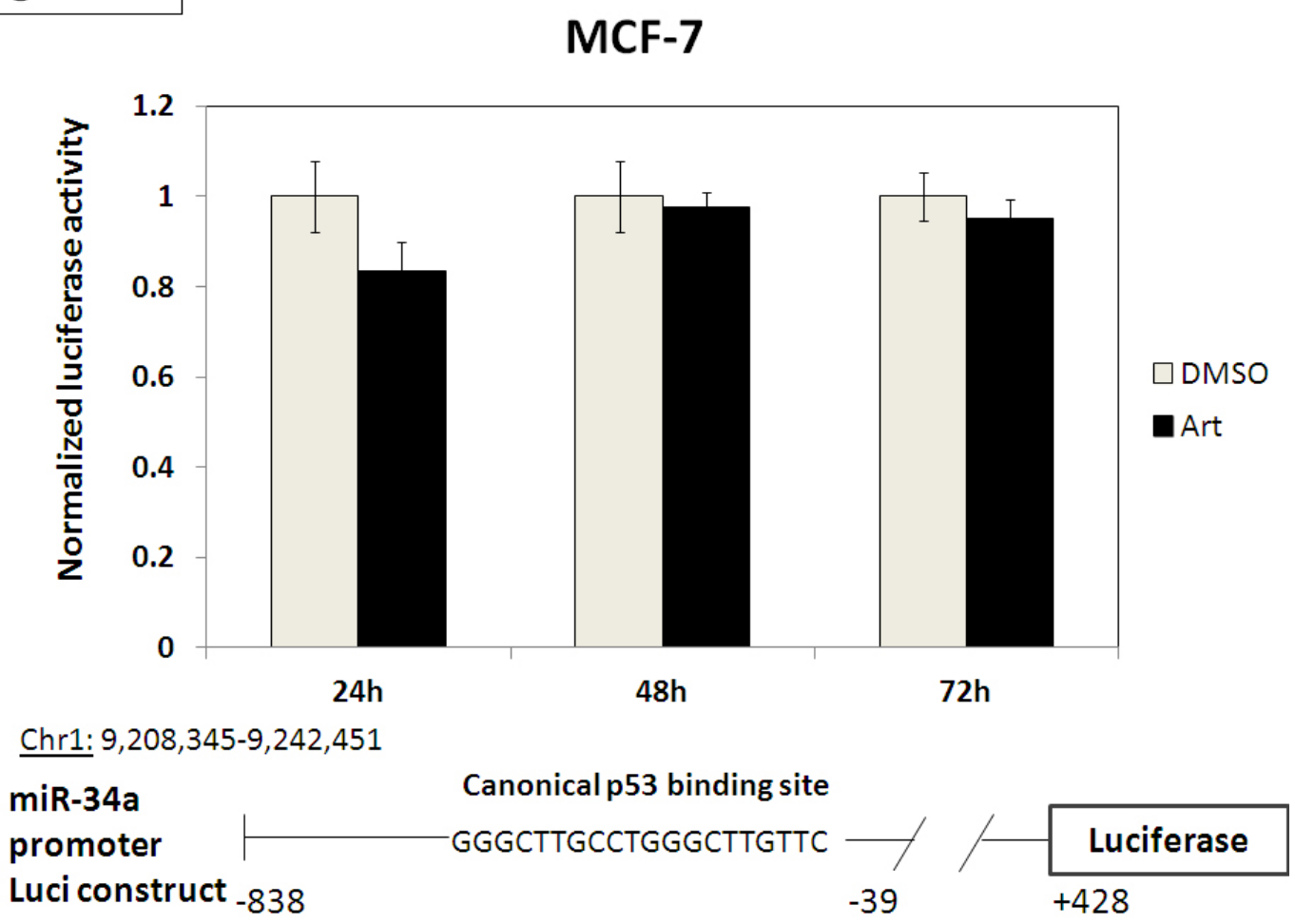
MCF-7
Normalized luciferase activity
1.2
1
0.8
0.6
0.4
0.2
0
24h
48h
72h
DMSO
Art
Chr1: 9,208,345-9,242,451
miR-34a
promoter
Luci construct
Canonical p53 binding site
GGGCTTGCCTGGGCTTGTTC
-838
-39
+428
Luciferase

Figure 5B

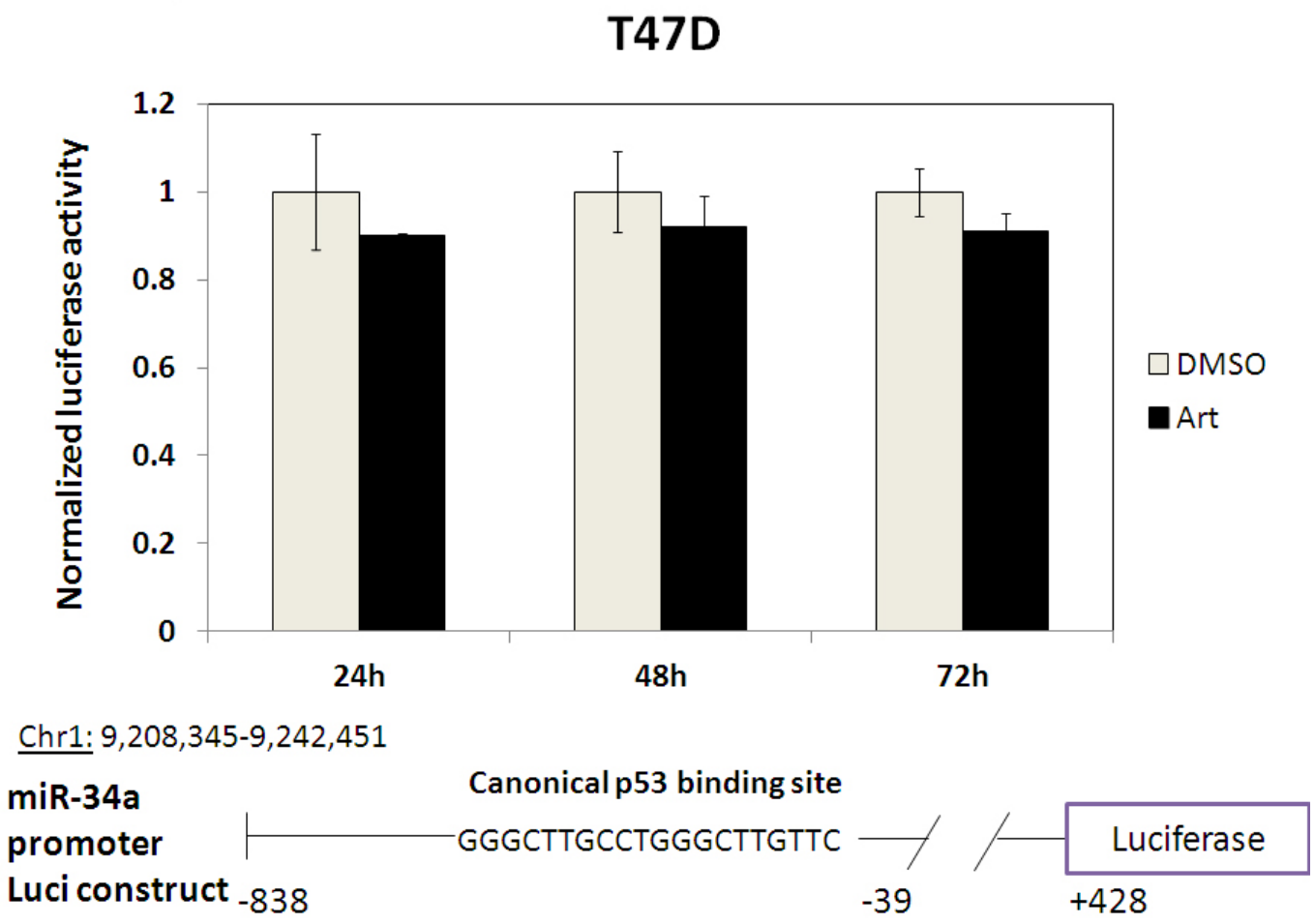
T47D
Normalized luciferase activity
1.2
1
0.8
0.6
0.4
0.2
0
24h
48h
72h
DMSO
Art
Chr1: 9,208,345-9,242,451
miR-34a promoter Luci construct
Canonical p53 binding site
GGGCTTGCCTGGGCTTGTTC
Luciferase
-838
-39
+428

Figure 6. Artemisinin upregulates primary miR-34a transcript levels. A) MCF-7 and **B)** T47D cells were treated with or without 300μM artemisinin for the indicated time points and total RNA extracted. The transcript levels of primary miR-34a (pri-34a) and GAPDH were determined by qualitative RT-PCR analysis using specific primers as described in "Materials and Methods." Products were fractionated by electrophoresis on a 1.5% agarose gel and visualized with an ultraviolet transilluminator. GAPDH was used as a loading control. Fold change in mature miR-34a levels as detected by Taqman qPCR analysis of the same RNA extracts is indicated.

Figure 6

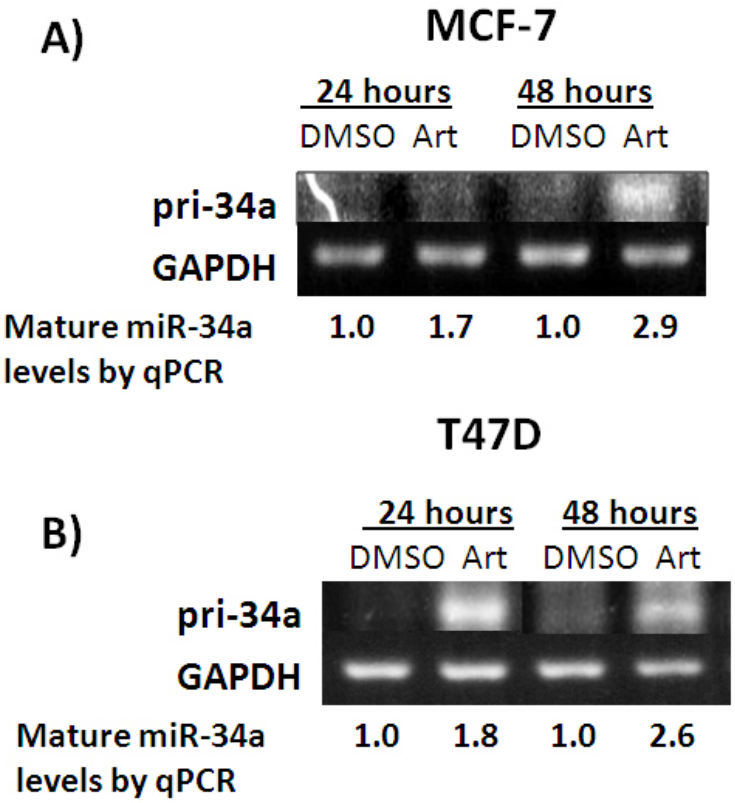
A)
MCF-7
24 hours
48 hours
DMSO Art DMSO Art
pri-34a
GAPDH
Mature miR-34a levels by qPCR
1.0 1.7 1.0 2.9
T47D
B)
24 hours
48 hours
DMSO Art DMSO Art
pri-34a
GAPDH
Mature miR-34a levels by qPCR
1.0 1.8 1.0 2.6

miR-34a inhibition reverses artemisinin mediated down-regulation of CDK4 and ERα

To determine the molecular mechanism by which miR-34a contributes to artemisinin mediated cell cycle arrest, MCF-7 and T47D cells were transfected with miR-34a inhibitors and target gene expression assessed by Western blot analysis. Cells were transfected with 100nM of miR-34a locked nucleic acid inhibitors (LNA's) or a non-specific control, and upon overnight incubation, treated with or without 300μM artemisinin for 48 hours. LNA's are non-translatable microRNA targets that reduce microRNA function by sequestering their target microRNA in highly stable heteroduplexes (Exiqon, Woburn, MA.) As described in a previous section, miR-34a induction by artemisinin correlates with a dose and time-dependent decrease in protein levels of the cell cycle regulators cyclin D1 and CDK4 as well as the hormone signaling component, estrogen receptor alpha (ERα) (Figure 3A-3B). All three proteins can regulate the G1 to S phase transition in the cell and cyclin D1 and CDK4 are confirmed direct targets of miR-34a inhibition (Melmed 2008, Hermeking 2007).

miR-34a inhibition in MCF-7 and T47D cells ablates artemisinin mediated down-regulation of CDK4 and attenuates ERα regulation (Figure 7A-7B). Cyclin D1 protein levels were downregulated by artemisinin in either cell line regardless of miR-34a inhibition and p53 protein expression remained the same (Figure 7C-7D). All of these data suggest that functional miR-34a is required for artemisinin mediated down-regulation of ERα and CDK4 in human breast cancer cells while having no effect on cyclin D1 or p53 expression.

miR-34a directly inhibits CDK4 expression upon artemisinin treatment

To confirm if artemisinin treatment mediates miR-34a inhibition of CDK4, MCF-7 and T47D cells were transfected with a luciferase construct containing the miR-34a binding site in CDK4 mRNA attached to the firefly luciferase gene (CDK4-34a Luci). In this assay, translation of luciferase mRNA will be inhibited if miR-34a binds to the CDK4 target site resulting in decreased light expression upon the addition of luciferase substrate. A luciferase construct containing a mutated version of the miR-34a binding site preventing miR-34a inhibition was used as a control for microRNA specificity (ΔCDK4-34a Luci). Vectors expressing luciferase under the control of an unregulated promoter or an empty neomycin vector were used as positive and negative controls.

Upon overnight incubation, transfected MCF-7 and T47D cells were treated with or without 300μM artemisinin for 48 hours. Cells were then harvested, a luciferase assay performed and relative light units normalized to protein expression. The results revealed that artemisinin significantly decreased luciferase activity in MCF-7 and T47D cells transfected with the CDK4-34a Luci construct while levels remained unchanged in artemisinin treated ΔCDK4-34a Luci cells (Figure 8). Such data suggests that artemisinin directly inhibits CDK4 translation through miR-34a mediated repression in human breast cancer cells.

Figure 7. Loss of functional miR-34a reverses artemisinin inhibition of CDK4 and ERα. MCF-7 and T47D cells were transfected with 100nM control or locked nucleic acid inhibitors (LNA's) against miR-34a and upon overnight incubation, treated with or without 300μM artemisinin for 48 hours. LNA's are non-translatable microRNA targets that reduce microRNA function by sequestering their target microRNA in highly stable heteroduplexes Western blot analysis was performed on protein extracts using antibodies specific to CDK4, ERα, p53, cyclin D1 and actin using the procedure described in "Materials and Methods." Protein expression of CDK4 and ERα in **A)** MCF-7 and **B)** T47D cells as well as expression of cyclin D1 and p53 in **C)** MCF-7 and **D)** T47D cells is depicted. Actin was used as a loading control.

Figure 7

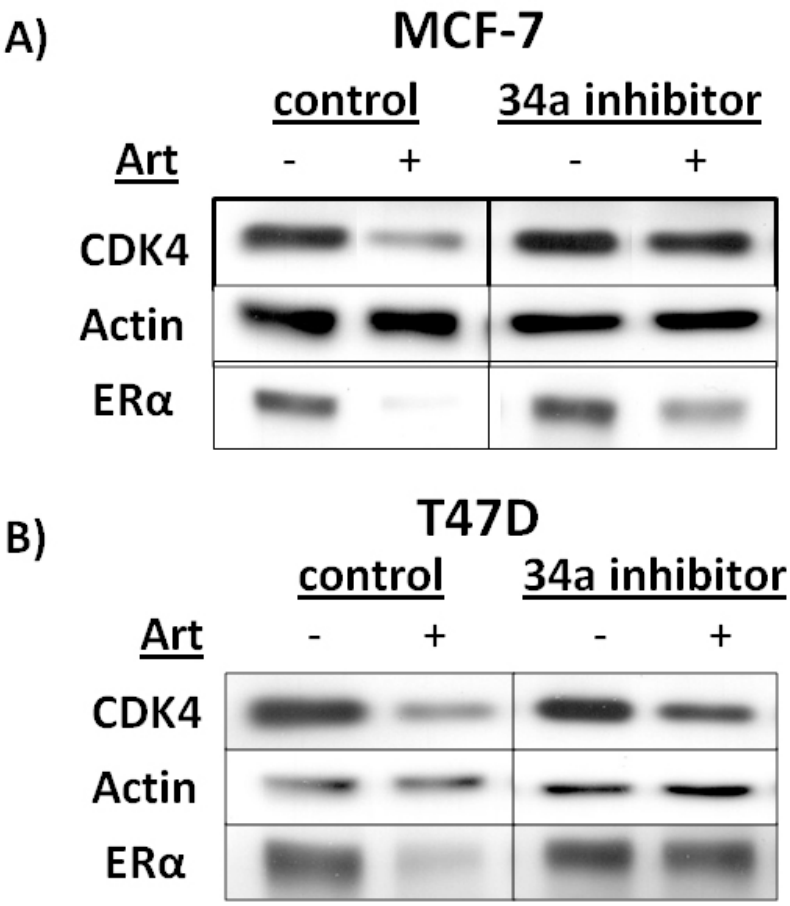
A)
MCF-7
control
34a inhibitor
Art
-
+
-
+
CDK4
Actin
ERα
B)
T47D
control
34a inhibitor
Art
-
+
-
+
CDK4
Actin
ERα

Figure 7

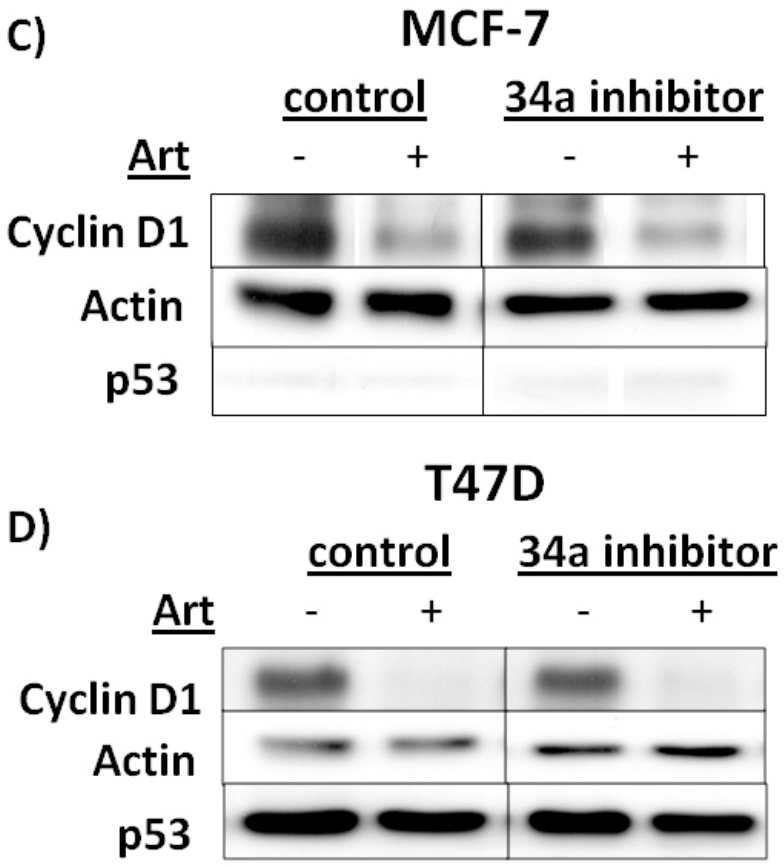
C)
MCF-7
control
34a inhibitor
Art
- + - +
Cyclin D1
Actin
p53
D)
T47D
control
34a inhibitor
Art
- + - +
Cyclin D1
Actin
p53

Figure 8. miR-34a directly inhibits CDK4 expression upon artemisinin treatment.
MCF-7 and T47D cells were transfected with a luciferase construct containing the miR-34a binding site in CDK4 mRNA attached to the firefly luciferase gene (CDK4-34a Luci) while a mutated version of the miR-34a binding site preventing miR-34a inhibition was used as a control for microRNA specificity (ΔCDK4-34a Luci). Upon overnight incubation, transfected MCF-7 and T47D cells were treated with or without 300μM artemisinin for 48 hours. Cells were then harvested, a luciferase assay performed as described in "Materials and Methods" and relative light units normalized to protein expression. Bar graphs represent average normalized protein expression of three independent experiments and error bars indicate standard deviation.

Figure 8

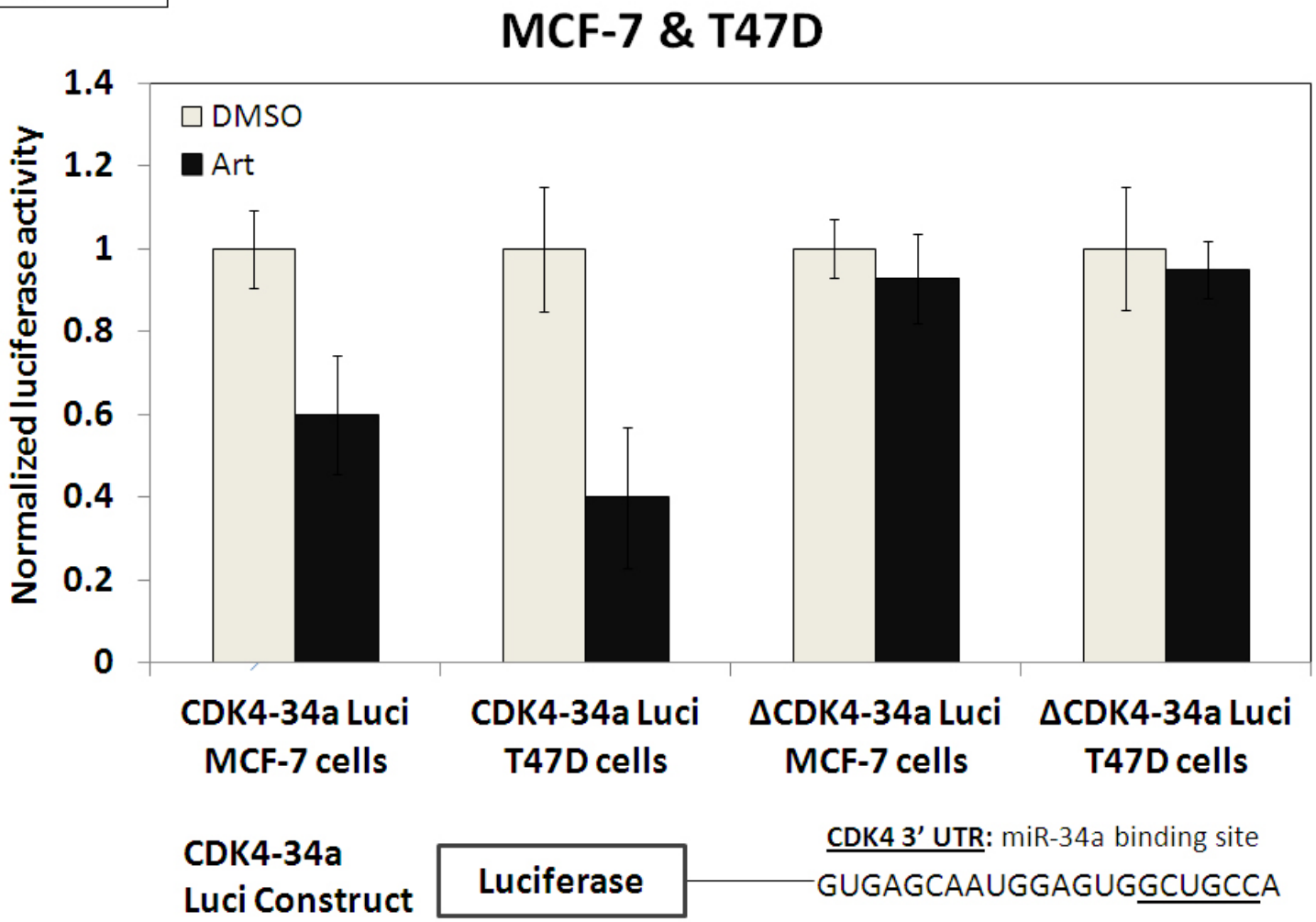
MCF-7 & T47D
Normalized luciferase activity
1.4
1.2
1
0.8
0.6
0.4
0.2
0
DMSO
Art
CDK4-34a Luci MCF-7 cells
CDK4-34a Luci T47D cells
ΔCDK4-34a Luci MCF-7 cells
ΔCDK4-34a Luci T47D cells
CDK4-34a Luci Construct
Luciferase
CDK4 3' UTR: miR-34a binding site
GUGAGCAAUGGAGUGGCUGCCA

DISCUSSION

The results of my study indicate that the tumor suppressive microRNA miR-34a is a key component of artemisinin mediated cell cycle arrest. Artemisinin treatment upregulated mature miR-34a levels in a dose and time-dependent manner that correlated with the growth arrest of human breast cancer cells and decrease in the proliferation regulatory proteins CDK4 and estrogen receptor alpha (ERα). Transfection of miR-34a inhibitors attenuated artemisinin mediated down-regulation of either protein, indicating a requirement for functional miR-34a in CDK4 and ERα inhibition. Luciferase assays in which cells were transfected with a constructs containing a wild-type or mutated miR-34a binding site for CDK4 downstream of the luciferase gene confirmed artemsinin mediates miR-34a inhibition of CDK4. Luciferase activity decreased in artemisinin treated cells transfected with the wild-type CDK4 binding site while no change was observed in those transfected with the mutated binding site, indicating miR-34a specific regulation.

Artemisinin induction of miR-34a appears to be p53-independent. Artemisinin can upregulate miR-34a expression levels in cell lines containing wild-type or mutant p53 and transfection of non-functional p53 into wild-type p53 cell lines does not affect miR-34a induction. In addition, artemisinin appears to transcriptionally regulate miR-34a expression in a promoter region outside the canonical p53 binding site. Luciferase activity was not detected in cells transfected with the p53 binding region of the miR-34a promoter regulating luciferase expression yet levels of primary miR-34a increased as detected by RT-PCR. The increase in primary transcripts upon artemisinin treatment suggests artemisinin regulates miR-34a gene expression in a region outside the p53 binding site.

All of these data suggest a novel p53-independent mechanism of miR-34a regulation. miR-34a activity has traditionally been associated with p53 functionality and transcriptional regulation (Hermeking 2009, He 2007-review). Genome-wide analysis for p53 induced miRNA, direct correlation of p53 status to miR-34a expression levels and identification of a consensus p53 binding site within the miR-34a promoter indicate miR-34a is an active component of the p53 tumor suppressor pathway (Bommer 2007, Chang 2007, Corney 2007, He 2007, Raver-Shapria 2007, Tarasov 2007). The implication of a p53-independent means of miR-34a regulation provides an exciting opportunity to therapeutically regulate miR-34a in p53 mutant cancers. A recent study of miR-34a transcription could provide alternate methods for regulating miR-34a expression. Christoffersen and colleagues demonstrated the ETS family transcription factor, Elk1 can upregulate miR-34a to mediate senescence of human primary fibroblasts independent of p53 status (Christoffersen 2010). Constitutive activation of B-RAF increased Elk1 interaction with identified binding sites in the miR-34a promoter, resulting in an upregulation in mature miR-34a levels and miR-34a mediated inhibition of c-Myc expression. miR-34a induction occurred in the presence of dominant-negative p53 or p53 siRNA, yet siRNA

mediated ablation of Elk-1 expression significantly impaired B-RAF induction of miR-34a. It remains to be seen if Elk-1 can regulate miR-34a levels in conjunction with cell cycle arrest or in the context of human breast cancer.

The loss of ERα expression upon miR-34a inhibition suggests a novel role for miR-34a in the regulation of hormonal signaling. ERα is a steroid receptor that encourages cell proliferation through transcriptional regulation of target genes involved in cell cycle progression, senescence, and apoptosis (Welboren 2009, Melmed 2008). Loss of ERα expression is associated with advanced stages of breast cancer however 80% of diagnosed cases are hormone responsive and estrogen receptor positive (American Cancer Society 2013). The MCF-7 and T47D cell lines utilized in this study are indicative of such cases (ER+, hormone responsive) and the observed artemisinin inhibition of ERα through miR-34a could represent a natural means of reducing the pro-proliferative estrogen response in these cancer types. While ERα itself does not possess a miR-34a binding site, a recent study suggests miR-34a can decrease ERα expression indirectly through translational inhibition of the ERα regulatory protein, lemur tyrosine kinase 3 (LMTK3) (Zhao 2013). LMTK3 is a serine-threonine-tyrosine kinase shown to regulate ERα expression by phosphorylation at residues that prevent proteosomal mediated degradation (Giamas 2011). LMTK3 can also influence ERα expression indirectly by decreasing Akt and protein kinase C (PKC) signaling to upregulate forkhead box O3 (FOXO3) transcription of the ERα promoter. Detection of LMTK3 expression levels in cells transfected with or without miR-34a inhibitors could provide an indication of whether this process is responsible for miR-34a mediated inhibition of ERα upon artemisinin treatment. Other microRNA that have been shown to regulate ERα expression in human breast cancer cells include miR-21, miR-221/222, miR-206, miR-375 and the miR-17-92 locus (Simonini 2010, Pandey 2009, Castellano 2009, Liu Zhao 2008, Adams 2007).

All of these data suggest that miR-34a regulation is a critical component of artemisinin mediated cell cycle arrest in human breast cancer cells. Such evidence not only further elucidates the potential of artemisinin as a treatment for p53 mutant breast cancer but suggests miR-34a could regulate hormonal signaling in a p53-independent manner.

CHAPTER 3

The Artemisinin Derivative Artesunate Inhibits Growth of Human Breast Cancer Cells and Upregulates miR-34a to Inhibit CDK4 with Enhanced Efficiency Compared to the Parent Compound

ABSTRACT

Artesunate is a semi-synthetic derivative of the sweet wormwood extract artemisinin that demonstrates enhanced efficiency in malaria treatment. The pro-apoptotic activity of artesunate against cancer cell lines and tumors has recently been demonstrated yet its ability to growth arrest cancer cells is still under investigation. This study demonstrates that artesunate growth arrests human breast cancer cells at concentrations far less than its parent compound. Cell cycle arrest correlates with a dose-dependent increase in the tumor suppressive microRNA, miR-34a, and decrease in protein levels of the cyclin dependent kinase, CDK4. Luciferase assays demonstrate that artesunate treatment directs miR-34a mediated inhibition of CDK4. Taken together, these data suggest that artesunate is more effective than artemisinin in growth arresting human breast cancer cells and that miR-34a mediated inhibition of CDK4 could be a mechanism for artesunates anti-proliferative activity.

INTRODUCTION

Artemisinin, a sesquiterpene lactone derived from the sweet wormwood plant *Artemisia annua*, has been successfully used as a malaria treatment since its isolation by the Chinese government in 1972. The processing of heme iron by the malaria parasite cleaves the endoperoxide bridge of the compound, releasing reactive oxygen species that irreparably damages the parasites food vacuole (Efferth 2009, Gautam 2009, Cui 2009, Meschnick 2002). Artemisinins poor solubility in water lead to the synthesis of more highly soluble derivates such as artesunate derived from a reduction of the compounds carbonyl group (Wells 2013 , McGovern 2010, Haynes 2007, Adjuik 2004). Artesunate is more effective at clearing malaria parasites than artemisinin and is currently the most highly used combination partner for malaria treatment (McGovern 2010, Efferth 2009, Haynes 2007).

The observation that cancer cells contain higher iron content than their primary tissue counterparts prompted researchers to investigate the anti-cancer activity of artesunate. Artesunate treatment has been shown to inhibit angiogenesis, reduce tumor growth and induce apoptosis in a variety of cancer cell lines and tumor models including leukemia, liver, lung, breast, melanoma and pancreatic cancer (McGovern 2010, Du 2010, Efferth 2009, Sundar 2009). Reactive oxygen species formation through endoperoxide cleavage has been shown to mediate artesunate apoptosis in lung and breast cancer cells however microarray as well as *in vitro* studies suggests artesunate treatment primarily induces its cytotoxic effects through the regulation of target genes (Zhou 2012, Hamacher-Brady 2011, Sundar 2009, Hou 2008, Nakase 2008, Anfosso 2006, Efferth 2003, Efferth 2002). Artesunate can inhibit angiogenesis by down-regulation of the vascular endothelial growth factor (VEGF) and its associated receptor while increasing the pro-apoptotic factor Bax to induce apoptosis in hepatoma cell lines (He 2011, Hou 2008, Chen 2004). Artesunate has also been shown to growth arrest cancer cells however the molecular mechanisms involved have yet to be fully elucidated. Two studies suggest that artesunate mediated growth arrest correlates with decreased expression of the cyclin-dependent kinase CDK4 in p53 mutant and p53 null cancer cell lines yet the upstream targets responsible for such regulation are currently unknown (Liu 2011, Hou 2008).

The following study demonstrates that artesunate growth arrests human breast cancer cells and downregulates expression of CDK4 through miR-34a mediated inhibition. Cell cycle arrest and miR-34a induction occur at much lower doses than artemisinin, indicating that artesunate is more effective than its parent compound in inhibiting the proliferation of breast cancer cells. Such data further elucidates the anti-cancer potential of artesunate while implicating a critical for tumor-suppressive microRNA.

MATERIALS & METHODS

Cell Culture

Cells were grown to sub-confluency in a humidified incubator at 37°C containing 5% CO2. MCF-7 and T47D cell lines were cultured as described by the American Tissue Culture Collection (Manassas, VA). Cells were treated for the indicated time points in complete medium with artemisinin or artesunate (Sigma, St. Louis, Missouri) dissolved 1000X in DMSO. Pure DMSO (Sigma-Aldrich, Milwaukee, WI) was used as a control. The medium was changed every 24 hours for the duration of each experiment.

Flow cytometry

For cell cycle analysis, attached and non-adherent cells treated in 6-well plates were collected within the media, rinsed with PBS and hypotonically lysed in 0.5 ml of propidium iodide buffer (0.5mg/ml propidium iodide, 0.1% sodium citrate, 0.05% Triton X-100). Samples were analyzed on a Beckman-Coulter (Fullerton, CA) EPICS XL flow cytometer with laser output adjusted to deliver 15 MW at 488 nm. Ten thousand cells were counted. Cell cycle analysis was then performed using MultiCycle software WinCycle 32 (Phoenix Flow Systems, San Diego, CA).

RNA extraction

Cells were harvested in 1.0 ml TRIzol reagent (Invitrogen, Carlsbad, CA) and total RNA extracted following the manufacturer's protocol with the phase separation procedure being performed twice to extract microRNA. Removal of contaminating DNA was performed on 10µg of extracted RNA using a DNA-free Kit (Invitrogen, Carlsbad, CA) per the manufacturer's protocol. RNA integrity was confirmed by running a 1.5% formaldehyde (Sigma Chemical, St. Louis, MO) denaturing agarose gel (Invitrogen, Carlsbad, CA) using 1µg of RNA per sample and visualizing intact bands corresponding to the molecular weights of the 28S and 18S subunits of ribosomal RNA, the most abundant RNA species. Gels contained GelRed Nucleic Acid Gel Stain (Biotium, Hayward, CA) diluted to a 2X concentration for band visualization using short wavelength ultraviolet light.

Reverse Transcription and PCR

Total RNA was reverse transcribed using stem loop primers for miR-34a, miR-34b and miR-34c as well as random primers for β-actin, a housekeeping gene insensitive to artesunate or artemisinin treatment. Each reverse transcriptase reaction contained 10XRT buffer, 100mM dNTPS, 50U/µl MultiScribe reverse transcriptase, and 20U/µl RNAse inhibitor (Applied Biosystems, Foster City, California) dissolved in nuclease-free water. The reverse transcription reaction for β-actin contained 100ng of purified total RNA as well as 10X random primers while the reaction for microRNA reverse transcription contained 560ng of purified total RNA and 5X miR-34a stem-loop RT primer (Applied Biosystems, Foster City, California). The microRNA

reactions were incubated in a thermal cycler for 30 minutes at 16°C, 30 minutes at 42°C, and 5 minutes at 85°C while reactions for the control gene were incubated for 10 minutes at 25°C, 120 minutes at 37°C, and 5 minutes at 85°C.

Real-time PCR reactions for each miRNA (10 µl volume) were performed in triplicate, and each reaction mixture included 4 µl of diluted RT product (1:2 dilution), 5 µl of 2X TaqMan Universal PCR Master Mix, 0.2 µM TaqMan probe, 1.5 µM forward primer, 0.7 µM reverse primer with the probes and primers specific to mature miR-34a, mature miR-34b, mature miR-34c or β-actin (Applied Biosystems, Foster City, CA). Reactions were incubated in an Applied Biosystems 7900HT Fast Real-Time PCR system in 96-well plates at 95°C for 10 min, followed by 40 cycles at 95°C for 15 seconds and 60°C for 1 min. Changes in fluorescence levels of miR-34 were normalized to β-actin, and fold changes compared between the target sample (miR-34 levels in cells treated with artemisinin or artesunate) and calibrator samples (miR-34 levels in DMSO treated cells).

Immunoblotting

Cell extracts were harvested in RIPA lysis buffer containing inhibitors, and standardized to 20-30ug protein using the Bradford protein assay. Equal protein amounts were subjected to SDS-PAGE on an 8% or 10% poly-acrylamide gel, transferred onto nitrocellulose membranes, and incubated for 1 hour at room temperature with blocking solution (5% milk dissolved in TBST). Primary antibodies to p53, HSP90 (Cell Signaling Technology, Beverly, MA) p21, CDK4, CDK6, and estrogen-receptor alpha (ERα) (Santa Cruz Biotechnologies, Santa Cruz, CA) were incubated overnight at 4°C. After three washes in 5% milk dissolved in TBST, membranes were incubated with anti-mouse or anti-rabbit horseradish peroxidase-conjugated antibodies for 1.5 hours at room temperature. Following an additional five washes in 5% milk, chemo luminescent signals were generated by incubation with Western Lightning ECL reagents according to the manufactures instructions (Perkin Elmer, Shelton, CT) and the results transferred to ECL-sensitive film (GE Healthcare, United Kingdom).

Transfections and Luciferase Assay

2µg of CDK4-miR-34a luciferase constructs were transfected into MCF-7 and T47D cells using Superfect reagent (Qiagen, Germantown, Maryland). Upon overnight incubation, cells were treated with or without 300µM artemisinin or varying doses of artesunate for 48 hours and harvested in ice-cold PBS. The cells were then centrifuged at 14,000 rpm for 5 minutes at 4°C, combined with 1X Passive lysis buffer, and Promega Luciferase assay performed according to the manufacturer's instructions (Promega, San Luis Obispo, CA). Relative light units were normalized to protein expression as determined by the Bradford protein assay. CDK4-miR-34a luciferase constructs were a kind gift of Dr. Lin He, University of California, Berkeley.

RESULTS

Artesunate growth arrests human breast cancer cells and downregulates CDK4

To determine the profile of artesunate mediated growth arrest in human breast cancer cells in comparison to artemisinin, MCF-7 (wild-type p53) and T47D (p53 mutant) human breast cancer cells were treated with or without 0.1μM-20.0 μM artesunate or 300μM artemisinin for 48 hours and flow cytometry analysis using propidium iodide staining performed to determine effects on the cell cycle. Both artemisinin and artesunate growth arrested MCF-7 and T47D cells in the G1 phase of the cell cycle with a concomitant decrease of cells in the S phase (Figure 1A-1D). Artesunate mediated growth arrest occurred in a dose-dependent manner with 10.0μM and 1.0μM causing the maximal effects in MCF-7 and T47D cells respectively (Figure 1A-1B). 10.0 μM artesunate and 300μM artemisinin increased the G1 cell cycle population of MCF-7 cells (Figure 1C) by 20-24% while 5.0 μM artesunate and 300μM artemisinin growth arrested T47D cells by approximately 15% (Figure 1D). Such data suggests that artesunate growth arrests human breast cancer cells at doses 30-100x less than artemisinin.

To determine artesunate effects on cell cycle regulatory proteins as well as p53 expression, Western blot analysis was performed on MCF-7 and T47D cells treated with or without 0.1μM-20.0 μM artesunate or 300μM artemisinin for 48 hours. The cyclin-dependent kinases CDK4 and CDK6 phosphorylate the retinoblastoma protein to regulate the G1 to S phase transition in the cell cycle while estrogen receptor-alpha (ERα) can influence cell cycle progression through transcriptional upregulation of target genes including cyclin D1 and the transcription factor c-Myc (Melmed 2008 Reed 1997). Previous research in our lab also showed that artemisinin treatment can downregulate ERα expression (Sundar 2008). CDK6 expression remain unchanged with artemisinin or artesunate treatment while CDK4 and ERα levels decreased in a dose-dependent manner with either phytochemical (Figure 2A-2B). p53 was undetected in MCF-7 cells (Figure 2A) while levels remained high in T47D cells (Figure 2B) consistent with the over-expression of mutant-type p53 in this cell line ((Lukashchuk 2007, Olivier 2010, Nigro 1989). p53 expression levels in T47D cells were not affected by artemisinin or artesunate treatment.

Figure 1. Artesunate growth arrests human breast cancer cells.
A) MCF-7 and **B)** T47D breast cancer cell lines were treated with or without 300μM artemisinin (Art) or the indicated concentrations of artesunate (AE) for 48 hours and subjected to flow cytometry analysis of the cell cycle as described in "Materials and Methods."The bar graphs indicate the average DNA content corresponding to the phases of the cell cycle as detected in three independent experiments. Error bars represent standard deviation. Representative flow cytometry profiles for 48 hour treatments with or without 300μM artemisinin and 10.0μM or 5.0μM artesunate are provided for **C)** MCF-7 and **D)** T47D cells.

Figure 1A

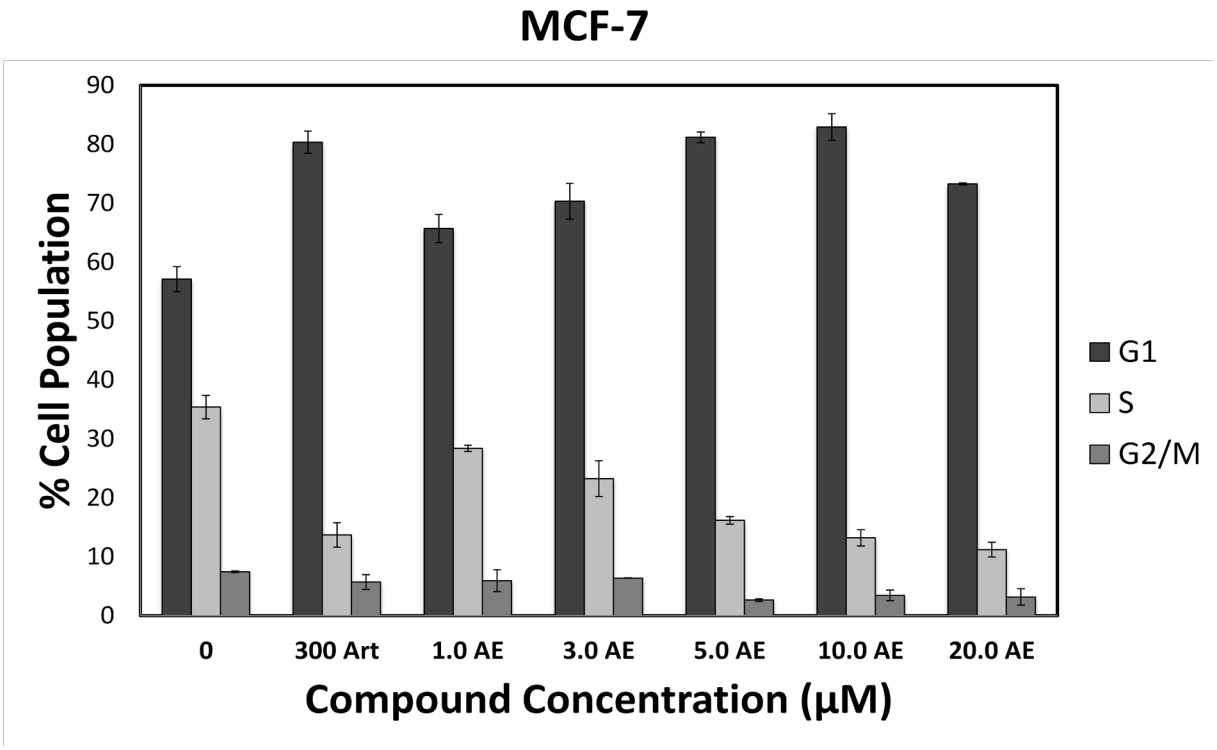

Figure 1B

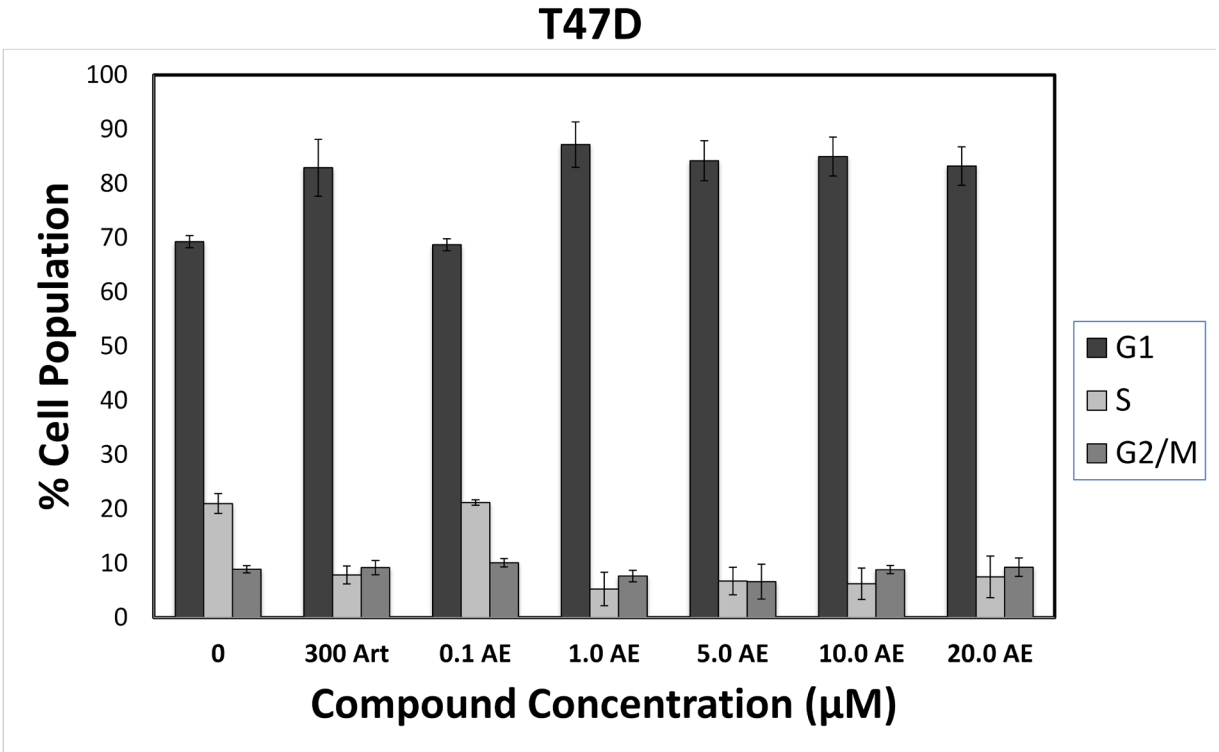

Figure 1C

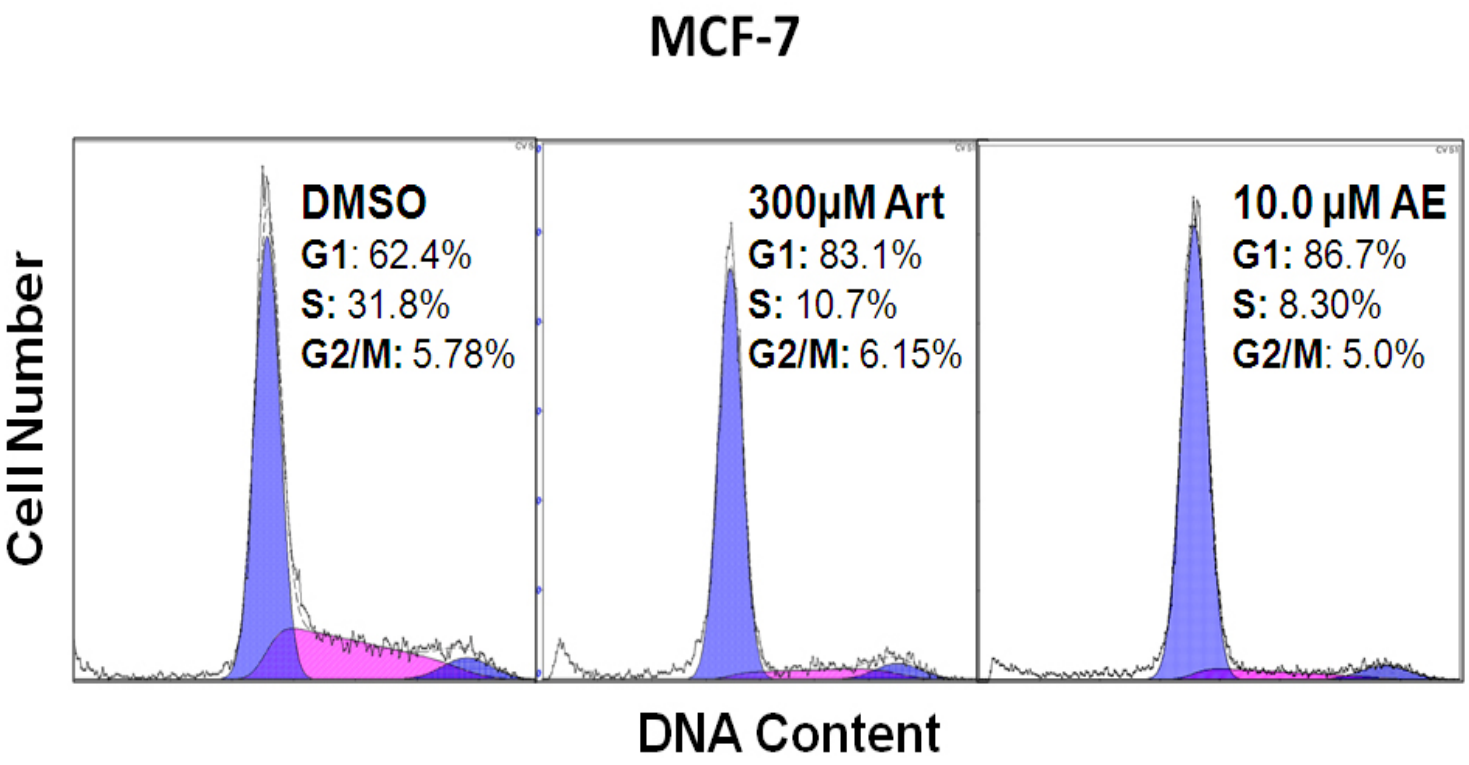
MCF-7
Cell Number
DMSO
G1: 62.4%
S: 31.8%
G2/M: 5.78%
300μM Art
G1: 83.1%
S: 10.7%
G2/M: 6.15%
10.0 μM AE
G1: 86.7%
S: 8.30%
G2/M: 5.0%
DNA Content

Figure 1D

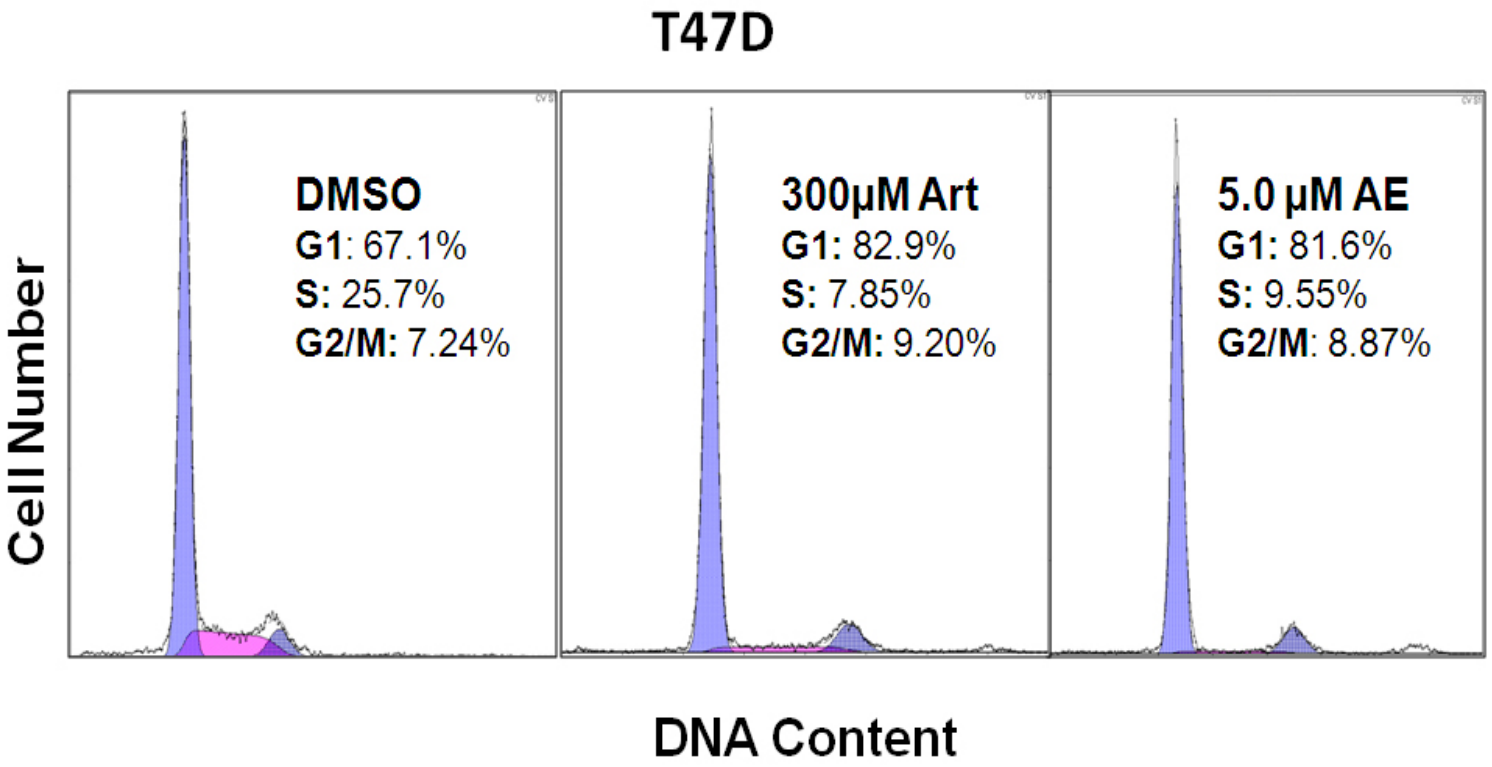
T47D
Cell Number
DMSO
G1: 67.1%
S: 25.7%
G2/M: 7.24%
300μM Art
G1: 82.9%
S: 7.85%
G2/M: 9.20%
5.0 μM AE
G1: 81.6%
S: 9.55%
G2/M: 8.87%
DNA Content

Figure 2. Artesunate downregulates CDK4 and ERα protein expression. A) MCF-7 cells and **B)** T47D cells were treated with or without 300μM artemisinin (Art) or the indicated concentrations of artesunate (AE) for 48 hours and protein levels of CDK4, CDK6, ERα, HSP90 and p53 determined by Western blot as described in "Materials and Methods." HSP90 was used as a loading control.

Figure 2A

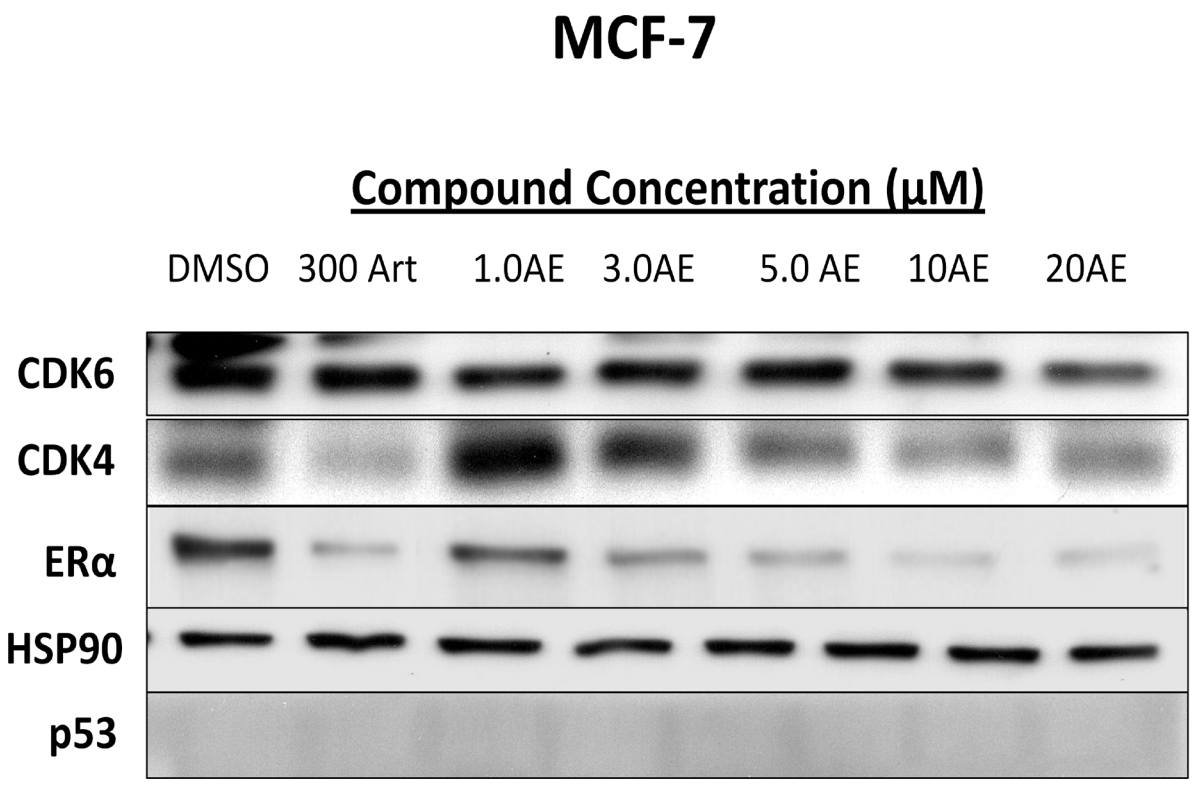
MCF-7
Compound Concentration (µM)
DMSO
300 Art
1.0AE
3.0AE
5.0 AE
10AE
20AE
CDK6
CDK4
ERα
HSP90
p53

Figure 2B

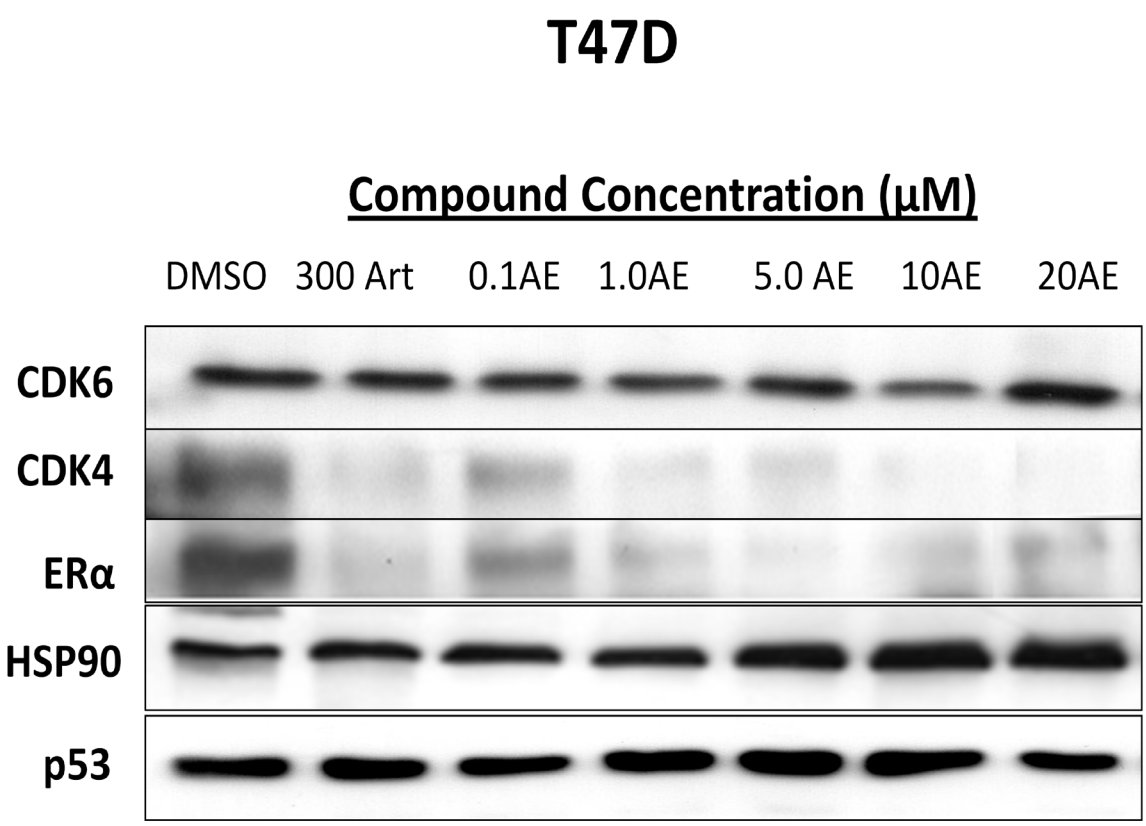
T47D
Compound Concentration (µM)
DMSO
300 Art
0.1AE
1.0AE
5.0 AE
10AE
20AE
CDK6
CDK4
ERα
HSP90
p53

Artesunate upregulates miR-34a in human breast cancer cells at lower concentrations than artemisinin

To assess the possibility of artesunate regulation of miR-34 family expression under conditions of cell cycle arrest, MCF-7 and T47D cells were treated with or without 0.1μM-20.0 μM artesunate or 300μM artemisinin for 48 hours and Taqman quantitative PCR analysis performed on extracted RNA. Total RNA was reverse transcribed using stem loop primers for miR-34a, miR-34b and miR-34c and the cDNA amplified in real-time using primers and dual-labeled fluorogenic probes specific to miR-34a, miR-34b, miR-34c or β-actin as a negative control. Changes in fluorescence levels of miR-34 were normalized to β-actin, and fold changes compared between the target sample (miR-34 levels in artemisinin and artesunate treated cells) and calibrator samples (miR-34 levels in DMSO treated cells). A fold-change of two is indicative of a significant change, thus artesunate upregulated miR-34a in a dose-dependent manner in MCF-7 cells (Figure 3A). Significant upregulation occurred at all artesunate doses with 10.0μM artesunate increasing miR-34a levels more than 2.5 fold, an induction greater than the approximately 2-fold increase mediated by artemisinin. miR-34a levels were also significantly upregulated by artesunate and artemisinin in T47D cells (Figure 3B). 5.0μM-20.0μM artesunate increased miR-34a levels by greater than 4-fold while artemisinin upregulated expression by approximately 3.5 fold. Maximal miR-34a induction in T47D cells occurred at nearly 7-fold with 5.0μM artesunate treatment, an increase nearly twice that of artemisinin. miR-34b levels were minimally affected by artesunate or artemisinin treatment in either cell line while mature miR-34c was undetected. Taken together, these data suggest that artesunate significantly upregulates miR-34a at lower doses and to greater expression levels than artemisinin in human breast cancer cells. miR-34a was significantly upregulated at doses correlating with artesunate mediated cell cycle arrest, suggesting it could play a critical role in the process.

Figure 3. Comparison of effectiveness of miR-34a expression in artesunate versus artemisinin treated cells. A) MCF-7and **B)** T47D cells were treated with or without 300μM artemisinin (Art) or the indicated concentrations of artesunate (AE) for 48 hours. Reverse transcription with stem-looped primers for each member of the miR-34 family or random primers for β-actin was performed on purified RNA extracts followed by Taqman semi-quantitative PCR using dual-labeled fluorogenic probes for mature miR-34a, miR-34b, miR-34c and β-actin, a housekeeping gene insensitive to artemisinin treatment. Triplicate results were normalized to expression of β-actin and bar graphs represent average fold change in miR-34a and miR-34b as determined in three independent experiments. miR-34c was undetected. The dotted line represents the two-fold significance threshold of microRNA experiments and error bars indicate standard deviation.

Figure 3A

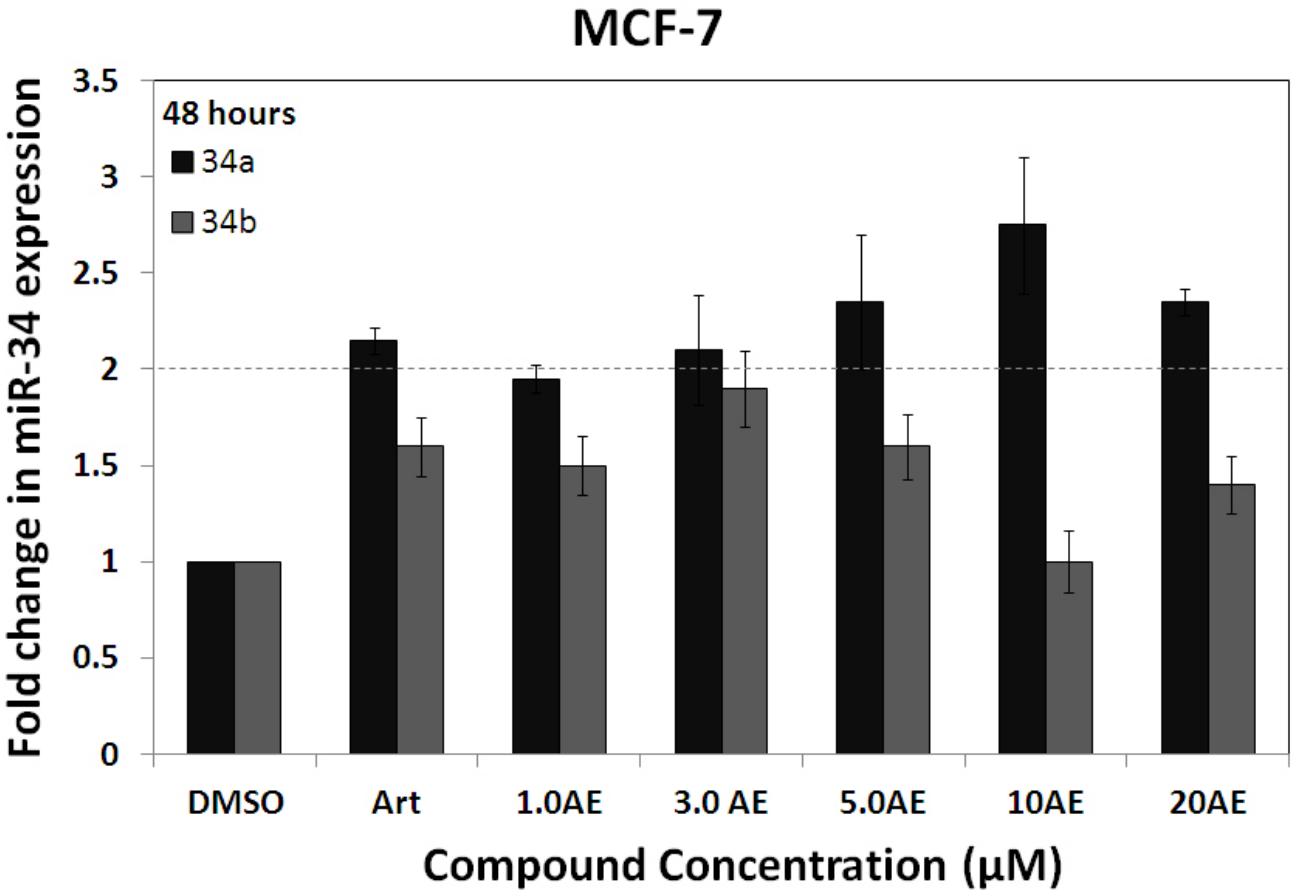
MCF-7
48 hours
34a
34b
Fold change in miR-34 expression
3.5
3
2.5
2
1.5
1
0.5
0
DMSO
Art
1.0AE
3.0 AE
5.0AE
10AE
20AE
Compound Concentration (µM)

Figure 3B

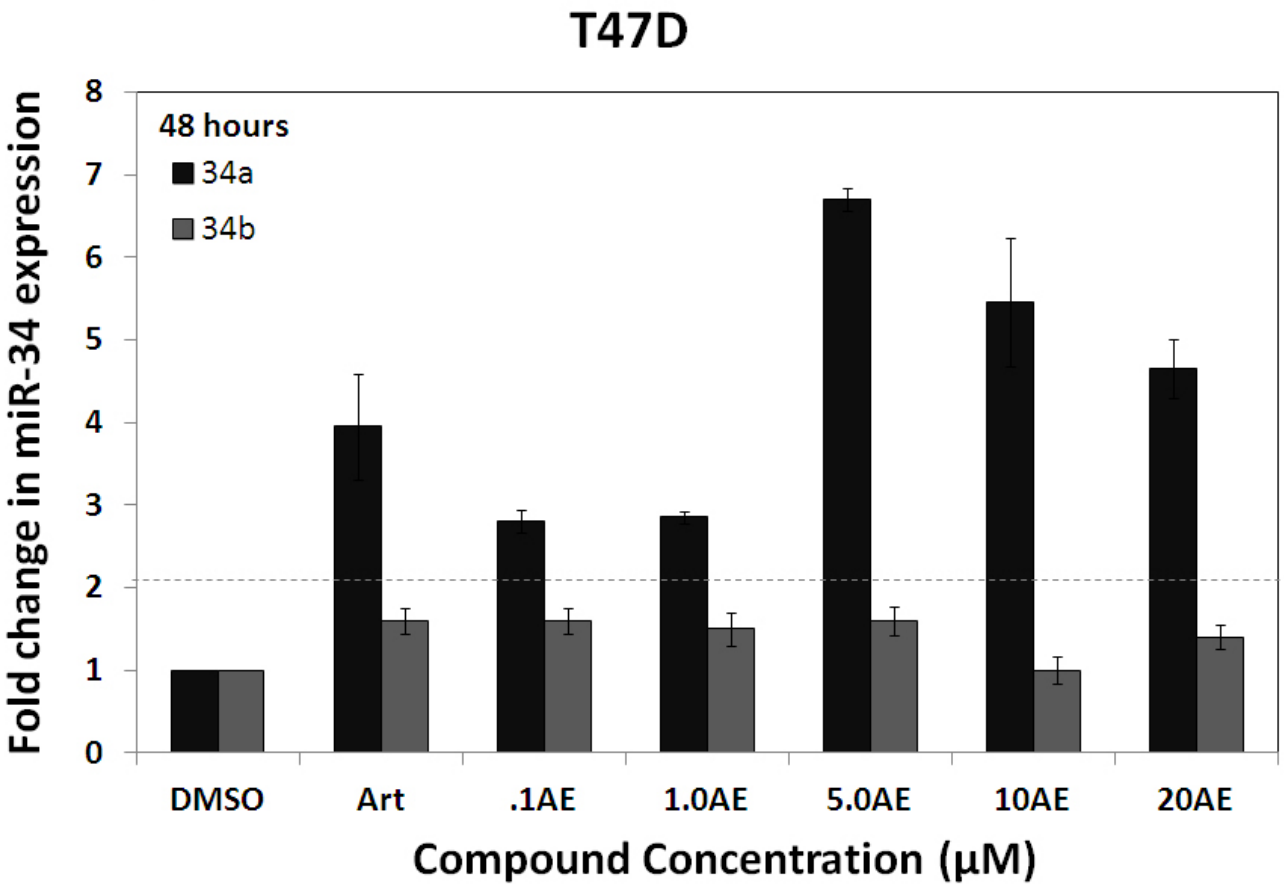
T47D
48 hours
34a
34b
Fold change in miR-34 expression
0
1
2
3
4
5
6
7
8
DMSO
Art
.1AE
1.0AE
5.0AE
10AE
20AE
Compound Concentration (µM)

miR-34a directly inhibits CDK4 upon artesunate treatment

CDK4 is a direct target of miR-34a translational inhibition (Hermeking 2007). To determine if artesunate treatment mediates miR-34a inhibition of CDK4, MCF-7 and T47D cells were transfected with a luciferase construct containing the miR-34a binding site in CDK4 mRNA attached to the firefly luciferase gene (CDK4-34a Luci). In this assay, translation of luciferase mRNA will be inhibited if miR-34a binds to the CDK4 target site resulting in decreased light expression upon the addition of luciferase substrate. A luciferase construct containing a mutated version of the miR-34a binding site preventing miR-34a inhibition was used as a control for microRNA specificity (ΔCDK4-34a Luci). Vectors expressing luciferase under the control of an unregulated promoter or an empty neomycin vector were used as positive and negative controls.

Upon overnight incubation, transfected MCF-7 and T47D cells were treated with or without artesunate or 300μM artemisinin for 48 hours. Cells were treated with doses at which artesunate maximally induced miR-34a expression levels, thus MCF-7 cells underwent 10μM and 20μM artesunate treatment while T47D cells were treated with 1.0uM or 5.0μM artesunate. Upon 48 hours of treatment, cells were harvested, a luciferase assay performed and relative light units normalized to protein expression. The results revealed that artemisinin and artesunate significantly decreased luciferase activity in MCF-7 and T47D cells transfected with the CDK4-34a Luci construct while levels remained unchanged in artemisinin or artesunate treated ΔCDK4-34a Luci cells (Figure 4A-4B). These data suggest that artemisinin and artesunate directly inhibits CDK4 translation in breast cancer cells and that such inhibition occurs through miR-34a mediated repression.1.0μM and 5.0μM artesunate reduced CDK4-34a-luci expression more substantially than artemisinin in T47D cells, indicating artesunate is more efficient at inhibiting CDK4 expression (Figure 4A). CDK4 expression was also inhibited by artesunate and artemisinin treatment of MCF-7 cells (Figure 4B). 20.0uM artesunate decreased CDK4-34a-luci activity by a nearly a third while 300 μM artemisinin was less effective, providing further evidence of the increased efficiency of artesunate in directing miR-34a mediated inhibition.

Figure 4. miR-34a directly inhibits CDK4 expression upon artesunate treatment.
MCF-7 and T47D cells were transfected with a luciferase construct containing the miR-34a binding site in CDK4 mRNA attached to the firefly luciferase gene (CDK4-34a Luci) while a mutated version of the miR-34a binding site preventing miR-34a inhibition was used as a control for microRNA specificity (ΔCDK4-34a Luci). Upon overnight incubation, transfected MCF-7 and T47D cells were treated with or without 300μM artemisinin (Art) or the indicated concentrations of artesunate (AE) for 48 hours. Cells were then harvested, a luciferase assay performed as described in "Materials and Methods" and relative light units normalized to protein expression. Bar graphs represent average normalized protein expression of three independent experiments in **A)** T47D and **B)** MCF-7 cells while error bars indicate standard deviation.

Figure 4A

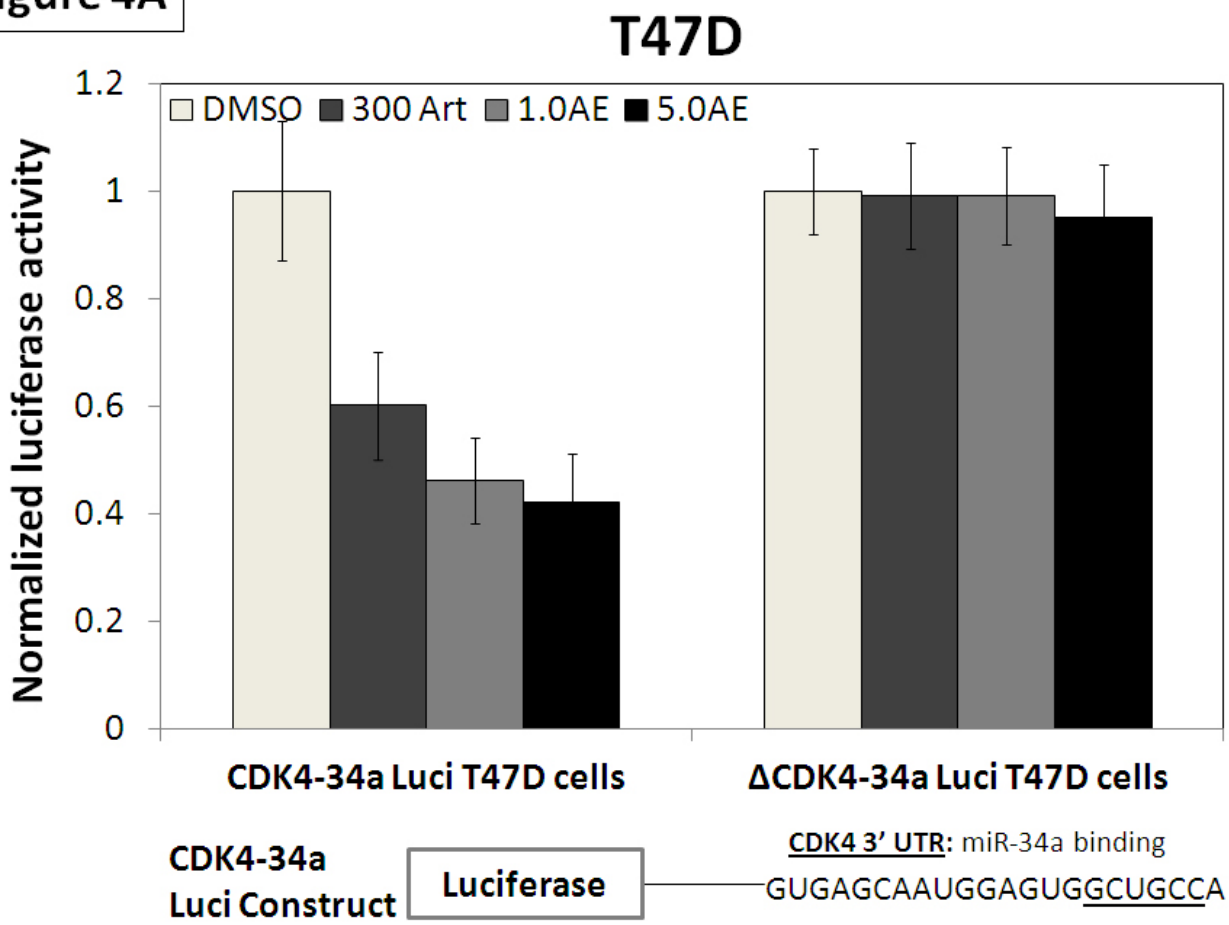
T47D
DMSO
300 Art
1.0AE
5.0AE
Normalized luciferase activity
1.2
1
0.8
0.6
0.4
0.2
0
CDK4-34a Luci T47D cells
ΔCDK4-34a Luci T47D cells
CDK4-34a
Luci Construct
Luciferase
CDK4 3' UTR: miR-34a binding
GUGAGCAAUGGAGUGGCUGCCA

Figure 4B

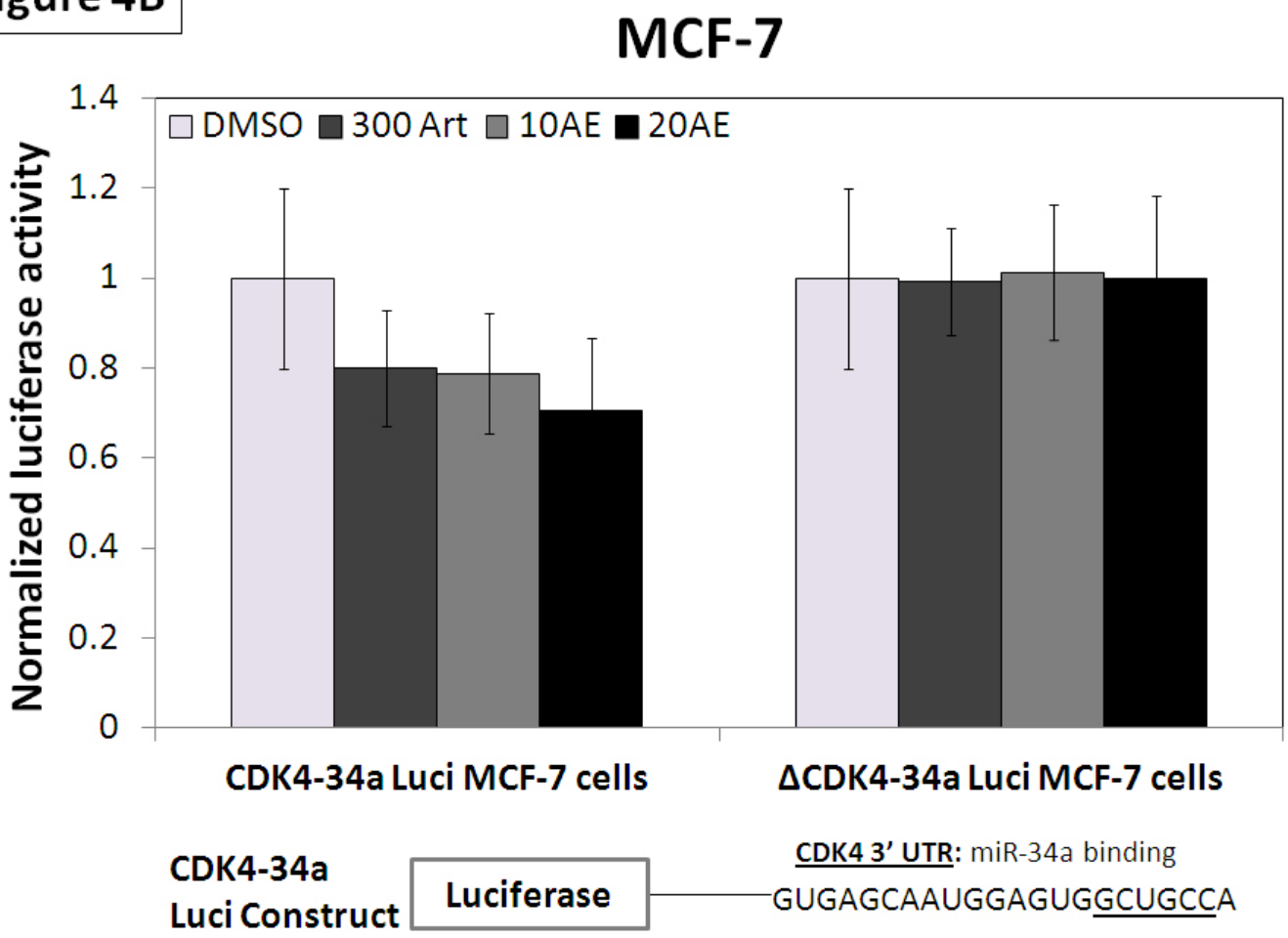
MCF-7
DMSO
300 Art
10AE
20AE
Normalized luciferase activity
1.4
1.2
1
0.8
0.6
0.4
0.2
0
CDK4-34a Luci MCF-7 cells
ΔCDK4-34a Luci MCF-7 cells
CDK4-34a
Luci Construct
Luciferase
CDK4 3' UTR: miR-34a binding
GUGAGCAAUGGAGUGGCUGCCA

DISCUSSION

My study demonstrates that artesunate growth arrests human breast cancer cells and regulates the tumor suppressive microRNA miR-34a. Upregulation of miR-34a occurs in a dose-dependent manner that correlates with a G1 cell cycle arrest and down-regulation of the growth promoting proteins estrogen receptor alpha (ERα) and CDK4. Luciferase assays in which cells were transfected with constructs containing a wild-type or mutated miR-34a binding site for CDK4 downstream of the luciferase gene confirmed artesunate mediates miR-34a inhibition of CDK4. Luciferase activity decreased in artesunate treated cells transfected with the wild-type CDK4 binding site while no change was observed in those transfected with the mutated binding site, indicating miR-34a specific regulation. Artesunate induction of miR-34a appears to p53-independent as artesunate can upregulate miR-34a expression levels in cell lines containing wild-type or mutant p53.

Artesunate exerted its growth inhibitory effects as well as regulation of miR-34a at concentrations 30-100X less than artemisinin. This indicates enhanced efficiency over the parent compound, a finding that correlates with the increased efficiency of artesunate over artemisinin in its activity as a malaria treatment (McGovern 2010, Efferth 2009, Haynes 2007). Artesunate is also more water-soluble than artemisinin and is currently undergoing clinical trials for the treatment of metastatic breast cancer (ClinicalTrials.gov). The results of the current study provide further evidence for the anti-cancer activity of artesunate while implicating the use of miR-34a as a diagnostic tool to determine phytochemical treatment. Future directions include identifying the p53-independent mechanism of miR-34a induction as well as additional cell cycle regulatory proteins that are affected by miR-34a inhibition.

FUTURE DIRECTIONS

The studies presented in this dissertation provide direct evidence that the tumor suppressive microRNA miR-34a is involved in the anti-cancer effects of the phytochemicals indole-3-carbinol (I3C), artemisinin and artesunate. miR-34a is critical for I3C mediated growth inhibition and artemisinin inhibition of the cyclin-dependent kinase CDK4 while mediating CDK4 downregulation by artesunate in human breast cancer cells. My studies also suggest that miR-34a can be regulated in a p53-independent manner as artemsinin and artesunate can upregulate miR-34a in cells containing mutant or dominant negative p53. These data suggest tumor suppressive microRNA play a critical role in the anti-proliferative effects of phytochemicals and that the canonical p53 dependent pathway of miR-34 regulation is not the only means to regulate this microRNA family. Future directions of this project could be as follows:

In-vivo experiments: Animal models can be utilized to determine the role of miR-34a on the anti-tumorigenic effects of phytochemicals. Immunodeficient nude mice could be xenografted with human breast cancer cell lines containing wild-type or mutant p53 as well as wild-type or depleted miR-34a expression. MiR-34a knockdown cells would be generated via stable transfection of cells with lentiviral vectors expressing decoy miR-34a targets in the 3'UTR of green fluorescent protein (GFP). Lentiviral vectors enable decoy integration into the genome, permitting stable expression of non-functional miRNA targets and thus continuous repression of target miRNA activity (Gentner 2009). In effect, transfected cells will become saturated with exogenous, non-translatable targets, causing endogenous targets to be re-expressed by lack of microRNA repression. To assess vector transfection efficiency, fluorescence levels of GFP will be standardized to the copy number of GFP mRNA. Fluorescence levels will be detected by fluorescence activated cell sorting (FACS) while quantitative PCR will be used to determine GFP mRNA copy number. If the knockdown is successful, miR-34a knockdown cells should have low fluorescence levels, due to miR-34 mediated repression of the GFP-miRT construct. Confirmed miR-34a knockdown cells would then be transfected into immunodeficient nude mice. Upon tumor development to a palpable size, each mouse will receive daily subcutaneous injections of I3C, artemisinin, artesunate or DMSO, using concentrations equivalent to the amount shown previously to decrease tumor formation in mouse models exhibiting that particular cell type. Weekly observations will be made of body weight, tumor size and tumor volume. After a cell-type specific treatment period for maximal phytochemical affects, excised tumors will be weighed, measured for size, gross observations made regarding level of vascularization and Western blot and quantitative RT-PCR performed on extracted tissues to assess levels of total and active p53, mature miR-34a and phytochemically induced miR-34a repressed cell cycle regulators such as CDK4. If miR-34a is critical for artesunate, artemisinin or I3C mediated tumor reduction, levels of miR-34a should increase in wild-type xenografts while tumor volume and size would remain unchanged upon phytochemical treatment in xenografts

derived from miR-34a knockdown cells. p53 mutant xenografts may be resistant to I3C treatment given this dissertations evidence that functional p53 is required for miR-34a induction.

An alternate mechanism of *in vivo* analysis would be to generate a miR-34a knockout mouse and determine phytochemical responsiveness. The mouse could be generated by incorporating Cre-lox recombination of a miR-34a deletion cassette into a nude mouse model. Human breast cancer xenografts would then be generated and upon tumor development to a palpable size, each mouse would receive daily subcutaneous injections of I3C, artemisinin, artesunate or DMSO, using concentrations equivalent to the amount shown previously to decrease tumor formation in mouse models exhibiting that particular cell type.. If miR-34a is critical for the anti-tumorigenic effects of artemisinin, artesunate and I3C, tumor volume upon excision should be similar between phytochemically treated and control treated mice.

Identification of p53-independent mechanism of miR-34a regulation: Research in this dissertation showed artemisinin can upregulate mature miR-34a levels in p53-mutant cell lines, while assessment of primary miR-34a levels suggested artemisinin upregulates miR-34a on a transcriptional level. To identify the transcriptional mechanism of artemisinin mediated mR-34a regulation, computational analysis of the miR-34a promoter region could be performed to identify potential binding sites of known artemisinin regulated transcription factors such as Sp-1, E2F1 and NFκB (Tran 2013, Tin 2012, Willoughby 2009). Chromatin immunoprecipitation would then be performed on artemisinin treated breast cancer cells using antibodies for the identified transcription factors under conditions of miR-34a induction. Increased binding to the identified sites in the miR-34a promoter for a specific transcription factor upon artemisinin treatment could indicate its involvement in miR-34a regulation. siRNA of the transcription factor should attenuate artemisinin mediated miR-34a induction and would confirm this hypothesis. Each of these experiments should be performed in both p53 wild-type and p53 mutant breast cancer cell lines to re-confirm p53 is not involved in the process of miR-34a induction.

Biopsy evaluation for miR-34a requirement in phytochemical sensitivity: Biopsies of breast cancer patients with various disease states could be utilized to determine phytochemical responsiveness in correlation with miR-34a and p53 gene status. The p53 gene is mutated in nearly half of all human tumors while CpG methylation of the miR-34a promoters has been detected in the most commonly diagnosed carcinomas (Serra 2012, Vogt 2011, Olivier 2010, Lodygin 2008, Toyota 2008, Lujambio 2008, Kozaki 2008, Vogelstein 2000). The shared chromosomal locus of miR-34a and p53 (1p36) is also one of the most frequently deleted in cancer (Wong 2011, Hermeking 2009, He-review 2007, Welch 2007, Chang 2007, Bommer 2007). Biopsies would be assessed for miR-34a gene expression by Taqman qPCR detection of mature miR-34a levels while promoter methylation status would be determined through bisulfate sequencing. Karyotyping using fluorescent probes specific to the miR-34a and p53 genes would detect the shared chromosomal locus of both genes (1p36) while Western blot analysis and protein sequencing analysis could determine p53 expression and mutation status. Primary cell

lines would then be derived from biopsies with differing miR-34a or p53 gene status and the phytochemical responsiveness determined through flow cytometry, qPCR and Western blot analysis upon artemisinin, artesunate, or I3C treatment. It would be interesting to see if phytochemical mediated inhibition of cell growth was altered in any way due to changes in miR-34a or p53 gene status.

Expansion into other cancer types: Phytochemical regulation of miR-34 could also be assessed in other cancer types. Two possibilities are lung or prostate cancer, disease states that often express low levels of the miR-34 family and are responsive to I3C, artemisinin and artesunate treatment (Hahn 2013, Gaofolo 2013, Kasinki 2012, Hermeking 2009, Kokhlin 2008, Gao 2013, Willoughby 2009, Kassie 2010, Choi 2010, Adler 2011, Wu 2012, Wang 2012, Zhou 2012, Zhao 2011, Efferth 2001). Cell cycle analysis, miR-34 and p53 expression status and miR-34 target gene expression would be determined by flow cytometry, Taqman qPCR, and Western blot analysis. It would be interesting to see if miR-34b or miR-34c were significantly regulated by any of these phytochemicals in addition to miR-34a and if any member of this tumor suppressive microRNA family could affect phytochemically induced apoptosis.

REFERENCES

1. Colozza M, et al (2008). Aromatase inhibitors: a new reality for the adjuvant endocrine treatment of early-stage breast cancer in postmenopausal women. *Mini Rev Med Chem* 8, 564-574.
2. Croce, C.M. and George Adrian Calin. (2006). MicroRNA-Cancer Connection: The beginning of a new tale. *Cancer Research.* 66, 7390-7394**.**
3. He, et al. (2007). microRNAs join the p53 network-another piece in the tumor-suppression puzzle. *Nature Reviews Cancer.* 7, 819-822.
4. Kim VN, Han J and Mikiko C. Siomi. (2009). Biogenesis of small RNAs in animals. *Nature Reviews Molecular Cell Biology* 10, 126-139.
5. Yates LA, Norbury CJ and Robert JC Gilbert. (2013). The Long and Short of MicroRNA. *Cell* 153, 516-519.
6. Zinovyev A, et al. (2013). Mathematical modeling of microRNA-mediated mechanisms of translational repression. *Adv Exp Med Biol* 774, 189-224.
7. Filipowicz W., Bhattacharyya S.N., and N, Sonenberg (2008). Mechanisms of post-transcriptional regulation by microRNAs: are the answers in sight? *Nat.Rev. Genet*. 9, 102–114.
8. Lujambio A, and Scott W. Lowe. (2012). The microcosmos of cancer. *Nature* 482, 347-355.
9. Friedman RC, et al. (2009). Most mammalian mRNAs are conserved targets of microRNAs. *Genome Research* 19, 92-105.
10. Lewis B, Burge C and Bartel D (2005). Conserved seed pairing, often flanked by adenosines, indicates that thousands of human genes are microRNA targets. *Cell* 120, 15-20.
11. Xie X, et al (2005). Systematic discovery of regulatory motifs in human promoters and 3' UTRs by comparison of several mammals. *Nature* 434, 338-345.
12. Aranha MM, et al (2011). miR-34a regulates mouse neural stem cell differentiation. *PLoS One* 6:e21396.
13. Bak M, et al (2008). MicroRNA expression in the adult mouse central nervous system. *RNA* 14, 432-444.
14. Bommer GT, et al (2007). p53-mediated activation of miRNA-34 candidate tumor-suppressor genes. *Current Biology* 17, 1298-1307.
15. Bouhallier F, et al (2011). Role of miR-34c microRNA in the late steps of spermatogenesis. *RNA* 16, 720-731.
16. Caraval LA and JJ Manfredi (2013). Another fork in the road--life or death decisions by the tumour suppressor p53.*EMBO Rep* 14, 414-21.
17. Chang TC, et al (2007). Transactivation of miR-34a by p53 broadly influences gene expression and promotes apoptosis. *Molecular Cell* 26, 745-752.
18. Corney DC, et al (2007). MicroRNA-34b and MicroRNA-34c are targets of p53 and cooperate in control of cell proliferation and adhesion-independent growth. *Cancer Research* 67, 8433-8488.
19. Courteau LA, Storey KB, and Morin P Jr (2012). Differential expression of microRNA species in a freeze tolerant insect, Eurosta solidaginis. *Cryobiology* 65, 210-214.

20. Fujita Y, et al (2008). Effects of miR-34a on cell growth and chemoresistance in prostate cancer PC3 cells. *Biochemical and Biophysical Research Communications* 377, 114-119.
21. Hermeking, H (2009). The miR-34 family in cancer and apoptosis. *Cell Death and Differentiation* 17, 193-199.
22. Hermeking, H (2007). p53 enters the microRNA world. *Cancer Cell* 12, 414-418.
23. He L, et al (2007). A microRNA component of the p53 tumor suppressor network. *Nature* 447, 1130-1134.
24. He L, et al (2007). microRNAs join the p53 network-another piece in the tumor-suppression puzzle. *Nature Reviews Cancer* 7, 819-822.
25. Jiang P, et al (2012). MiR-34a inhibits lipopolysaccharide-induced inflammatory response through targeting Notch1 in murine macrophages. *Exp Cell Res* 318, 1175-1184.
26. Lujambio A, et al. A microRNA DNA methylation signature for human cancer metastasis. *PNAS USA* 105, 13556-13561.
27. Luan S, Sun L, and Fengping Huang (2010). microRNA-34a: a novel tumor suppressor in p53-mutant glioma cell line U251. *Archives of Medical Research* 41, 67-74.
28. Liu N, et al (2012). The microRNA miR-34 modulates ageing and neurodegeneration in Drosophila. *Nature* 482, 519-523.
29. Lodygin D, (2008). Inactivation of miR-34a by aberrant CpG methylation in multiple types of cancer. *Cell Cycle* 7, 2591–2600.
30. Lyons PJ, et al (2013). Identification of differentially regulated microRNAs in cold-hardy insects. *Cryo Letters* 34, 83-89.
31. Miska EA, *et al* (2004). Microarray analysis of microRNA expression in the developing mammalian brain. *Genome Biol* 5, R68.
32. Olivier M, Hollsetin M and P Hainaut (2010). Tp53 mutations in human cancers: origins, consequences and clinical use. *Cold Spring Harb Perspect Biol* 2, a001008.
33. Raver-Shapira N, et al. (2007). Transcriptional activation of miR-34a contributes to p53-mediated apoptosis. *Molecular Cell* 26, 731-743.
34. Rao D, et al (2010). microRNA-34a perturbs B lymphocyte development by repressing the forkhead box transcription factor Foxp1. *Immunity* 33, 48-59.
35. Riley T, et al (2008). Transcriptional control of human p53-regulated genes. *Nat Rev Mol Cell Bio* 9, 402-412.
36. Sempere L, et al (2004). Expression profiling of mammalian microRNAs uncovers a subset of brain-expressed microRNAs with possible roles in murine and human neuronal differentiation. *Genome Biol* 5, R13.
37. Serra PL and M Esteller (2012). DNA methylation-associated silencing of tumor-suppressor microRNAs in cancer. *Oncogene* 31, 1609-1622.
38. Soni K, et al (2013). miR-34 is maternally inherited in Drosophila melanogaster and Danio rerio. *Nucleic Acids* 41, 4470-4480.
39. Stadanlick JE, et al (2011). Developmental arrest of T cells in Rpl22-deficient mice is dependent upon multiple p53 effectors. J Immunol, 187, 664-675.
40. Tarantino C, et al (2010). miRNA34a, 100, and 137 modulate differentiation of mouse embryonic stem cells. *FASEB* 24, 3255-3263.
41. Tarasov V, et al (2007). Differential regulation of microRNAs by p53 revealed by massively parallel sequencing: miR-34a is a p53 target that induces apoptosis and G1-arrest. *Cell Cycle* 6, 1586-1593.

42. Toyota M, et al (2008). Epigenetic silencing of the microRNA-34b/c and B-cell translocation gene is associated with CpG island methylation in colorectal cancer. *Cancer Res* 68, 4123-4132.
43. Vogelstein B, Lane D and AJ Levine (2000). Surfing the p53 network. *Nature* 408, 307-310.
44. Vogt M, et al (2011). Frequent concomitant inactivation of miR-34a and miR-34b/c by CpG methylation in colorectal, pancreatic, mammary, ovarian, urothelial, and renal cell carcinomas and soft tissue sarcomas. *Virchows Arch* 458, 313-322.
45. Wei J, et al (2012). miR-34s inhibit osteoblast proliferation and differentiation in the mouse by targeting SATB2. *J Cell Bio* 197, 509-521.
46. Wong, et al (2011). microRNA-34 family and treatment of cancers with mutant or wild-type p53. *International Journal of Oncology* 38, 1189-1195.
47. Yamakuchi M and CJ Lowenstein (2009). MiR-34, SIRT1 and p53: the feedback loop. *Cell Cycle*. 8, 712-725.
48. Yamakuchi M, Ferlito M, and CJ Lowenstein (2008). miR-34a repression of SIRT1 regulates apoptosis. *PNAS* 105, 13421-13426.
49. Zhao T, Li J, and Alex F. Chen (2010). microRNA-34a induces endothelial progenitor cell senescence and impedes it angiogenesis via suppressing silent information regulator 1. *Am J Physiol Endocrinol* 299, e110-e116.
50. Dawood S, Hu R, Homes MD, et al. (2011). Defining breast cancer prognosis based on molecular phenotypes: results from a large cohort study. *Breast Cancer Res Treat* 126, 185-92.
51. Carey LA, Perou CM, Livasy CA, et al. (2006). Race, breast cancer subtypes, and survival in the Carolina Breast cancer Study. *JAMA*. 295, 2492-2502.
52. O'Brien KM, et al. (2010) Intrinsic breast tumor subtypes, race, and long-term survival in the Carolina Breast Cancer Study. *Clin Cancer Res*. 24, 6100-10.
53. Koboldt DC, Fulton RS, McLellan MD, et al. (2012). Cancer Genome Atlas Network. Comprehensive molecular portraits of human breast tumours. *Nature*. 490, 61-70.
54. Kao, J et al. (2009). Molecular Profiling of Breast Cancer Cell Lines Defines Relevant Tumor Models and Provides a Resource for Cancer Gene Discovery. *PLoS One* 4(7).
55. Chavez, KJ (2010). Triple Negative Breast Cancer Cell Lines: One Tool in the Search for Better Treatment of Triple Negative Breast Cancer. *Breast Dis*. 32, 35–48.
56. Soule HD, Maloney TM, Wolman SR, Peterson WD, Jr., Brenz R, et al. (1990) Isolation and characterization of a spontaneously immortalized human breast epithelial cell line, MCF-10. *Cancer Res* 50, 6075–6086.
57. Cowell JK, LaDuca J, Rossi MR, Burkhardt T, Nowak NJ, et al (2005). Molecular characterization of the t(3;9) associated with immortalization in the MCF10A cell line. *Cancer Genet Cytogenet* 163, 23–29.
58. Leivonen, SK et al. (2013). High-throughput screens identify microRNAs essential for HER2 positive breast cancer cell growth. *Mol Oncol.* 13, 00141-5.
59. Iorio MV, et al (2005). MicroRNA gene expression deregulation in human breast cancer. *Cancer Res*. 16, 7065-70.
60. Blenkiron, C et al. (2007) MicroRNA expression profiling of human breast cancer identifies new markers of tumor subtypes. *Genome Biology* 8, R214.
61. Sempere LF, et al. (2001). Altered microRNA expression confined to specific epithelial cell sub-populations in breast cancer. *Cancer Research* 67, 11612-11620.

62. Cheng C, Fe X, Alves P and Mark Gerstein (2009). mRNA expression profiles show differential regulatory effects of microRNAs between estrogen-receptor positive and estrogen receptor-negative breast cancer. *Genome Biology* 10, R90.
63. Verghese ET, Hanby AM, Speirs V and TA Hughes. (2008). Small is beautiful: microRNAs and breast cancer-where are we now? *J Pathology* 215, 214-221.
64. Shi M and Ning Guo (2009). MicroRNA Expression and its implications for the diagnosis and therapeutic strategies of breast cancer. *Cancer Treat Rev* 35, 328-334.
65. Kondo N, et al. (2008). miR-206 expression is down-regulated in estrogen-receptor alpha-positive breast cancer. *Cancer Res* 68, 5004-8.
66. O'Day E and Shish Lal (2010). microRNAs and their target gene networks in breast cancer. *Breast Cancer Research* 12, 201.
67. Bockmeyer CL, et al (2011). microRNA profiles of healthy basal and luminal mammary epithelial cells are distinct and reflected in different breast cancer subtypes. *Breast Cancer Research Treatment* 130, 735-745.
68. Mackiewicz M, et al (2011).Identification of the receptor tyrosine kinase Axl in breast cancer as a target for the human miR-34a microRNA . *Breast Cancer Research Treatment* 130, 633-679.
69. Peurala H, et al (2011). miR-34a expression has an effect for lower risk of metastasis and associates with expression patterns predicting clinical outcome in breast cancer. *PLoS One* 6, e26122.
70. Iorio MV, et al (2011). Breast cancer and microRNAs: therapeutic impact. *Breast* S3,S63-S70.
71. Li X, et al (2012). microRNA-34a modulates chemosensitivity of breast cancer cells to adriamycin by targeting Notch1. *Archives of Medical Research* 43, 514-521.
72. Liu, Huiping (2012). microRNAs in breast cancer initiation and progression. *Cell Mol Life Sc*i. 69, 3587-3599.
73. Yang S, et al (2013). microRNA-34 suppresses breast cancer invasion and metastasis by directly targeting Fra-1. *Oncogene* 32, 4294-4303.
74. Wiggins JF, et al (2010). Development of a lung cancer therapeutic based on the tumor suppressor microRNA-34. *Cancer Research* 14, 5923-5930.
75. Chen Y, et al (2010). Nanoparticles modified with tumor-targeting scFv deliver siRNA and miRNA for cancer therapy. *Mol Ther* 9, 1650-1656.
76. Tazawa H, et al (2007). Tumor-suppressive miR-34a induces senescence-like growth arrest through modulation of the E2F pathway in human colon cancer cells. *Proc Natl Acad Sci* 39, 15472-15477.
77. Kota J, et al (2009). Therapeutic microRNA delivery suppresses tumorigenesis in a murine liver cancer model. *Cell* 137, 1005–17.
78. Trang P, et al (2010). Regression of murine lung tumors by the let-7 microRNA. *Oncogene* 29, 1580–1587.
79. Janssen HL, et al. (2013). Treatment of HCV infection by targeting microRNA. *New England Journal of Medicine* \18, 1685-1694.
80. Grimm D, et al. (2006). Fatality in mice due to oversaturation of cellular microRNA/short hairpin RNA pathways. *Nature* 441, 537-541.
81. Esquela-Kerscher A, et al (2008). The let-7 microRNA reduces tumor growth in mouse models of lung cancer. *Cell Cycle* 7, 759–64.

82. Liu X and Lv K (2013). Cruciferous vegetables intake is inversely associated with risk of breast cancer: a meta-analysis. *Breast* 3, 309-313.
83. Hoezl C, et al (2008). Consumption of Brussels sprouts protects peripheral human lymphocytes against 2-amino-1-methyl-6-phenylimidazo[4,5-b]pyridine (PhIP) and oxidative DNA-damage: results of a controlled human intervention trial. *Mol Nutr Food Res.* 3, 330-341.
84. Altundag K, Gundeslioglu O and O Altundag. (2006). Increased cabbage intake may inhibit metastatic and invasive capacity of breast cancer cells by inhibiting CXCL12(SDF-1 alpha)/CXCR4. *Mol Hypotheses*, 3, 672.
85. Kristal AR and JL Stanford (2004). Cruciferous vegetables and prostate cancer risk: confounding by PSA screening. *Cancer Epidemiol Biomarkers Prev* 7, 1265.
86. Kristal AR and JW Lampe (2002). Brassica vegetables and prostate cancer risk: a review of the epidemiological evidence. *Nutr Cancer* 1, 1-9.
87. J.H. Cohen, A.R. Kristal, and J.L. Stanford (2000). Fruit and vegetable intakes and prostate cancer risk. *J. Natl. Cancer Inst*. 92, 61–68.
88. J.V. Higdon, et al (2007).Cruciferous vegetables and human cancer risk: epidemiologic evidence and mechanistic basis, *Pharmacol. Res.* 55, 224–236.
89. D.T. Verhoeven, et al (1996).Epidemiological studies on brassica vegetables and cancer risk, Cancer Epidemiol. *Biomarkers Prev.* 5, 733–748**.**
90. Bradlow HL, et al (1991). Effects of dietary indole-3-carbinol on estrogen metabolism and spontaneous mammary tumors in mice. *Carcinogenesis* 12, 1571-1574.
91. Terry P, et al (2002). Dietary factors in relation to endometrial cancer: a nationwide case-control study in Sweden. *Nutr Cancer* 42, 25-32.
92. Terry, P et al. (2001) Brassica vegetables and breast cancer risk. *J. Am. Med. Assoc.* 285, 2975–2977.
93. Bell, M. C. et al (2000). Placebo-controlled trial of indole-3-carbinol in the treatment of CIN. *Gynecol. Oncol*. 78, 123–129.
94. Del Priore G, et al (2009). Oral diindolylmethane (DIM): pilot evaluation of a nonsurgical treatment for cervical dysplasia. *Gynecol Oncol* 116, 464-7.
95. Dalessandri KM, et al (2004). Pilot study: Effect of 3,3'-diindolylmethane supplements on urinary hormone metabolites in postmenopausal women with a history of early-stage breast cancer. *Nutr Cancer* 50, 161-7.
96. Reed GA, et al (2006). Single-dose and multiple-dose administration of indole-3-carbinol to women: Pharmacokinetics based on 3,3'-diindolylmethane. *Cancer Epidemiol Biomarkers* Prev 15, 2477-81.
97. Reed GA, et al (2005). A phase I study of indole-3-carbinol in women: tolerability and effects. *Cancer Epidemiol Biomarkers Prev* 14, 1953-60.
98. Acharya A, et al (2010). Chemopreventive properties of indole-3-carbinol, diindolylmethane and other constituents of cardamom against carcinogenesis. *Recent Pat Food Nutr Agric* 2,166-77
99. Aggarwal, B.B and Haruyo Ichikawa. (2005). Molecular targets and anti-cancer potential of indole-3-carbinol. *Cell Cycle* 4, 1201-1215.
100. Firestone, GL and Shyam N. Sundar (2009). Mini-review: modulation of hormone receptor signaling by dietary anti-cancer indoles. *Molecular Endocrinology* 23, 1940-1947.

101. Weng et al. 2008). Indole-3-carbinol as a chemopreventive and anti-cancer agent. *Cancer Letters* 262, 153-163.
102. Wattenberg L W and W D Loub (1978). Inhibition of polycyclic aromatic hydrocarbon-induced neoplasia by naturally occurring indoles. *Cancer Research* 38, 1410-1413.
103. Wattenberg LW, et al (1985). Inhibition of carcinogenesis by some minor dietary constituents. *Princess Takamatsu Symp 1985* 16, 193-203.
104. Sharma, S. et al (1994). Screening of potential chemopreventive agents using biochemical markers of carcinogenesis. *Cancer Research* (54) 5848-5855.
105. Bradlow HL, et al. (1995) Indole-3-carbinol. A novel approach in breast cancer prevention. *Ann. N. Y. Acad. Sci*. 768, 180-200.
106. Chatterji U, et al (2004). Indole-3-carbinol stimulates transcription of the interferon gamma receptor 1 gene and augments interferon responsiveness in human breast cancer cells. *Carcinogenesis* 25, 1119-1128.
107. Bradlow HL, et al. (1991). Effects of dietary indole-3-carbinol on estrogen metabolism and spontaneous mammary tumors in mice. *Carcinogenesis* 12, 1571–1574.
108. Riby JE, Firestone GL, and LF Bjeldanes. (2008) 3,3'-diindolylmethane reduces levels of HIF-1alpha and HIF-1 activity in hypoxic cultured human cancer cells. *Biochem Pharmacol* 9, 1858-1867.
109. Chang X, et al (2005). 3,3'-diindolylmethane inhibits angiogenesis and the growth of transplantable human breast carcinoma in athymic mice. *Carcinogenesis* 26, 771-778.
110. Hong, et al (2002). 3,3'-diindolylmethane (DIM) induces a G1 cell cycle arrest in human breast cancer cells that is accompanied by Sp1-mediated activation of p21 expression. *Carcinogenesis* 23, 1297-1305.
111. Hong C, Firestone GL and Leonard F. Bjeldanes (2002). Bcl-2 family mediated apoptotic effects of 3,3'-diindolylmethane (DIM) in human breast cancer cells . *Biochemical Pharmacology* 63, 1085–1097.
112. Rahman, et al (2007). Inactivation of NF-κB by 3,3'-diindolylmethane contributes to increased apoptosis induced by chemotherapeutic agent in breast cancer cells. *Mol Cancer Ther* 10, 2757-2765.
113. Rahman KM, Aranha O, and Fazul H. Sarkar (2003). Indole-3-carbinol (I3C) induces apoptosis in tumorigenic but not in non-tumorigenic breast epithelial cells. *Nutrition and Cancer* 45, 101-112.
114. McGuire et al (2006). 3,3'-diindolylmethane and Paclitaxel act synergistically to promote apoptosis in Her-2/Neu human breast cancer cells. *Journal of Surgical Research* 132, 208-213.
115. Rahimi M, Huang KL, and Careen K. Tang (2010). 3,3'-diindolylmethane (DIM) inhibits the growth and invasion of drug-resistant human cancer cells expressing EGFR mutants. *Cancer Letters* 295, 59-68.
116. Xue L, et al (2008). 3,3'-diindolylmethane stimulates murine immune function in vitro and in vivo. *Journal of Nutritional Biochemistry* 19, 336-344.
117. Riby JE, et al (2006). Activation and potentiation of interferon-gamma signaling by 3,3'-diindolylmethane in MCF-7 breast cancer cells. *Mol Pharmacol.* 2, 430-439.
118. Xue L, Firestone GL, and LF Bjeldanes. (2005). DIM stimulates IFNgamma gene expression in human breast cancer cells via the specific activation of JNK and p38 pathways. *Oncogene* 14, 2343-2353.

119. Chatterji U, et al (2004). Indole-3-carbinol stimulates transcription of the interferon gamma receptor 1 gene and augments interferon responsiveness in human breast cancer cells. *Carcinogenesis* (7) 1119-1128.
120. Marconett CN, et al (2012). Indole-3-carbinol disrupts estrogen receptor-alpha dependent expression of insulin-like growth factor-1 receptor and insulin receptor substrate-1 and proliferation of human breast cancer cells. *Mol Cell Endocrinol* 363, 74-84.
121. Aronchik I, et al (2012). Target protein interactions of indole-3-carbinol and the highly potent derivative 1-benzyl-I3C with the C-terminal domain of human elastase uncouples cell cycle arrest from apoptotic signaling. *Mol Carcinog*. 11, 881-894.
122. Marconett CN, et al (2011). Indole-3-carbinol downregulation of telomerase gene expression requires the inhibition of estrogen receptor-alpha and Sp1 transcription factor interactions within the hTERT promoter and mediates the G1 cell cycle arrest of human breast cancer cells. *Carcinogenesis* 9,1315-1323.
123. Aronchik I, Bjeldanes LF, and GL Firestone. (2010). Direct inhibition of elastase activity by indole-3-carbinol triggers a CD40-TRAF regulatory cascade that disrupts NF-kappaB transcriptional activity in human breast cancer cells. *Cancer Res* 12, 4961-4967.
124. Marconett CN, et al. (2010). Indole-3-carbinol triggers aryl hydrocarbon receptor-dependent estrogen receptor (ER)alpha protein degradation in breast cancer cells disrupting an ERalpha-GATA3 transcriptional cross-regulatory loop. *Mol Biol Cell*. 7,1166-1177.
125. Brew CT, et al (2009). Indole-3-carbinol inhibits MDA-MB-231 breast cancer cell motility and induces stress fibers and focal adhesion formation by activation of Rho kinase activity. *Int J Cancer* 124, 2294-2302.
126. Nguyen HH, et al (2008). The dietary phytochemical indole-3-carbinol is a natural elastase enzymatic inhibitor that disrupts cyclin E protein processing. *Proc Natl Acad Sci U SA.* (50):19750-5
127. Sundar SN, et al (2006). Indole-3-carbinol selectively uncouples expression and activity of estrogen receptor subtypes in human breast cancer cells. *Mol Endocrinol*. 12, 3070-3082.
128. Wang TT, et al (2006). Estrogen receptor alpha as a target for indole-3-carbinol. *J Nutr Biochem*.10, 659-64.
129. Brew CT, et al (2006). Indole-3-carbinol activates the ATM signaling pathway independent of DNA damage to stabilize p53 and induce G1 arrest of human mammary epithelial cells. *Int J Cancer.* 4, 857-68.
130. Garcia HH, et al (2005).Indole-3-carbinol (I3C) inhibits cyclin-dependent kinase-2 function in human breast cancer cells by regulating the size distribution, associated cyclin E forms, and subcellular localization of the CDK2 protein complex. *J Biol Chem.* 10, 8756-64.
131. Cover CM, et al (1998). Indole-3-carbinol inhibits the expression of cyclin-dependent kinase-6 and induces a G1 cell cycle arrest of human breast cancer cells independent of estrogen receptor signaling. *J Biol Chem.* 273, 3838-3847.
132. Cram EJ, et al (2001). Indole-3-carbinol inhibits CDK6 expression in human MCF-7 breast cancer cells by disrupting Sp1 transcription factor interactions with a composite element in the CDK6 gene promoter. *J Biol Chem*. 25,22332-22334.
133. Adjuik M, et al (2004). Artesunate combinations for treatment of malaria: meta-analysis. *Lancet* 363, 9-17.

134. Anfosso, L. et al. (2006) Microarray expression profiles of angiogenesis-related genes predict tumor cell response to artemisinins. *Pharmacogenomics Journal* 6, 269-278.
135. Bosman A, and KN Mendis. (2007) A major transition in malaria treatment: the adoption and deployment of artemisinin-based combination therapies. *Am J Trop Med Hyg* 77, 193–197.
136. Chen, H et al (2004). Inhibitory effects of artesunate on angiogenesis and on expressions of vascular endothelial growth factor and VEGF receptor KDR/flk-1. *Pharmacology* 71, 1–9.
137. Cui L and Xin-zhuan Su (2009). Discovery, mechanisms of action and combination therapy of artemisinin. *Expert Rev Anti Infect Ther* 8, 999-1013.
138. Du JH, et al (2010). Artesunate induces oncosis-like cell death in vitro and has antitumor activity against pancreatic cancer xenografts in vivo. *Cancer Chemother Pharmacol* 65, 895-890.
139. Efferth T and B Kaina (2010). Toxicity of the antimalarial artemisinin and its derivatives. *Crit Rev Toxicol* 40, 405-421.
140. Efferth T and K Ramawat (2009). *Herbal Drugs: Ethno-medicine to Modern Medicine*. Springer-Verlag Berlin. Heidelberg, Germany.
141. Efferth T and F Oesch (2004). Oxidative stress response of tumor cells: microarray-based comparison between artemisinins and anthracyclines. *Biochem Pharmacol* 68, 3-10.
142. Efferth, T. et al. (2004) Enhancement of cytotoxicity of artemisinins toward cancer cells by ferrous iron. *Free Radical Biology and Medicine* 37, 998-1009.
143. Efferth, T. et al. (2003). Molecular modes of action of artesunate in tumor cell lines. *Molecular Pharmacology* 64, 382-394.
144. Efferth T., Olbrich A. and R Bauer (2002). mRNA expression profiles for the response of human tumor cell lines to the antimalarial drugs artesunate, arteether, and artemether. *Biochemical Pharmacology* 64, 617-623.
145. Efferth T, et al (2001). The anti-malarial artesunate is also active against cancer. *Int J Oncol.* 4, 767-773.
146. Firestone GL, and Shyam N. Sundar (2009). Anticancer activities of artemisinin and its bioactive derivatives. *Expert Rev Mol Med* 11, 1-15.
147. Gautam, A. et al. (2009) Pharmacokinetics and pharmacodynamics of endoperoxide antimalarials. *Current Drug Metabolism* 10, 289-306.
148. Gao W, et al (2013). Artemisinin induces A549 cell apoptosis dominantly via a reactive oxygen species-mediated amplification activation loop among caspase-9, -8 and -3. *Apoptosis* 18, 1201-1213.
149. Gong Y, et al (2013). Effects of transferrin conjugates of artemisinin and artemisinin dimer on breast cancer cell lines. *Anticancer Research* 33, 123-132.
150. Hamacher-Brady A, et al (2011). Artesunate activates mitochondrial apoptosis in breast cancer cells via iron-catalyzed lysosomal reactive oxygen species production. *J Biol Chem* 286, 6587-601.
151. Haynes R, et al (2007). Artesunate and dihydroartemisinin (DHA): unusual decomposition products formed under mild conditions and comments on the fitness of DHA as an anti-malarial drug. *ChemMedChem* 2, 1448-1463.
152. He Y, et al (2011). The anti-malaria agent artesunate inhibits expression of vascular endothelial growth factor and hypoxia-inducible factor-1α in human rheumatoid arthritis fibroblast-like synoviocyte. *Rheumatol* 31, 53-60.

153. Hou, J. et al. (2008) Experimental therapy of hepatoma with artemisinin and its derivatives: in vitro and in vivo activity, chemosensitization, and mechanisms of action. *Clinical Cancer Research* 14, 5519-5530.
154. Langroudi L, et al (2010). A comparison of low-dose cyclophosphamide treatment with artemisinin treatment in reducing the number of regulatory T cells in murine breast cancer model. *Int Immunopharmcol* 10, 1055-1061.
155. Lai, H. and Singh, N.P. (2006) Oral artemisinin prevents and delays the development of 7,12-dimethylbenz[a]anthracene (DMBA)-induced breast cancer in the rat. *Cancer Letters* 231, 43-48.
156. Lai H, Sasaki T, and NP Singh (2005). Targeted treatment of cancer with artemisinin and artemisinin-tagged iron-carrying compounds. *Expert Opin Ther Targets*. 9, 995-1007.
157. Lai H, et al (2005a). Effects of artemsinin-tagged holotransferrin on cancer cells. *Life Sci* 76, 1267-1279.
158. Lai H, et al (2005b) Targeted treatment of cancer with artemisinin and artemisinin-tagged iron-carrying compounds. *Expert Opin Ther Targets* 9, 995-1007.
159. Liu, WM et al (2011). The antimalarial agent artesunate possess anticancer properties that can be enhanced by combination strategies. *Int J Cancer* 128, 1471-1480.
160. McGovern, et al (2010). Anticancer activity of botanical compounds in ancient fermented beverages. *International Journal of Oncology* 37, 5-14.
161. Mercer AE, et al (2011). The role of heme and the mitochondrion in the chemical and molecular mechanisms of mammalian cell death induced by the artemisinin anti-malarials. *J Biol Chem* 286, 987-996.
162. Meschnick, SR et al (2002). Artemisinin: mechanisms of action, resistance and toxicity. *Int J Parasitology* 32, 1655-1660.
163. Milller, LH (2013). Malaria biology and disease pathogenesis: insights for new treatments. *Nature Medicine* 19, 156-167.
164. Miller, LH and Xinzhuan Su (2011). Artemisinin: discovery from the Chinese herbal garden. *Cell* 146, 855-858.
165. Nakase, I. et al. (2009) Transferrin receptor dependent cytotoxicity of artemisinin-transferrin conjugates on prostate cancer cells and induction of apoptosis. *Cancer Letters* 274, 290-298.
166. Nakase, I et al (2008). Anticancer properties of artemisinin derivatives and their targeted delivery by transferrin conjugation. *International Journal of Pharmaceutics* 354, 28-33.
167. Sadava D, et al (2002). Transferrin overcomes drug resistance to artemisinin in human small-cell lung carcinoma cells. *Cancer Letters* 179, 151-156.
168. Sertel S, (2010). Pharmacogenomic identification of c-Myc/Max-regulated genes associated with cytotoxicity of artesunate towards human colon, ovarian and lung cancer cell lines. *Molecules* 15, 2886-2910.
169. Sundar SN, et al (2008). Artemisinin selectively decreases functional levels of estrogen receptor-alpha and ablates estrogen-induced proliferation in human breast cancer cells. *Carcinogenesis* 29, 2252-2258.
170. Sinclair D, et al (2012). Artesunate versus quinine for treating severe malaria. *Cochrane Database Syst Rev* 6, CD005967.

171. Tin AS, et al (2012). Anti-proliferative effects of artemisinin on human breast cancer cells requires the downregulated expression of the E2F1 transcription factor and loss of E2F1-target cell cycle genes. *Anticancer Drugs* 4, 370-379.
172. Wartenberg, M. et al. (2003) The anti-malaria agent artemisinin exerts anti-angiogenic effects in mouse embryonic stem cell-derived embryoid bodies. *Laboratory Investigation* 83, 1647-1655.
173. Willoughby JA Sr, et al (2009). Artemisinin blocks prostate cancer growth and cell cycle progression by disrupting Sp1 interactions with the cyclin-dependent kinase-4 (CDK4) promoter and inhibiting CDK4 gene expression. *J Biol Chem* 284, 2203-2213.
174. YouyouTu (2011). The discovery of artemisinin (qinghaosu) and gifts from Chinese Medicine. *Nature Medicine* 17, 1217-1220.
175. Zhang HT, et al (2013). Artemisinin inhibits gastric cancer cell proliferation through upregulation of p53. *Tumour Biol.*
176. Zhou C, et al (2012). Artesunate induces apoptosis via a Bak-mediated caspase-independent intrinsic pathway in human lung adenocarcinoma cells. *J Cell Physiol.* 227, 3778-3786.
177. Zhou, H.J. et al. (2007) Artesunate inhibits angiogenesis and downregulates vascular endothelial growth factor expression in chronic myeloid leukemia K562 cells. *Vascular Pharmacology* 47, 131-138.
178. Li Y, et al. (2010). Regulation of microRNAs by natural agents: an emerging field in chemoprevention and chemotherapy research. *Pharm Res*. 6, 1027-41.
179. Izzotti A, et al (2010). Chemoprevention of cigarette smoke-induced alterations of MicroRNA expression in rat lungs. *Cancer Prev Res (Phila*). 3, 62-72.
180. Melkamu T, et al (2010). Alteration of microRNA expression in vinyl carbamate-induced mouse lung tumors and modulation by the chemopreventive agent indole-3-carbinol. *Carcinogenesis*. 2, 252-258.
181. Ahmad A, et al (2013). 3, 3'-Diindolylmethane enhances the effectiveness of herceptin against HER-2/neu-expressing breast cancer cells. *PLoS One*. 8: e54657.
182. Soubani O, et al (2012). Re-expression of miR-200 by novel approaches regulates the expression of PTEN and MT1-MMP in pancreatic cancer. *Carcinogenesis*. 33, 1563-71.
183. Jin Y (2011). 3, 3'-Diindolylmethane inhibits breast cancer cell growth via miR-21-mediated Cdc25A degradation. *Mol Cell Biochem.* 358, 345-354.
184. Kong D, et al (2012). Loss of let-7 up-regulates EZH2 in prostate cancer consistent with the acquisition of cancer stem cell signatures that are attenuated by BR-DIM. *PLoS One*. 7, e33729.
185. Li Y, et al (2010). miR-146a suppresses invasion of pancreatic cancer cells. *Cancer Res.* 70, 1486-95.
186. Li Y, et al (2009). Up-regulation of miR-200 and let-7 by natural agents leads to the reversal of epithelial-to-mesenchymal transition in gemcitabine-resistant pancreatic cancer cells. *Cancer Res*. 69, 6704-12.
187. Jin Y, et al (2011). 3, 3'-Diindolylmethane inhibits breast cancer cell growth via miR-21-mediated Cdc25A degradation. *Mol Cell Biochem.*358, 345-54.
188. Paik WH, (2013). Chemosensitivity induced by down-regulation of microRNA-21 in gemcitabine-resistant pancreatic cancer cells by indole-3-carbinol. *Anticancer Res*. 3, 1473-81.

189. Pani A, et al (2011). Computational identification of sweet wormwood (Artemisia annua) microRNA and their mRNA targets. *Genomics Proteomics Bioinformatics*. 6, 200-210.
190. Pérez-Quintero AL, et al (2012). Mining of miRNAs and potential targets from gene oriented clusters of transcripts sequences of the anti-malarial plant, Artemisia annua. *Biotechnol Lett.* 34, 737-745.
191. Corcoran C, et al (2011). Intracellular and extracellular microRNAs in breast cancer. *Clin Chem*. 57, 18032.
192. Markey, M and Berberich SJ (2008). Full-length hdmX transcripts decrease following genotoxic stress. *Oncogene* 27, 6657-6666.
193. Chi V. Dang (1999). c-Myc Target Genes Involved in Cell Growth, Apoptosis, and Metabolism. *Molecular and Cellular Biology*. 19, 1-11.
194. Perini G, et al (2005). In vivo transcriptional regulation of N-Myc target genes is controlled by E-box methylation. Proc Natl Acad Sci USA 102, 12117-12122.
195. Melmed S, et al (2008). *Hormonal Control of Cell Cycle*. Springer-Verlag Berlin. Heidelberg, Germany.
196. Chen et al. (2005). Real-time quantification of microRNAs by stem-loop RT-PCR. *Nucleic Acids Research* 33, 1-9.
197. Heid et al. (1996). Real Time Quantitative PCR. *Genome Research*. 6, 986-994.
198. Reed, SI. (1997). SI. Control of the G1/S transition. *Cancer Survival.* 29, 7-23.
199. Livak K and Thomas D. Schmittgen (2001). Analysis of relative gene expression data using real-time quantitative PCR and the $2^{-\Delta\Delta C}{}_{T}$ method. *Methods* 15, 56-61.
200. Sheen JH and RB Dickson. (2002). Over-expression of c-Myc alters G (1)/S arrest following ionizing radiation. *Molecular Cell Biology* 122, 1819-1833.
201. Shaulian, E et al (1992). Identification of a minimal transforming domain of p53: negative dominance through abrogation of sequence-specific DNA binding. *Molecular and Cellular Biology* 12, 5581-5592.
202. Juntilla M and Evan G (2009). p53-a Jack of all trades but master of none. *Nat Rev Cancer* 9, 821-829.
203. Jump, SM et al (2008). N-Alkoxy derivatization of indole-3-carbinol increases the efficacy of the G1 cell cycle arrest and of I3C-specific regulation of cell cycle gene transcription and activity in human breast cancer cells. *Biochem Pharmacol* 75, 713-724.
204. Nguyen HH, et al (2010). 1-Benzyl-indole-3-carbinol is a novel indole-3-carbinol derivative with significantly enhanced potency of anti-proliferative and anti-estrogenic properties in human breast cancer cells. *Chem Biol Interact* 186, 255266.
205. Firestone GL and LF Bjeldanes (2003). Indole-3-carbinol and 3-3'-diindolylmethane anti-proliferative signaling pathways control cell-cycle gene transcription in human breast cancer cells by regulating promoter-Sp1 transcription factor interactions. *J Nutr.* 133, 2448S-2455S.
206. Aas T, et al (1996). Specific P53 mutations are associated with de novo resistance to doxorubicinin breast cancer patients. *Nat Med* 2, 811–814.
207. Bergh J, et al (1995). Complete sequencing of the p53 gene provides prognostic information in breast cancer patients, particularly in relation to adjuvant systemic therapy and radiotherapy. *Nat Med* 1, 1029–1034.
208. Olivier M, et al (2006).The clinical value of somatic TP53 gene mutations in 1,794 patients with breast cancer. *Clin Cancer Res* 12, 1157–1167.

209. Langerod A, et al (2007). TP53 mutation status and gene expression profiles are powerful prognostic markers of breast cancer. *Breast Cancer Res* 9, R30.
210. Petitjean A, et al (2007). TP53 mutations in human cancers: Functional selection and impact on cancer prognosis and outcomes. *Oncogene* 26, 2157–2165.
211. Chrisanthar R, et al **(**2008**).** CHEK2 mutations affecting kinase activity together with mutations in TP53 indicate a functional pathway associated with resistance to epirubicin in primary breast cancer. *PLoS ONE* 3**,** e3062.
212. Geisler S, et al (2003). TP53 gene mutations predict the response to neoadjuvant treatment with 5-fluorouracil and mitomycin in locally advanced breast cancer. *Clin Cancer Res* 9, 5582-5588.
213. Geisler S, et al (2001). Influence of TP53 gene alterations and c-erbB-2 expression on the response to treatment with doxorubicin in locally advanced breast cancer. *Cancer Res* 61, 2505-2512.
214. Aas T, et al (2003). Predictive value of tumour cell proliferation in locally advanced breast cancer treated with neoadjuvant chemotherapy. *Eur J Cancer* 39, 438-446.
215. Berns EM et al (2000). Complete sequencing of TP53 predicts poor response to systemic therapy of advanced breast cancer. *Cancer Res* 60, 2155-2162.
216. Bertheau P et al (2002). Effect of mutated TP53 on response of advanced breast cancers to high-dose chemotherapy. *Lancet* 360, 852-854.
217. Nigro JM, et al (1989). Mutations in the P53 Gene Occur in Diverse Human Tumour Types, *Nature* 342, 705-708.
218. Mikhail Blagosklonny (2000). p53 from complexity to simplicity: mutant p53 stabilization, gain-of-function, and dominant-negative effect. *FASEB J* 14, 1901-1907.
219. Zhao G, et al (2013). microRNA-34a suppresses cell proliferation by targeting LMTK3 in human breast cancer MCF-7 cell line. *DNA and Cell Biology* 0, 1-9.
220. Giamas G, et al (2011). Kinome screening for regulators of the estrogen receptor identifies LMTK3 as a new therapeutic target in breast cancer. *Nature Medicine* 17, 715-719.
221. Simonini P, et al (2010).Epigenetically deregulated microRNA-375 is involved in a positive feedback loop with estrogen receptor α in breast cancer cells. *Cancer Research* 70, 9175-9184.
222. Pandey D and Didier Picard (2009). miR-22 inhibits estrogen signaling by directly targeting the estrogen receptor α mRNA. *Molecular and Cell Biology* 29, 3783-3790.
223. Castellano L, et al (2009). The estrogen receptor-α induced microRNA signature regulates itself and its transcriptional response. *PNAS* 106, 15732-15737.
224. Zhao J, et al (2008). microRNA-221/222 negatively regulates estrogen receptor α and is associated with tamoxifen resistance in breast cancer. *Journal of Biological Chemistry* 283, 31079-31086.
225. Adams B, et al (2007). The micro-ribonucleic acid (miRNA) miR-206 targets the human estrogen receptor α (ERα) and represses ERα messenger RNA and protein expression in breast cancer cell lines. *Mol Endocrinology* 21, 1132-1147.
226. Migley CA and DP Lane (1997). p53 protein stability in tumour cells is not determined by mutation but is dependent on Mdm2 binding. *Oncogene* 15, 1179-1189.
227. Choi YJ, et al (2011). miR-34 miRNAs provide a barrier for somatic cell reprogramming. *Nature Cell Biology* 13, 1353-1360.

228. Welboren WJ, et al (2009). Genomic actions of estrogen receptor alpha: what are the targets and how are they regulated? *Endocr Relat Cancer*. 16, 1073-1089.
229. Adler S, Rashid G, and A Klein (2011). Indole-3-carbinol inhibits telomerase activity and gene expression in prostate cancer cell lines. *Anticancer Res*. 31, 3733-3777.
230. Wu TY, et al (2012). In vivo pharmacodynamics of indole-3-carbinol in the inhibition of prostate cancer in transgenic adenocarcinoma of mouse prostate (TRAMP) mice: involvement of Nrf2 and cell cycle/apoptosis signaling pathways. *Mol Carcinog*. 51, 761-770.
231. Wang TT, et al (2012). Broccoli-derived phytochemicals indole-3-carbinol and 3,3'-diindolylmethane exerts concentration-dependent pleiotropic effects on prostate cancer cells: comparison with other cancer preventive phytochemicals. *Mol Carcinog.* 51, 244-256.
232. Jeong YM, et al (2011). Indole-3-carbinol inhibits prostate cancer cell migration via degradation of beta-catenin. *Oncol Res*. 19, 237-43.
233. Kassie F, et al (2010). Inhibition of lung carcinogenesis and critical cancer-related signaling pathways by N-acetyl-S-(N-2-phenethylthiocarbamoyl)-l-cysteine, indole-3-carbinol and myo-inositol, alone and in combination. *Carcinogenesis*. 31, 1634-1644.
234. Choi HS, et al (2010). Indole-3-carbinol induces apoptosis through p53 and activation of caspase-8 pathway in lung cancer A549 cells. *Food Chem Toxicol*. 48, 883-890.
235. Gao W, et al (2013). Artemisinin induces A549 cell apoptosis dominantly via a reactive oxygen species-mediated amplification activation loop among caspase-9, -8 and -3. *Apoptosis*. 18, 1201-1213.
236. Zhou C, et al (2012). Artesunate induces apoptosis via a Bak-mediated caspase-independent intrinsic pathway in human lung adenocarcinoma cells. *J Cell Physiol.* 227, 3778-3786.
237. Zhao Y, et al (2011). Artesunate enhances radiosensitivity of human non-small cell lung cancer A549 cells via increasing NO production to induce cell cycle arrest at G2/M phase. *Int Immunopharmacol.*11, 2039-2046.
238. Cailleau R, et al (1974). Breast Tumor Cell Lines From Pleural Effusions. *J Natl Cancer Inst.* 53, 661-674.
239. Fogh J and T Orfeo (1977). One hundred and twenty-seven cultured human tumor cell lines producing tumors in nude mice. *J Natl Cancer Inst* 59, 221-226.
240. Keydar I, et al (1979). Establishment and characterization of a cell line of human breast carcinoma origin. *Eur J Cancer* 15, 659-670.
241. Levenson AS and VC Jordan (1997). MCF-7: the first hormone-responsive breast cancer cell line. *Cancer Res* 57, 3071-3078.
242. Cole KA, et al (2008). A functional screen identifies miR-34a as a candidate neuroblastoma tumor suppressor gene. *Mol Cancer Res* 6, 735-742.
243. Welch C, Chen Y and RL Stallings (2007). MicroRNA-34a functions as a potential tumor suppressor by inducing apoptosis in neuroblastoma cells. *Oncogene* 26, 5017-5022.
244. Kozaki K, et al (2008). Exploration of tumor-suppressive microRNAs silenced by DNA hypermethylation in oral cancer. *Cancer Res* 68, 2094-2105.